Seismic Refraction and Uphole Logging Based Geophysical Engineering Survey of Rawat Area

&

Development of Moisture Recording Instrument and Derivation of a Velocity-Moisture Empirical Relation

By

AMBER LATIF

BS Geophysics

2016-2020

Department of Earth Sciences

Quaid-I-Azam University

Islamabad, Pakistan

IN THE NAME OF ALLAH,

The Most Merciful & Mighty

"This is by the Grace of my Lord to test me whether I am grateful or ungrateful! And whoever is grateful, truly, his gratitude is for (the good of) his own self, and whoever is ungrateful, (he is ungrateful only for the loss of his own self). Certainly! My Lord is Rich (Free of all wants), Bountiful" **[Al-Naml: 40]**

CERTIFICATE

This dissertation submitted by **AMBER LATIF** D/o **ABDUL LATIF TAHIR** is accepted in its present form by the Department of Earth Sciences,

Quaid-i-Azam University Islamabad as satisfying the partial requirement for the award of Bachelors Science BS degree in Geophysics.

RECOMMENDED BY

Dr. MUMTAZ SHAH _____

(Supervisor)

Department of Earth Sciences

Dr. AAMIR ALI _____

(Chairperson)

Department of Earth Sciences

EXTERNAL EXAMINER _____

DEDICATION

*This thesis is dedicated to my **Parents**, **sister and brother,** they always taught me that the best kind of knowledge to have is that which is learned for its own sake. It is also dedicated to **My Teachers**, who taught me that even the largest task can be accomplished if it is done one step at a time.*

ACKNOWLEDGMENT

First of all thanks to **Almighty ALLAH,** the most the most Beneficent, Merciful ,cordial and sympathy whose great loving care and blessing always enabled us to perceive and pursue most difficult target of life, Alhamdulillah. I bear witness that **HOLY PROPHET HAZRAT MUHAMMAD (S.A.W)** is the last messenger, whose life is perfect model for the whole mankind till the Day of Judgment.

The work presented in this thesis would not have been possible without my close association with many people. I take this opportunity to extend my sincere gratitude and appreciation to all those who made this thesis possible. First and foremost among them is my supervisor Dr. Mumtaz Shah for his dedicated help, advice, inspiration, encouragement and continuous support.

I wish to express my deep gratitude to my advisor Dr. Khalid Amin Khan, Oil & Gas Development Company Ltd, for his continuous guidance and appreciation. He treated me as a child and helped me at every stage of this work like a father. His guidance throughout this endeavor was essential to its success from start to finish. Their help and direction provided me a framework that aided the progress toward my goal.

I specially acknowledge the prayers and efforts of my whole family, specially my parents for their encouragement, support and sacrifices throughout the study

I would like to say thanks to my friends especially Sana Kayani & Usama Younus for their moral support, guidance and companionship.

AMBER LATIF

ABSTRACT

Seismic refraction method is widely used to delineate the Low-Velocity Weathered Layers for computation of Statics corrections that are applied to the main reflection data. In addition it is considered as a valuable tool for near-surface geophysics & engineering, such as delineation of bed rock or basement and determining the engineering properties of ground. The refraction method utilizes the first arrival times of refracted waves propagating along the shallow subsurface layers. Variations in the near surface layers need to be mapped before the construction of any heavy industrial zone or highway. Uphole Logging and Near surface Seismic Refraction based Engineering survey of Rawat area is carried out for construction of heavy Engineering site, to map the near surface layers and estimate their velocities. In addition the near surface data is also used to compute Static corrections that can be applied to seismic reflection data for deep imaging of the Earth. The processing and interpretation of the data is performed on a highly interactive software, K-tron SeiRA along with Visual Oil Scripts and Golden Software Surfer. Weathered layer and Sub-weathered layer velocities are used to calculate Elastic properties for civil Engineering purposes to estimate the strength of Soil/Rock of Study Area. Contour maps of various important parameters; elastic moduli, standard penetration test, soil amplification factor, allowable bearing pressure, soil fundamental period, average horizontal spectral amplification are used for seismic zoning or classification of the study area.

As part of thesis work, an Arduino Based Moisture of Enginerring Recording Instrument has been developed which is capable of recording moisture of top soil and it can be used as a useful instrument for Engineering studies.

TABLE OF CONTENTS

LIST OF FIGURES

LIST OF TABLES

Chapter 1

Introduction

Seismic waves, gravity, magnetism and electrical fields in the earth are the foundation of modern *exploration geophysics.* The aim of exploration geophysics is the discovery of hidden geologic features. The non-invasive investigation of sub-surface conditions in the Earth includes measuring, analyzing and interpreting physical fields at the surface. Geophysical investigations of the interior of the Earth involve taking measurements at or near the Earth's surface that are influenced by the internal distribution of physical properties. Analysis of these measurements can reveal how the physical properties of the Earth's interior vary vertically and laterally. Geophysical interpreters create idealized models of the subsurface to better comprehend the structure and properties of the underlying geology. Geophysical instruments are designed to mapped spatial variation in the physical properties of the earth.

Hydrocarbons are among the earth's most important natural resources and hydrocarbons are the main constituents of petroleum (literally, "rock oil"), also called "oil," and natural oil. To explore the natural reserves particularly hydrocarbons, geophysical methods are most widely used. For the exploration of hydrocarbons, seismic methods are extensively used for the delineation of hydrocarbon.

1.1 Surveying Methods

Geophysical surveying, although sometimes prone to major ambiguities or uncertainties of interpretation, provides a relatively rapid and cost-effective means of deriving areally distributed information on subsurface geology. There is a broad division of geophysical surveying methods into those that make use of natural fields of the Earth and those that require the input into the ground of artificially generated energy.

- The natural field methods utilize the gravitational, magnetic and nuclear fields of the Earth, searching for local perturbations in these naturally occurring fields that may be caused by concealed geological features of economic or other.
- Artificial source Methods involve the generation of seismic waves whose propagation

velocities and transmission paths through the subsurface are mapped which provide information on the distribution of geological boundaries at depth.

A wide range of geophysical surveying methods exists, for each of which there is an "operative" physical property to which the method is sensitive. The methods are listed in Table 1.1.

Table 1.1 Geophysical Method (Kearey, P. M., & Hill, I. (2002))

Method	Measured parameter	Operative physical property
Seismic	Travel times of reflected/refracted seismic waves	Density and elastic moduli, which determine the propagation velocity of seismic waves.
Gravity	Spatial variations in the strength of the gravitational field of the Earth.	Density
Magnetic	Spatial variations in the strength of the geomagnetic field	Magnetic susceptibility and remanence
Electrical Resistivity	Earth resistance	Electrical conductivity
Induced polarization	Polarization voltages or frequency-dependent ground resistance	Electrical capacitance
Self-potential	Electrical potentials	Electrical conductivity
Electromagnetic	Response to electromagnetic radiation	Electrical conductivity and inductance
Radar	Travel times of reflected radar pulses	Dielectric constant

Geophysical methods are often used in combination. Among these techniques/methods, the most effective and the most adopted is based on the basic physical properties of waves that are reflection, refraction, diffraction and interference. The well-known technique is termed as the Seismic Technique (Kearey et al., 2002).

Reflection and Refraction methods are employed to map subsurface images, diffraction of seismic waves due to fault edges appear as noise on seismic traces while interference is helpful to improve the signal to noise ratio which is further helpful for getting better results.

1.2 Seismic Method Applications

Seismic methods are particularly well suited to the investigation of the layered sequences in sedimentary that are the primary targets for oil or gas. The seismic method has three important/principal applications (Yilmaz, O. (2001), where as Engineering properties can also be depicted from seismic waves.

a. Delineation of near-surface geology for engineering studies, and coal and mineral exploration within a depth of up to 1km: the seismic method applied to the near-surface studies is known as "***engineering seismology***".

b. Hydrocarbon exploration and development within a depth of up to 10 km: seismic method applied to the exploration and development of oil and gas fields is known as "***exploration seismology***".

c. Investigation of the earth's crustal structure within a depth of up to 100 km: the seismic method applies to the crustal and earthquake studies is known as "***earthquake seismology***".

1.2.1 Seismic Reflection Method

Seismic reflection is a method of exploration geophysics that provides information about the deeper sub-surface structures. In the case of seismic reflection, the down-going wavefield reflects off geological boundaries characterized by density and velocity contrasts before being recorded by an array of receivers. The strength of the seismic reflection method lies in its ability to gain insight into structural and stratigraphic relationships beneath the seafloor, as well as in investigating fluid flow processes. Seismic images, such as those derived from reflection data, provide crucial information for creating increasingly complex subsurface models of the earth.

1.2.2 Seismic Refraction Method

The seismic refraction method was developed for the exploration of hydrocarbons. The seismic refraction method was first developed in the nineteenth century when the first measurements were taken of speed and velocity of seismic waves through the number of earth materials. In 1924 it was first used for delineation of shallow salt domes. Due to some limitations, it was soon replaced with the seismic reflection method, which continues to be the main technique

for the exploration of hydrocarbons and imaging deep structures. Today the seismic refraction method is widely used to delineate the Low-Velocity Weathered Layers for computation of Statics corrections that are applied to the main reflection data. In addition, it is considered as a valuable tool for near-surface geophysics & engineering, such as delineation of bedrock or basement and determining the engineering properties of the ground.

- **Seismic Refraction Data Acquisition:** A seismic refraction recorder usually consists of 24 channels each of which is connected to a geophone. The geophones are placed along with a profile with variable geophone intervals. Two shots are taken at both ends of the profile, the first near geophone # 1 is called forward shooting while the second near geophone # 24 is called reverse shooting. This results in two seismic monitors each with 24 seismograms (traces) as shown below:

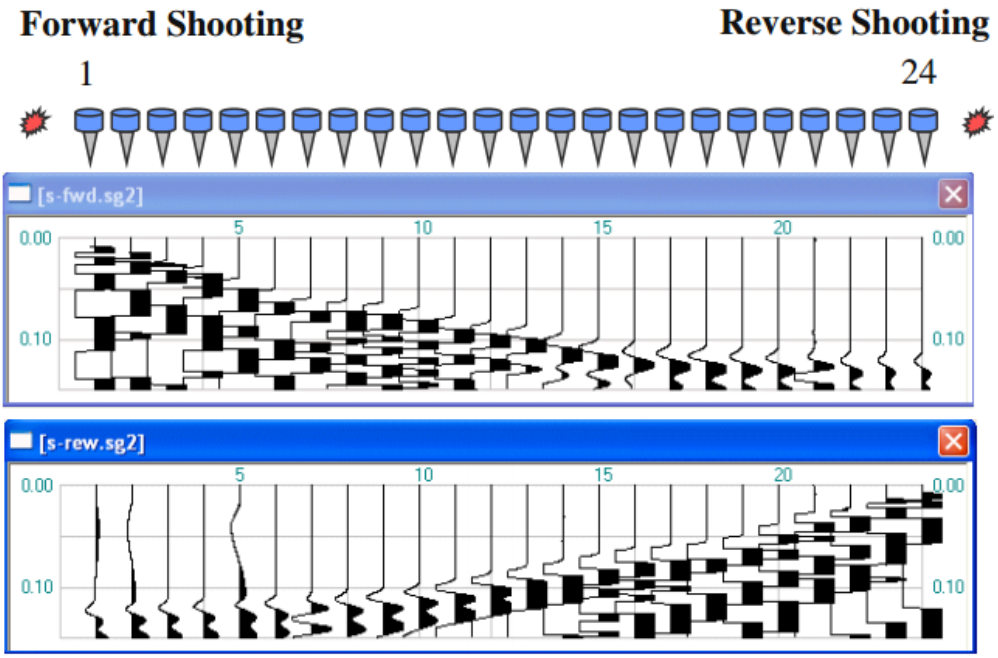

Fig 1.1 Surface Geometry for Forward & Reverse Shooting

1.3 Seismic Acquisition:

Seismic data acquisition consists of gathering and recording of continuous seismic signals from seismic stations. The seismic acquisition can take place either on the surface of the earth (land acquisition), or seafloor (marine acquisition). The generation of seismic waves (elastic waves) is carried out by the source. A source can be either natural such as earthquakes or controlled (induced) such as dynamite. For exploration purposes, controlled sources are used. A source such

as a vibrator unit, dynamite shot, or an air gun, generates acoustic or elastic vibrations that travel into the Earth, passes through strata with different seismic responses and filtering effects, and return to the surface to be recorded as seismic data. Seismic data can be acquired in different dimensions depending upon the objective of the survey and economy of the drilling company.

2D Seismic:

In two-dimensional seismic surveying both the sound source (shot) and the sound detectors/receivers (numbering up to a hundred or more per shot) are moved along a straight line. Thus Shot and receivers are in the same line. The next line is spaced kilometers away. In other words, 2D seismic data are acquired individually, as opposed to the multiple closely spaced lines acquired together that constitute 3D seismic data.

3D Seismic:

In a 3D survey, a shot is within the grid of multiple lines of receivers and the next line is spaced tens of meters away to create a 'three-dimensional volume' of data that is also referred to as a cube that represents a volume of the earth, it allows us to examine data in many different ways. The results are an improved understanding of the structures and nature of the earth beneath us and enhance the probability of finding recoverable reserves of hydrocarbon. The 3D seismic method often improves data density and provides detailed information about fault distribution and the sub-surface structure.

4D Seismic:

4D seismic survey is a three-dimensional (3D) seismic data acquired at different times over the same area to assess changes in a producing hydrocarbon reservoir with time. When 3D surveys are repeated in this way, they are often referred to as 4D seismic. The simplest, most direct method of using time-lapse seismic data is to qualitatively monitor reservoir changes due to production. 4D seismic data provides a baseline for the development of other oil and gas fields. It can help to locate an untapped pocket of oil and gas in a reservoir.

1.4 Introduction to the Survey

Refraction survey was carried out by Senshe in Rawat & was started on March 14, 2014, and lasted for almost two months. It comprises of surface shooting and uphole logging for the

weathered layer delineation and statics computation. Our aim of doing seismic refraction surveying is to calculate the thickness, velocities and Engineering properties of the near surface rock layers.

1.4.1 Location of Study Area

Rawat is located in Punjab province of Pakistan in Rawalpindi. It is bounded by Islamabad in the North, Jammu Kashmir in the East, Fateh Jang in the West and Gujar Khan in the South. It lies 650 above mean sea level and geographically it lies in Upper Indus Basin in Potwar Plateau. The geographical coordinates of the area are:

– **Latitude**: 33.4 to 33.6

– **Longitude:** 73.1 to 73.4

Location of the study area on Pakistan Map is shown in Figure 1.2.

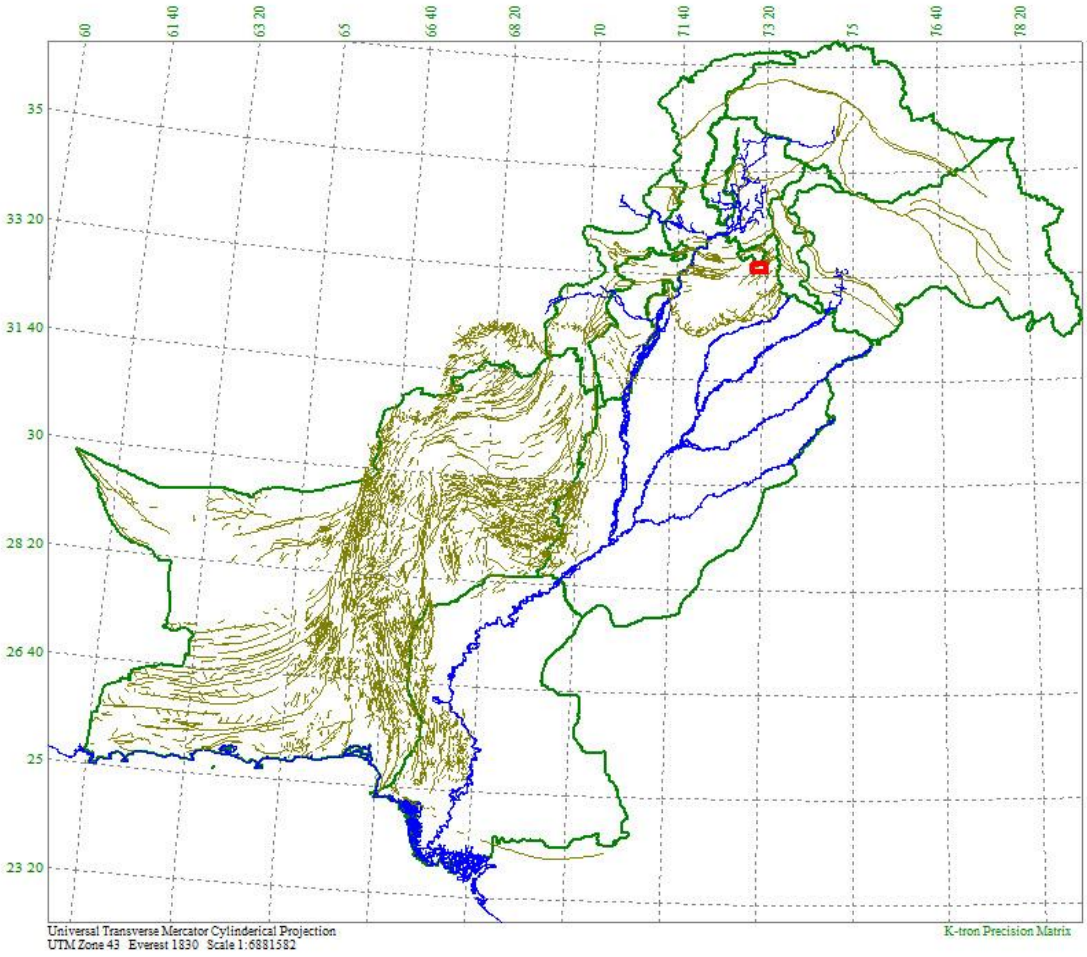

Fig 1.2 Location of Rawat in Pakistan Map Highlighted by red colour.

1.5 Base Map

The base map is an important component of interpretation, as it displays the spatial position or location of each refraction pickets. It also shows the spatial relationship of all seismic sections under consideration, their tie point locations and provides the framework for contouring. The base map is produced using some projection systems such as Lambert Conic projection or Universal Transverse Mercator (UTM) projection. The base map also shows grids of geographic latitude-longitudes and/or projected grid coordinates. The base map of the area, shown in Figure 1.3, is obtained by plotting data in Universal Transverse Mercator (UTM-42) geodetic reference system. These maps have been prepared using Precision Matrix an Integrated GeoSystems (Khan, 2000) application.

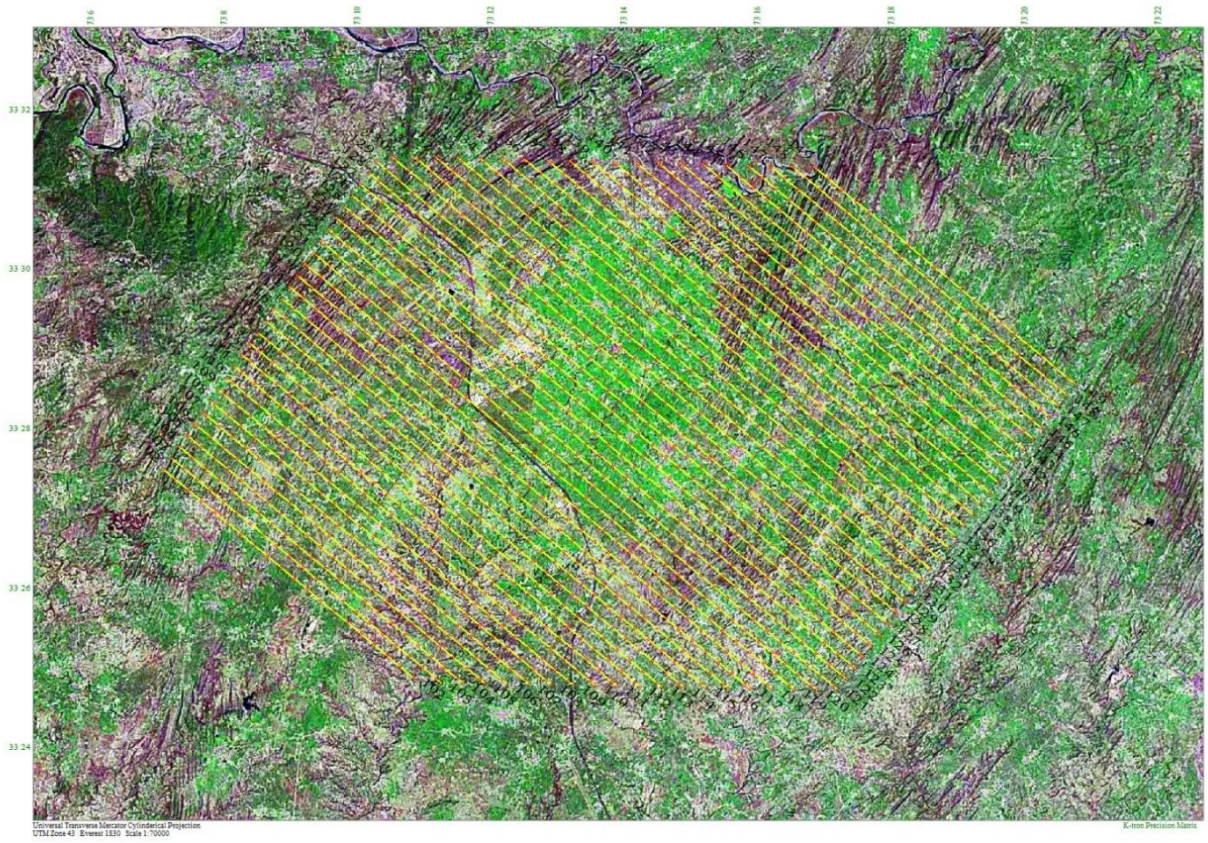

Fig 1.3 Base map with satellite imagery showing source and receiver lines, source point and receiver pickets.

1.5.1 Digital Elevation Model of Rawat

The digital elevation model (DEM) is a representation of geographic information in raster and consists of a regular grid of elevation points and is utilized to extract terrain parameters. The Shuttle Radar Topographic Mission (SRTM) Digital Elevation Model (DEM) (Farr et al, 2007) and imagery are obtained from a Spatial Data Infrastructure (SDI) for Pakistan (Khan et al., 2012). The base map of the survey lines along with SRTM30 digital elevation model contours is shown in Figure 1.4.

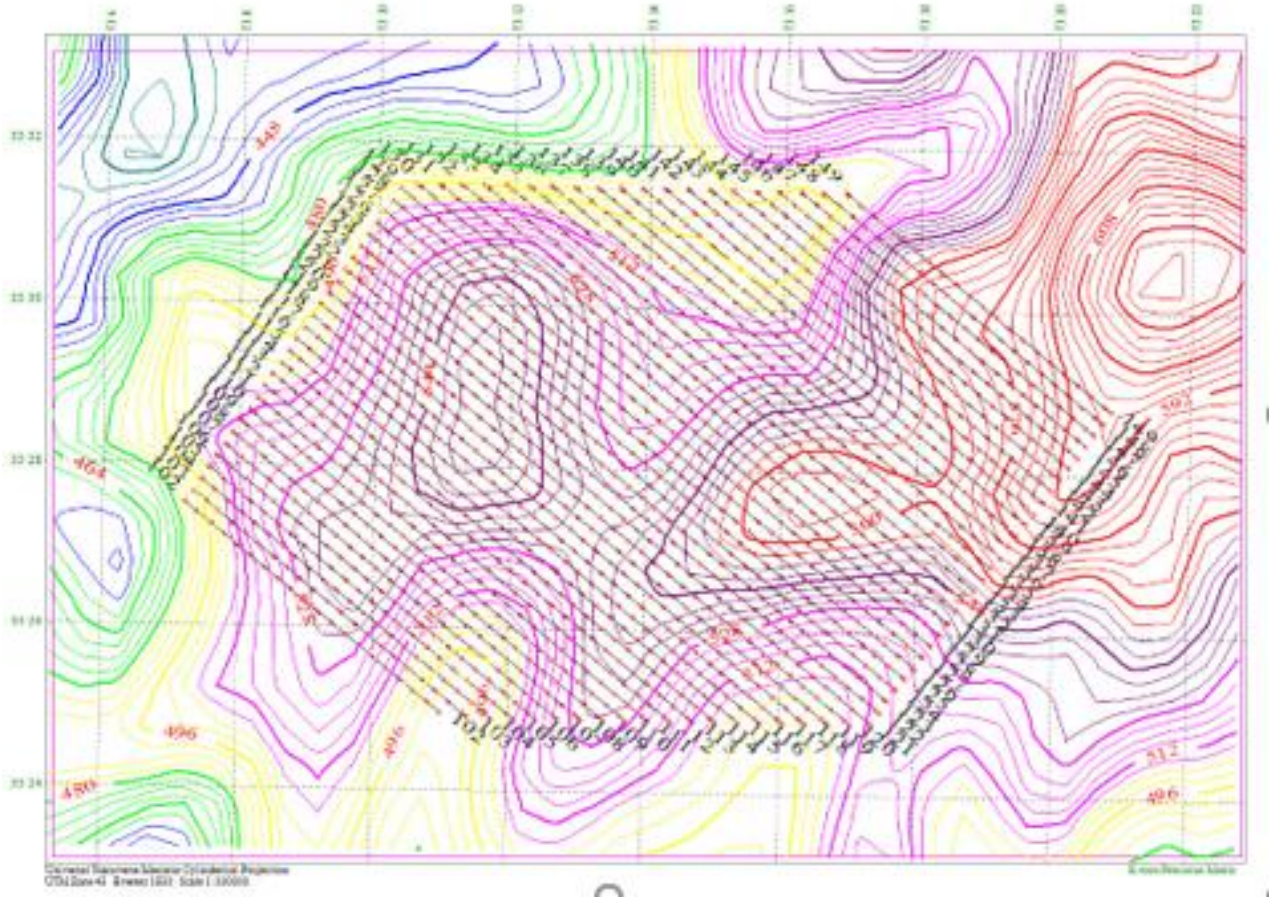

Fig 1.4 SRTM digital elevation model of Study area along with survey grid lines

1.6 Survey data

Survey data is obtained from Senshe Corporation. It includes Seismic Refraction forward-reverse shooting as well as Uphole Logging datasets.

1.6.1 Uphole Logging

In an area of 100 square kilometres, uphole logging has been carried out at 44 points. The circular uphole geometry for the survey is shown in Figure 1.5. The geophone offsets are 1, 2 and 3 meters and the total hole depth is 65 meters with 20 shots per hole.

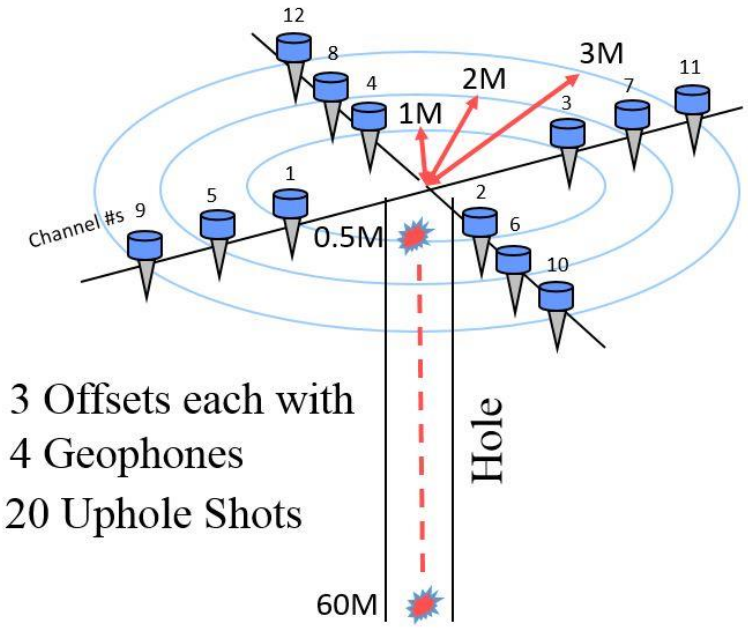

Fig 1.5. Uphole Circular Geometry Layout.

The survey datasets along with their formats are given in Table 1.2 while the uphole parameters are summarized in Table 1.3.

Table 1.2 Data Formats

DATA TYPE	FORMAT
Seismic Refraction Data	SEG-2 Format
Navigation Data	SPS and DBO format
Depth Files	DPT format

Table 1.3 Project Uphole Parameter

Geometry	Circular Shaped
Minimum Offset	1 meter
Maximum Offset	3 meters
Recording Depth	60 meters
Depth of Hole	65 meters
No of Detonators	20
Sample Rate	0.125ms
Record Length	100ms
No of Recorders	12
Source Pickets	44
Geophone	4.5 Hz
Mode of energy	Detonator

1.6.2 Surface Shooting

Surface Shooting was done at 12 Refraction Picket with Forward / Reverse shooting having a spread of 250m and an offset of 12m.

1.7 Software Applications

After obtaining the raw data, the next step is to load and process the data into different software. The software used for various tasks in the thesis work are discussed below.

I. **K-tron Precision Matrix:**

It is a geodetic transformations and GIS Mapping application and therefore used to generate all types of maps.

II. **K-tron SeiRA**:

It is a Seismic Refraction and Uphole Logging software which offers many interactive tools and processing modules, for first break picking, time-distance graphs and statics computation. It works in Integrated GeoSystems (IGS) base environment. S;

- **Autopick**

  Seismic (SEG-2) data is loaded and first breaks are picked and then the arrival times are saved in SeiRA file..

- **Refract**

  The arrival times are used for travel time inversion to generate the time distance (T-X) graph which gives the velocity of the weathered layer (Vo), the velocity of sub weathered layer (V1) and thickness of the weathered layer (ho).

- **Statcalc**

  It interpolates a near surface model using gridding and then computes statics.

III. **K-tron Visual OIL**

OIL (Output Input Language) is a data formatting language (Khan et al., 2010). All engineering and seismicity parameters have been computed using Visual OIL scripts. In addition, it is used to export the Elevation, Velocity & Thickness data from SeiRA to Surfer for gridding and contouring. In addition all

IV. **Golden Software Surfer**

Surfer is the standard gridding and contouring package and therefore it is used to generate contour maps of all parameters computed in the workflow.

Chapter 2

General Geology and Stratigraphy

2.1 Introduction

Geology is the science comprising the study of Earth, including the materials that it is made of, the physical and chemical changes that occur on its surface and in its interior, and the history of the planet and its life forms. Geoscientific research during the past two decades has established Pakistan as one of the most fascinating parts of the globe.

Geology gives imminent into the history of the Earth, as it provides the primary sign for plate tectonics, the evolutionary history of life, and past climates. In present times, geology is commercially important for mineral and hydrocarbon exploration and for evaluating water resources. Geology of an area plays very important role for a precise interpretation of seismic data, because same velocity effects can be generated from formations of different lithology. The information about location of faults, their penetration in subsurface and the presence of unconformities between rocks of different ages is also very essential from interpretation point of view.

2.2 Geology & Tectonic Framework of Pakistan

Pakistan comprises of three main geological subdivisions referred to as Laurasian, Tethyan and Gondwanaland domains. The geography of Pakistan is a profound blend of landscapes varying from plains to deserts, forests, hills, and plateaus ranging from the coastal areas of the Arabian Sea in the south to the mountains of the Karakoram Range in the North. The structural framework is the result of the collision and coalescence of three crustal plates: the Arabian Plate in the southwest, the Eurasian Plate in the northwest and north, and the Indo-Pakistan Plate in the southeast (Kazmi & Jan et al., 1997).

Pakistan has been geologically well-known for several decades for its great mountains, extensive glaciers, devastating earthquakes, exotic and prolific Neogene vertebrate fauna, chromite-bearing ophiolites, Precambrian and Paleozoic succession of the Salt Range, the abundant oroclinal flexures and enigmatic syntaxes in its mountain ranges, and the deep gorges and canyons that

highlight the antecedent drainage. Pakistan covers a land area of 796,096 km2 between the latitudes 24°N to 37°N and the longitudes 61°E to 76°E. Tectonics plays important, rather a basic role in configuration of basins. Tectonics zones of Pakistan are the Eurasian plate, Arabian plate and Indian plate which is part of Indo-Australian plate as shown in Figure 2.1. Pakistan overlaps with Indian and Eurasian tectonic plates. Sindh and Punjab lie on Indian Plate, Balochistan and KPK lie on Eurasian Plate.There is a three point junction of Indian, Eurasian and Arabian plate near Balochistan. The Northern areas and Azad Kashmir lie mainly in Central Asia along the edge of the Indian plate and hence prone to violent earthquakes where the two tectonic plates collide. In Pakistan there are three mountains ranges; Hindukush, Karakorm and Himalaya. Geographically two rivers Hunza and Indus separate them .The ranges in the west of Hunza River are Karakorm Ranges, between Hunza and Indus River (Northwest of Pakistan) are Hindukush Range and in the west of Indus River Himalayas are located.

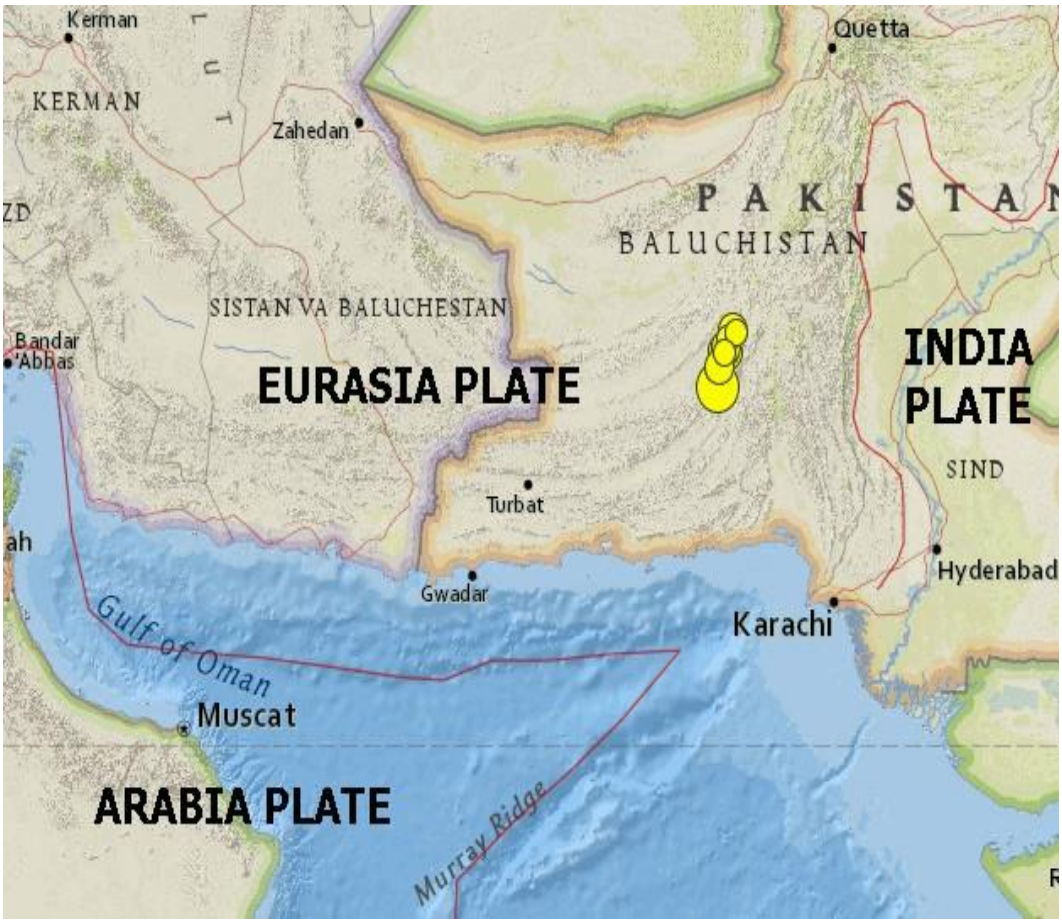

Fig 2.1 Movement of the Indian plate towards Eurasian Plate and formation of Himalaya (Kazmi, et al., 1997).

2.2.1 Tectonic Zones of Pakistan

Based on Plate tectonic features, geological structure, orogenic history (age and nature of deformation, magmatism and metamorphism) and lithofacies, Pakistan has been divided into the following zones i.e.

- Northwest Himalayan fold and thrust belts
- Indus Plate Form and Fore deep
- Kohistan-Ladakh Magmatic Arc
- East Baluchistan Fold and Thrust Belt
- Kakar Khorasan Flysch Basin and Makran Accretionary Zone
- Chagai Magmatic Arc
- Karakoram block

2.3 Sedimentary Basins:

Sedimentary basin is an area in which long term subsidence takes place and sediments are preserved for longer period of time. Sediments originate and transported by several transporting agents. Those sediments which are deposited at the same place where they are generated, are called molasses sediments. Those which rest at the basement of a basin form sedimentary cover. Pakistan is endowed with three major Sedimentary Basins (covering more than 2/3 of its total area) namely, Indus Basin in the East, Baluchistan Basin in the West and Pishin Basin in the North West as shown in Figure 2.2.

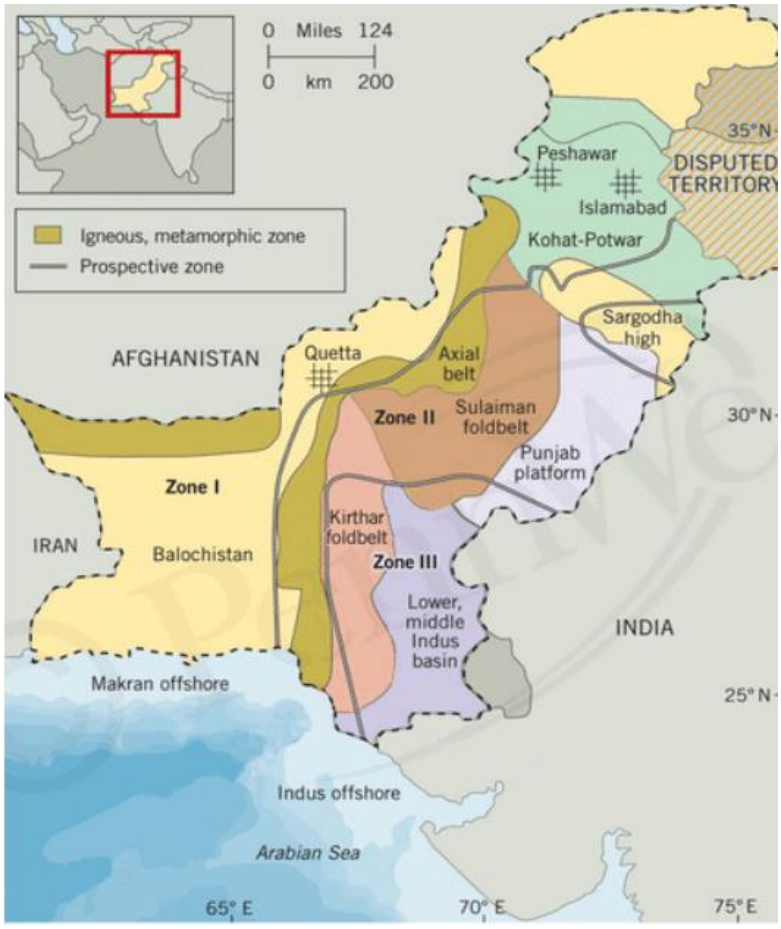

Fig 2.2 Basins of Pakistan

2.3.1 Intoduction to Basins of Pakistan

Indus and Baluchistan Basins are separated by Ornach-Nal transform fault zone and the Pishin Basin lies between Indus and Chamman transform fault. A variety of sub-basins, fold belts and monoclines with variable structural styles resulting from diverse geodynamic conditions have been identified in Baluchistan Basin and Indus Basin. The Indus basin is divided into a number of regimes i.e. compression regime at foreland margins, basement uplift in the Central Indus Basin and extensional regime in the Lower Indus Basin (Kadri, 1995). The Basin and their subdivision include the following:

1. Indus Basin

- Upper Indus Basin

  - ✓ Kohat Sub-Basin
  - ✓ Potwar Sub-Basin

- Lower Indus Basin
    - ✓ Central Indus Basinn
    - ✓ Southern Indus Basin

2. Baluchistan Basin

3. Pishin Basin

2.4 Indus Basin

Indus Basin is the largest and more thoroughly studied basin of Pakistan. The Indus Basin covers an area of about 533,500 km2 and contains more than 15,000 m thick sediments ranging in age from the Precambrian to Recent. It trends NE-SW for over 1600 km along its axis and width varies considerably with an average of 300 km. This basin is characterized by well-developed platform deposits of Jurassic throughout (Shah, 2009). Based on differences in structure, sedimentary facieses development, and chrono-stratigraphic sequences, Indus basin is classified into following basins:

- Upper Indus basin
- Lower Indus basin

The Sargodha High is considered to be the divide between the upper and lower Indus basin.

2.4.1 Upper Indus Basin

Upper Indus basin is located in the Northern Pakistan and is separated from the lower Indus basin by Sargodha high. The northern and eastern boundaries coincide with the main boundary thrust (MBT). The western boundary of basin is marked by an uplift of pre-Eocene sediments and eastward directed thrusting to the west of Bannu. The northern and eastern boundaries‟ coincide with Main Boundary Thrust (MBT). The MBT runs through the Margala Hills, Kala Chitta and Kohat ranges. (Kadri, 1995)**.** The study area, which includes Rawat and adjacent areas is located in Upper Indus Basin.

Upper Indus can be further sub-divided into:

- Kohat sub-basin
- Potwar sub-basin

These sub-basins although not much larger in size, depict important facies. Geographically, study area is located in Potwar Basin. The studied area is a part of the Potwar plateau where the

topography is undulating and characterized by a series of parallel ridges and valleys. Generally, they trend in E-W direction. Geologically it forms part of the foreland zone of the NW Himalayan fold and thrust belt. (Kazmi & Jan, 1997)

2.5 Potwar Sub-Basin

Potwar sub-basin preserves the sediments from Precambrian to Quaternary age in the subsurface and all of these are exposed in the Salt Range, a southern most thrust. The Tran-Indus ranges in south of the Kohat sub-basin expose sediments from Cambria to Pliocene age. Both Kohat and Potwar sub-basin are characterized by an unconformity between Cambrian and Permian. Mesozoic sediments are also exposed around the basin rim. However, this presence is governed by Pre-Paleocene erosion which progressively cut into older sequence from the Trans-Indus Ranges in the west to east Potwar through Salt Range.

- ***Geological boundaries***

The Potwar is a Fore-land fold and Thrust belt of Himalaya Orogeny that surrounded by Kalachitta ranges and Margala Hills to the North, the Indus River and Kohat Plateau to the West, the Jhelum River and the Hazara-Kashmir syntaxes to the East and Salt Range formation in the South. It is covered by the Siwalik sequence in large scale, although at some places upper Eocene shales and limestone's locally in folded outliers. The Soan syncline divides the Potwar Basin into two major zones as Northern Potwar Deformed Zone (NPDZ) and Southern Potwar Platform Zone (khawar, et al., 2012). It is characterized by a series of parallel ridges and valleys, generally trend in the E-W direction. Geologically, it forms part of the foreland zone of the NW Himalayan Fold-and-Thrust belt. Structurally Potwar Basin is divided into North Potwar Deform Zone (NPDZ) in the north, Soan Syncline and Southern Potwar Deformed Zone (SPDZ) in the south.

2.5.1 Structural style of Potwar Basin

The structural style of the central eastern and western parts of Potwar Plateau shows a marked difference. In the central western parts of Potwar Plateau, the deformation appears to have occurred by south-verging thrusting, whereas in the eastern part the deformation is mainly in northeast-southwest direction with tight and occasionally overturned anticlines separated by broad synclines. This difference may be related to lesser amount/thickness of salt in the lnfra-Cambrian in the eastern areas and very low dip of the basement (1°-1.5°) as compared to Central Potwar (20-30). The structure trend in the East-Potwar is long (NE-SW), continues and consisting of salt-cored

anticlines separated by broad synclines. Seismic, gravity and drill-hole data showed that, Potwar underlies a gently north dipping basement (1 -4 degree). (Kazmi & Jan, 1997). Structural style of Potwar Plateau is shown in Figure 2.3.

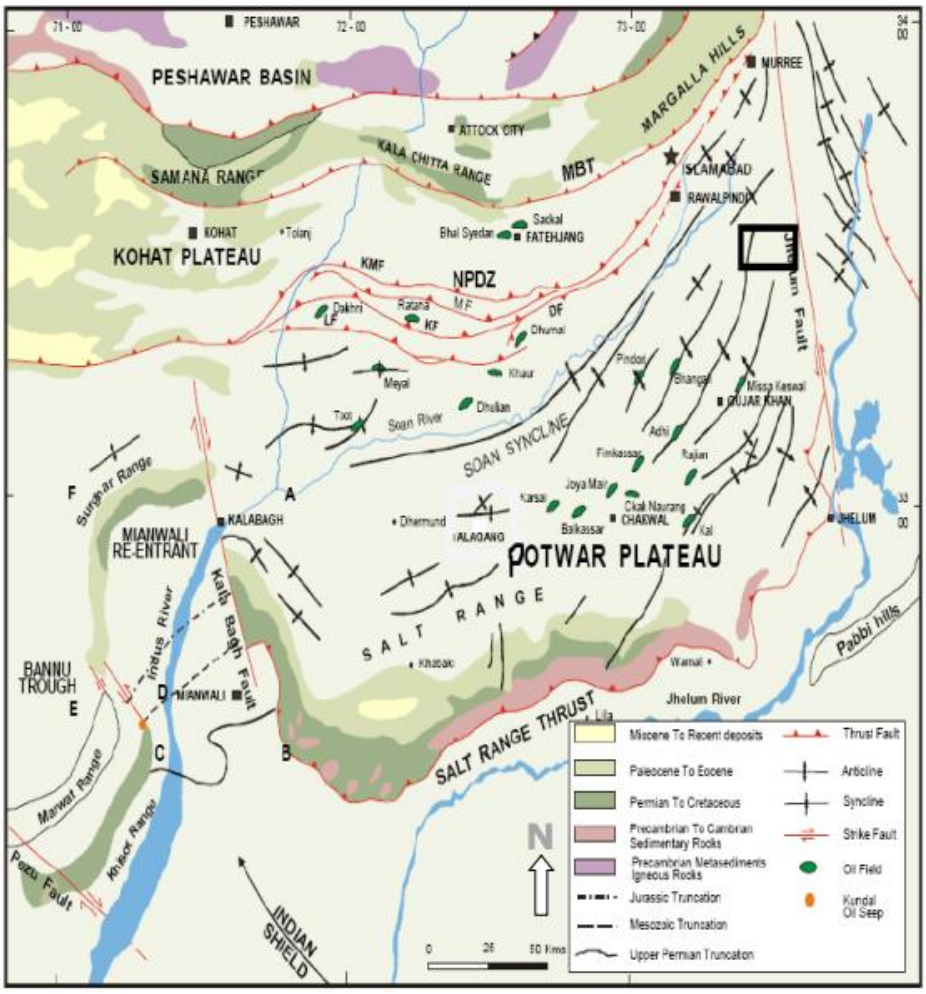

Fig 2.3 Geological and Structural map of Potwar Plateau (William, et al.,1998)

Major anticlinal and synclinal features are bounded by major thrusts and back thrusts trending almost E-W in the northern part, while in the eastern part fault trend is almost NE-SW. Based on the seismic interpretation, the structures in the Potwar area may be divided into:

- Pop-up anticlines
- Snake-head anticlines
- Salt cored anticlines
- Triangle zone. (Jadoon, et al., 1999)

Presence of different decollement levels has resulted in offset of the subsurface structures from their surface appearance. The main decollement level at the interface of platform deposits and evaporite sequence relates to the Pre-Cambrian salt particularly in the Salt Range an Southern Potwar. In eastern part, most of the deformation appear to have shifted toward shallower inter-molasse decollement horions due to progressive thinning of the salt layers. There may be some other local decollement level within under-compacted Neogene molasse sediments near the top of Kamlial Formation. During the Eocene to Oligocene, the creation of Himalayan mountain chain due to crustal thickening and loading from the north and west and terrestrial forland basin sedimentation in the Kohat-Potwar Fold belt. Cenozoic to recent sedimentation in these basins were punctuated by periods of uplift and erosion and the development of minor unconformities. It was during the Cenozoic that most traps were formed, as a series of large amplitude fold developed. Thrusting and Folding with associated terrestrial sedimentation continue to the present day as show in Figure 2.4.

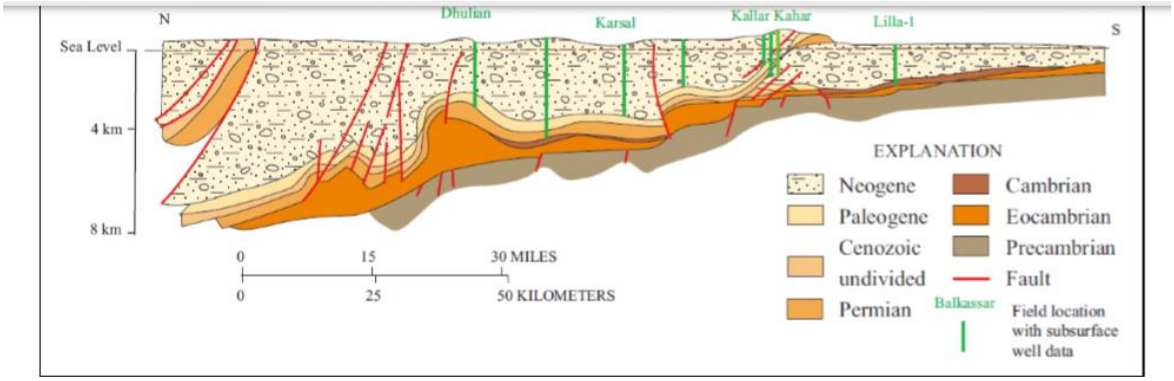

Fig 2.4 Thrusting and Foldimg with associated terrestrial sedimentation continue to the present day (Shah et al., 1977).

2.5.2 Tectonics of Potwar Basin

Tectonic history of basin is associated with plate movement that occurred from latest Paleozoic to the present. From Permian through middle Jurassic time, the Indian plate was located in the Southern Hemisphere -between the Africa, Antarctic and the Australian plates-and comprised part of southern Gondwana (USGS Bulletin). During early Cretaceous time, the Indian plate drift northward, entering warmer lattitudes. During the latest Cretaceous, the Indian plate continued to drift northward toward the Eurasian plate and seafloor of Bengal Basin began to form and flysch accumulated on all sides of the Indian plate. Northward plate movement continued

during the late Cretaceous, and a transform fault became active along the Ninety-East Ridge. From the late Cretaceous through middle Paleocene, trap deposits and basal sands continued to accumulate on the western, northern, and easrtern shelves of Indian plate. In the

Kohat-Potwar geologic province shallow northeast-trending anticlines and overturned folds developed above multiple detachment surfaces on the late Miocene. Today, uplift of the Himalyas and subduction of the Indian plate continues, and the growth rate of indus deltas remain high. In the Kohat-Potwar area crustal shortening also continues (USGS Bulletin). Tectonic in the Potwar is thin skin tectonic without significance involvement of basement.

2.5.3 Major Faults in Potwar Basin

Potwar represents the southern margin of Himalayan collisional zone, a variety of faults and folds can be seen in the area. Some of the major faults in the area are described below:

Riwat Fault (RF)

Riwat Fault (RF) is a passive roof thrust in the south of Soan syncline in the eastern Potwar plateau, and is hinterland dipping fault rather than foreland. At its southward terminus, the Riwat Fault dies along the southern flank of Chakbeli khan anticline and to the northeast it dies to the Soan syncline axis (Dobrin et al,. 1998).

Kanet Fault (KF)

Kanet Fault (KF) is a north dipping emergent thrust in the western part of the NPDZ, developed in the direction of tectonic transport, and in the eastern part of the NPDZ. It is underthrusted beneath the DBT. KF bound the Kanet syncline from the north (Jaswal, et al., 1997).

Mianwali Fault (MF)

Mianwali Fault is a high angle intraformational thrust at the surface that can be traced only in streams where good water exposure is present, on the basis of shear zones, fault breccia and secondary calcite. The rocks having steep dips are present in the area between MF and KMF and represent northern most exposure of Siwaliks (Jaswal, et al., 1997).

Dhurnal Back-thrust (DBT)

DBT (Dhurnal Back Fault) is a different fault due to different movement. DBT had been considered as the eastward extension of the Kanet Fault (KF). It joins the KF west of Dhurnal

and diverts towards the southwest, gradually dying out at the surface. Jadoon explained steep DBT becomes shallower to the south which dies out at a depth of 2 to 4 km (Jadoon, et al., 1995)

Sakhwal Fault (SF)

Sakhwal Fault is a north-northeast trending back thrust which merges into the south-verging Ahmadal fault in the south of the Nauthian and dies out in the Chinji Formation in the north of Sakhwal, is an overstep, passive roof thrust, developed in the roof sequence of Dhurnal backthrust. It cuts the surface just north of Dhurnal. (Palmer et,al, 1980)

Khair-i-Murat Fault (KMF)

Khair-i-Murat Fault is a north-dipping major emergent thrust in the NPDZ along which high velocity Eocene carbonates are thrusted southward over low velocity molasses. Due to back rotation, fault having steep dips at the surface and contains highly faulted of Murree Formation to its north where most of the area is covered with alluvium (Jaswal, et al., 1997).

2.5.4 Major Folds in the Potwar Sub-Basin

Joya-Mir Anticline

Joya-Mir Anticline is a doubly plunging anticline and plunges at 10° southwest and 4° northeast. The fold axis of anticline trends northeast-southwest and is cross-folded to form northeast-southwest trending Joya Mair antiformal syncline. The geologic, structural, seismic and borehole data shows that the Joya Mair structure is a triangle zone in the subsurface & lies in the Southern Potwar Platform zone and is segmented along left-lateral Vairo and Dhab Kalan Fault. The triangle zone is the result of southeast and northwest directed Himalayan thrusting. These faults are steeper and listric respectively. (Shami and Baig, 2002).

Mahesian Anticline

Mahesian anticline exposes Chinji Formation in its core. The fold is cut by two small faults, neither of which show surface displacement of more than a few meters. The southern end of the fold has an overturned limb (600-750) and a moderately dipping western limb (30°-40°) (Pennock et al., 1989).

Dhurnal Anticline

Dhurnal Anticline is a thrust formed anticline in a triangle zone hidden under an adjacent, foreland syncline. The surface expression is an east-trending monocline, which forms the northern limbs of the Soan Syncline. At Eocene level the Dhurnal structure is an east-northeast-

trending popup structure bounded by forward and backward thrusts. This is also the largest producing oil field in Pakistan (Jaswal, et al., 1997).

Adhi-Gungril Anticline

Adhi-Gungril Anticlines are relatively symmetrical structures. Seismic reflection data indicates the Adhi-Gungril structure is a popup bounded by reverse faults to the northwest and southeast. Adhi-5 well confirms the presence of the thick salt in the core thins to nearly zero in its adjacent syncline (Pennock et al.,1989).

Soan Syncline

Soan Syncline is a broad, wide and asymmetrical that divides the Potwar plateau into Northern Potwar deformed zone (NPDZ) and Southern Potwar deformed zone (SPDZ). Soan River marks its axis & developed at 2.1 to 1.8 Ma (Shaami and Baig, 2002). The area north of Soan Syncline is characterized by horizontal shortening and imbricate thrust faulting (Jaswal, et al., 1997).

Chak Naurang Anticline

Chak Naurang has two dipping limbs. These limbs are namely, southern limb which is dipping steeply while northern limb dipping moderately. Anticline is an example a fault-propagated fold. A strong northward-dipping basement reflector is there which is overlain by thick evaporite strata (Mari, et al., 1999).

2.5.5 Stratigraphy of Potwar Basin

The Stratigraphy of the Salt Range and Potwar Plateau is well established from outcrops in the Salt Range. The structural and stratigraphic study includes the out crop the formations at different places and the oil and water wells drilled in the area's the Salt Range-Potwar Foreland Basin. The oldest Formation of the cover sequence known to lie at the top of basement is the Cambrian Salt Range Formation which is available as outcrop and at many places it is also in the subsurface which is confirmed from the well log data. (Khawar, et al.,2012) The stratigraphy in the NPDZ is not that well constrained due to lack of deep drilling. Surface outcrops along the MBT and seismic profile, however, suggest the stratigraphy of NPDZ is similar to that of the Salt Rang and Potwar Plateau. Stratigraphic succession of the Potwar Basin is characterized by thick Infra-Cambrian evaporite deposits overlain by relatively thin stratigraphic succession of the Eocene to Cambrian. Thick Miocene-Pliocene molasses deposits are related to severe deformation in Late Pliocene to Middle Pleistocene (During Himalayan orogeny). Formations, age, and lithology is

given in Figure 2.5. The lithological formations are lying uncomfortably over Paleozoic formation, and the whole Mesozoic section is absent in and around the area which is the sign of unconformity. The Sakesar limestone and Chorgali Formations of Eocene age are the primary reservoir of this while Permian and Cambrian sandstones are secondary targets. The Eocene, Paleocene and Permian shales are supposed to be the potential source of oil and gas and cap rocks. (Khawar, et al., 2012). The rocks of Miocene-Pliocene age which are known as Nagri Formation and Chinji Formations are exposed in the core of the structure. Here thrust tectonics plays important role. (Kazmi, et al., 1982).

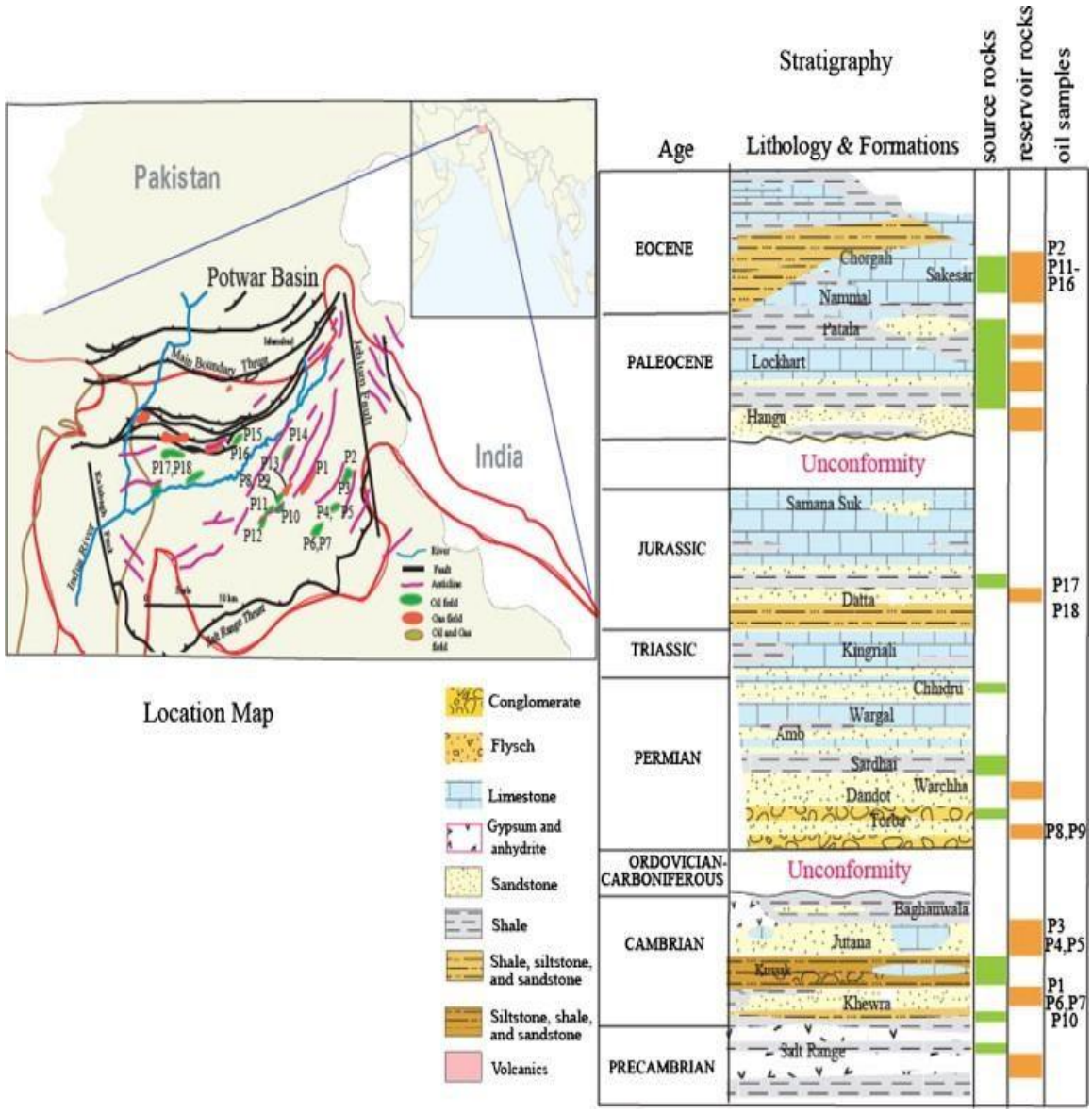

Fig 2.5 Genral Stratigraphy of Potwar Sub-Basin (Khawar, et al., 2012)

2.6 Geology & Sturctural Setting of Study Area

The Adhi Field area is part of the Himalayan fold and thrust belt, and is situated in a broad deformational zone, dominated by folding. The fold axis mostly trends in a north-east to south-west orientation in an En-echelon pattern. The anticlines in the area tend to be tightly compressed and separated by broad, open synclines. The Adhi Field structure, an anticline, broken by several longitudinal faults, is well expressed on surface outcrop.

The Kohat-Potwar province consists of a portion of the Indian plate structurally deformed by plate collision and overthrust of the Himalayas on the north and northwest. Important structural features include a series of faulted and un-faulted anticlines developed on multiple detachment surfaces as deep as Cambrian in age and thrust faults that trend generally southwest-northeast parallel to the plate-collision boundary.

2.7 Tectonic Setting & Stratigraphy of Study Area

From Permian through Middle Jurassic time, the Indian plate was located in the Southern Hemisphere between the Africa, Antarctic and the Australian plates-and comprised part of southern Gondwana. The area that is now the Indus Basin, Kohat Potwar geologic province, and the northern india, was a shallow continental shelf on which carbonates, shales, and sandstones were deposited. During the Late Jurassic,, Madagascar, India, Australia, Antarctica, and the Seychelles began to break away from Africa. Late Jurrasic rifting also initiated separation of Australia an Antarctica from india.

During early Cretaceous time, the Indian plate drift northward, entering warmer lattitudes. Along the eastern portion of Indian plate, the Rajmahal Trap volcanics were deposited. On the northwest margin of the plate, marine shales and limestones of the Lower Cretaceous Sembar and Goru Formations were deposited over a regional erosional surface on the Sulaiman Group. In Kohatg-Potwar area, this erosional surface is present at the top of the Samana Suk Formation and is overlain by sandstones and shales of the Lower Cretaceous Chichali Formation

Today, uplift of the Himalayas and subduction of the Indian plate continues, with crustal shortening continuing in the Kohat-Potwar area.

2.8 Petroleum Play of Potwar

Potwar marine facies has great potential of hydrocarbon. Previous drilling was restricted up to Eocene carbonate. Recent discoveries in Potwar result in delineation of deep subsurface crest. Potwar region which is traditional oil producing area of Pakistan has the average geo-thermal gradient of the order of 20C per 100 meters. Hence the oil window lies between 2750-5200 meters. (Kadri, 1995).

2.8.1 Source rocks

Different studies suggest that organic risch formation of Patala Formation of Paleocene age is major souce rock and charge most of the Potwar fields. Patala Formation is well developed in the area having good TOC and lies in the maturity zone. Tertiary Carbonates, shales of Jurassic age and shale of Salt Range Formation also contributing as source rocks. Paleocene sediments show oil and gas potential in Kohat-Potwar basin. TOC in Paleocene (Patala) source ranges up to 10.73% with good hydrocarbon potential. The coal and coaly shales in Patala Formation also exhibits good source potential (Government of Pakistan, 2010). The gray shales of the Mianwali (Triassic age), Datta (Jurassaic age) and Patala Formations (Paleocene age) are potential source rocks in Salt Range Potwar- Foreland Basin (SRPFB) (Khan et al, 1986).

2.8.2 Reservior rocks

Data formation is producing fromChanda and Markori Field in the west and Dhulian, Meyal & Toot Field in the east. The Cambrian, Permian, Jurassic, Paleocene and Eocene reservoirs are producing oil in Salt Range Potwar- Foreland Basin (SRPFB).Petroleum play reservoirs ranging in age from Infra-Cambrian to Miocene are present in the Kohat-Potwar fold belt. The target reservoirs are clastics and carbonates of Infra-Cambrian, Lower Cambrian, Clastic of Permian, clastics of lower to middle Jurassic, clastic of lower Cretaceous, carbonates of upper Paleocene and lower Eocene and clastics of Miocene. (Government of Pakistan, 2010). On Kohat-Potwar plateau oil and gas has been produced from the following formations (Khan, et al., 1986):

- Cambrian (i) Khewra Sandstone (ii) Kussak (iii) Jutana
- Permian (i) Tobra (ii) Amb (iii) Wargal
- Jurassic (i) Datta
- Cretaceous (i) Lumshiwal

- Paleocene (i) Khairabad (ii) Lockhart (iii) Patiala (iv) Nammal
- Eocene (i) Bhadrar (ii) Chorgali (iii) Margalla hill limestone
- Miocene (i) Murree Formation Production of more than one

2.9 Traps & Seals

Intraformational shale of different formations are acting cap rocks in the area of Potwar. However proven cap rock is shale/marl of Kuldana Formation in the Potwar area. Most of the fields discovered in Kohat-Potwar geological province to date are either due to overturned faulted anticlines, popup structures or fault-block traps. The latest trap-forming thrust event began at approximately 5 to 2 Ma (Jaswal, et al., 1997). Seals include fault truncations and interbedded shales and the thick shales and clays of the Miocene and Pliocene Siwalik group (C.J., et al., 2004). Thick layers of evaporite and shale have good sealing potential for Infra-Cambrian reservoir. Interbedded shale, mudstone and siltstone provide seal to Cambrian reservoirs. Limetones and intraformational shales are the potential seals for the Cenozoic and Mesozoic reservoirs. Paleocene shales (Patiala Formation) and Miocene shale are the regional seals in the area (Government of Pakistan, 2010).

Chapter 3

Seismic Refraction Processing & Interpretation

Seismic refraction is one of our most powerful methods for detecting subsurface structure. The seismic refraction surveying method uses seismic energy that returns to the surface after travelling through the ground along refracted ray paths. In seismic refraction techniques, we need to pick the first breaks times from the seismic traces. The first arrival of seismic energy at a detector offset from a seismic source always represents either a direct ray or a refracted ray. The picked first break arrival times, for both forward and reverse shooting, are plotted on a graph paper against their offsets and best-fit lines are passed through each segment of data, for both forward and reverse side, representing a subsurface layer. The method is normally used to locate refracting interfaces (refractors) separating layers of different seismic velocity, but the method is also applicable in cases where velocity varies smoothly as a function of depth or laterally. (Kearey et al, 2002). Then methods is used in near surface engineering applications and computation of Statics corrections for seismic reflection processing.

3.1 Introduction

Seismic data processing is the next step in seismic prospecting after acquisition i.e. to remove the noise, improve signal quality and thus improve signal to noise ratio and to apply all the required corrections so that we may be able to get a clear, error free picture of subsurface in order to get better results to make an easy way-out for interpretation. The interpretation thus defines our next step i.e. the best possible interpretation can be done only if the data is processed by using highly advance set of software's with the combination of intelligent human decisions. The better interpretation the better the results.

The software used for processing in my thesis work are:

- K-tron Visual OIL Version 2.10
- K-tron SeiRA Version 4.30.
- K-tron Precision matrix Version 4.10.
- Golden Software Surfer 8

3.2 Seismic Refraction Data Processing

Base map was being generated by using K-tron Precision Matrix an IGS base environment application (Khan, 2000) and contouring was done by using Visual OIL (Khan et al., 2010) and Surfer. The main Seismic Refraction processing and interpretation is carried out using in SeiRA.

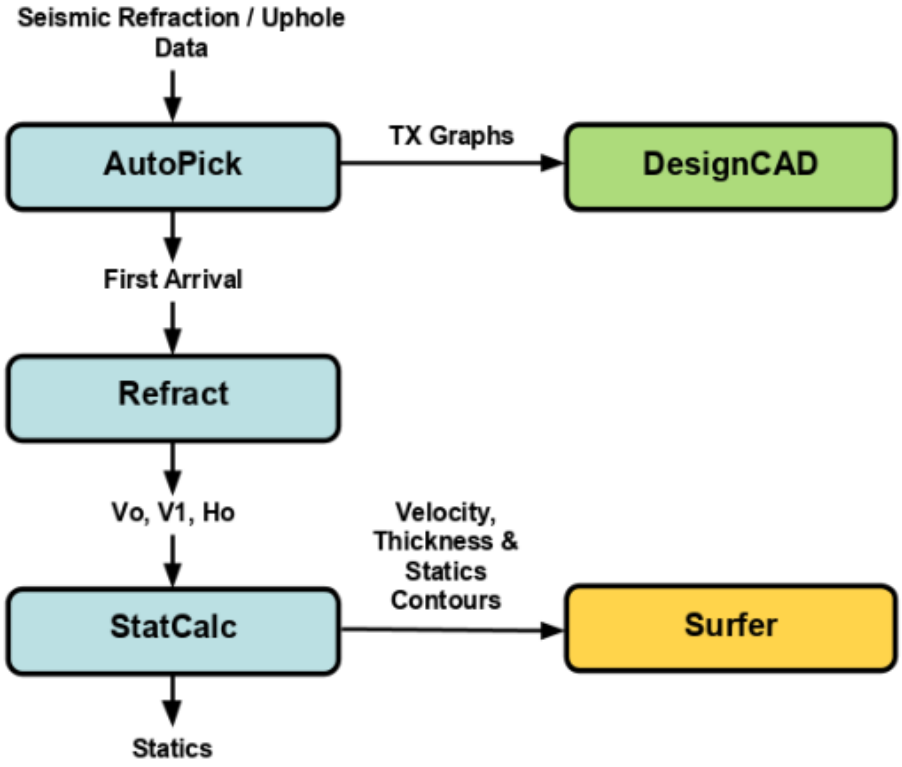

Fig 3.1. Flow chart of processing of refraction data.

3.3 Visual OIL (Output Input Language)

K-tron Visual OIL is a formatting engine along with a scripting language (Khan et al., 2010).. Visual OIL scripts are used to convert navigation data into DBO format. In addition, OIL scripts are used to invert Velocity into rock physics parameters for computing engineering and seismicity properties.

Visual OIL has a number of classes based on data types. For velocity inversion the “weathered layer data” class is used as shown in Figure 3.2.

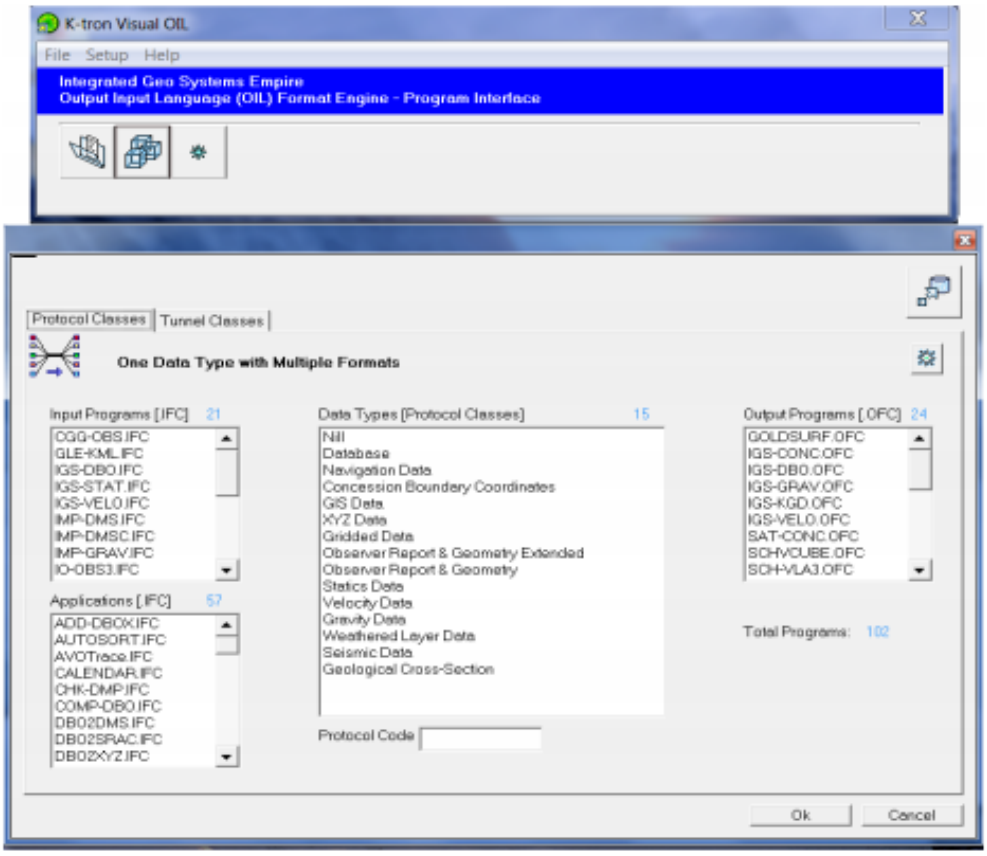

Fig 3.2. Data Type Classes in K-tron Visual OIL

3.4 Seismic Refraction Software

K-tron SeiRA comprises of three modules used for first break picking, travel time inversion and computation of statics. The three modules are listed below:

- SeiRA AutoPick
- SeiRA Refract
- SeiRA StatCalc

3.5 First Break Picking Software

First break picking was done by SeiRA AutoPick software, which has an Artificial intelligence based automated first break picking module. It reads seismic data in industry standard SEG-2 format, automatically picks arrival times and saves them in SeiRA data files [. SRA]. If required the use can QC and correct the mispicks.The seismic data can be viewed on the screen and several interactive QC and manual picking tools can be applied. The processing modules, including auto-

picking algorithms which can be applied to the seismic data. AutoPick also has a Job Engine through which a job sequence comprising of more than one processing module can be created and applied on the seismic data in a single step. SeiRA requires the following input files to process the data.

- Navigation files (DBO format)
- Depth files (DPT format)
- Offsets files (OFS format)
- Seismic data files (SG2 format)

3.5.1 Project Manager

Project Manager is specially designed to manage and process statics for large 2D/3D seismic surveys. A Project Manager is a system that registers all datasets involved in the project; all setup parameters and jobs used in the processing of data and keeps track of the current processing status of the project. Figure 3.3 shows that Project Manager along with GIS & Data Explorer.

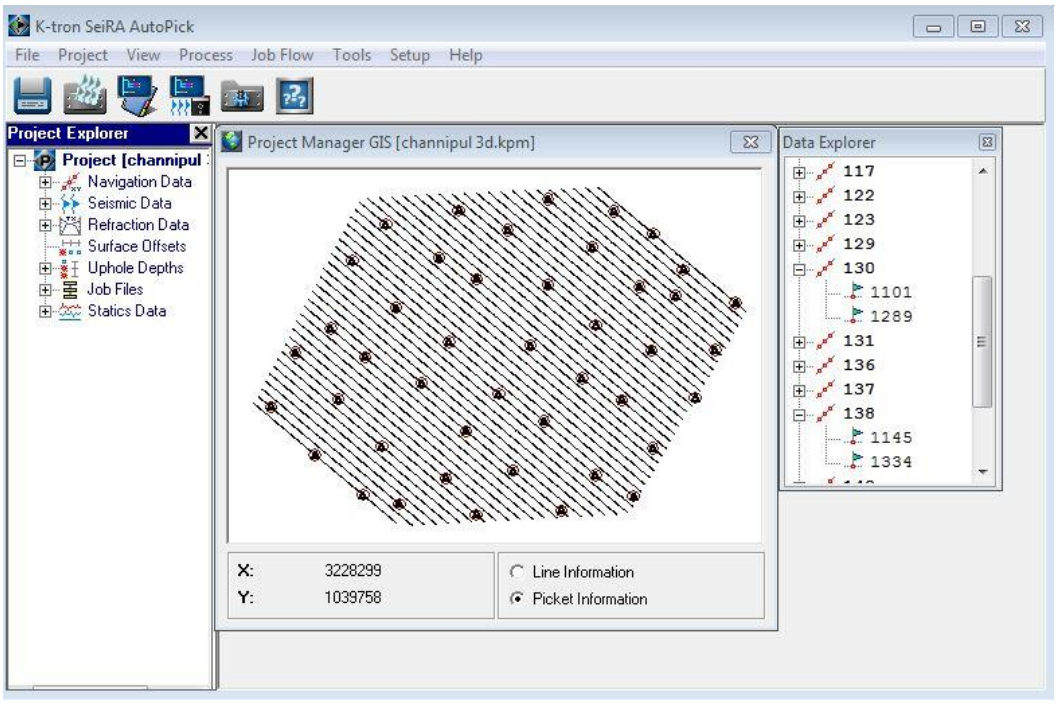

Fig 3.3. Project Manager with Project GIS Interface displaying the Map and Data Explorer with the list of lines ad their Refraction Pickets.

The Project Manager stores all information in a project database [.KPM]. Loading a KPM file would provide access to all datasets involved in the project. The Project Manager with Project GIS interface displays a project map, all seismic lines, in the project, are displayed along with the refraction survey pickets (Refraction Points). Autopick uses the Project Manager to manage hundreds of files in the project.

3.5.2 Loading of Seismic Data

Seismic refraction data is loaded using manual option as shown in Figure 3.4a:

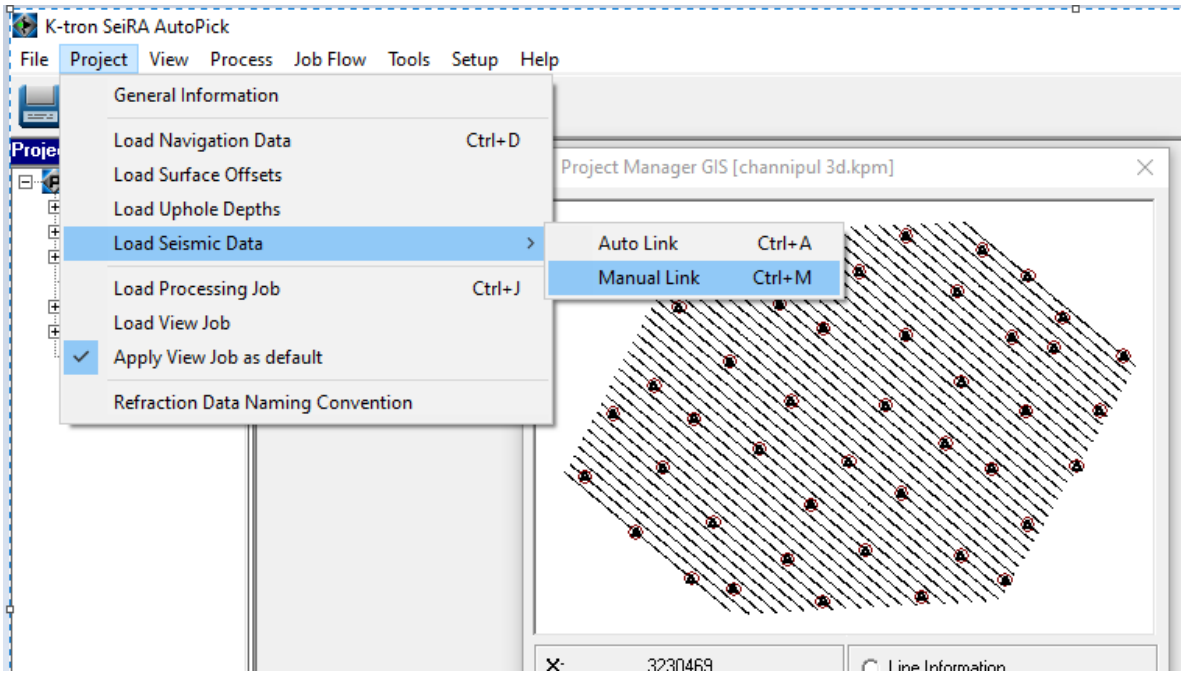

Fig 3.4(a). Loading of Seismic Data using the Manual Option.

Figure 3.4b shows Manual Data loading interface with Uphole files loading corresponding to their line and picket names and trace trace selection.

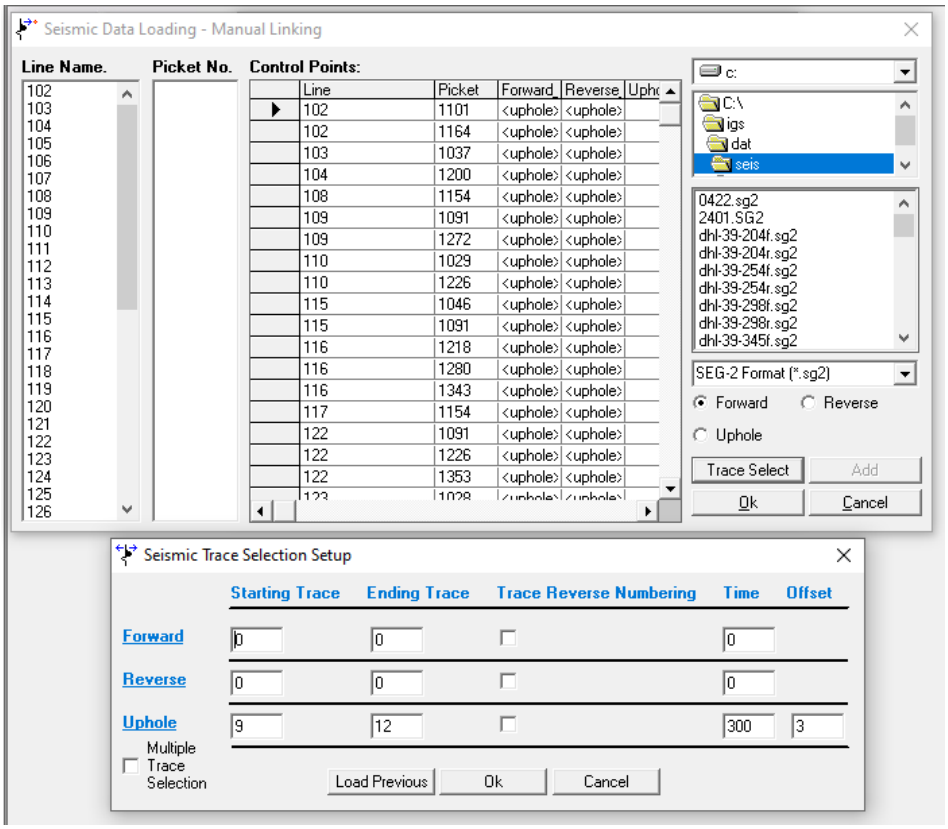

Fig 3.4(b). Trace selection setup and uphole files with their line and picket name.

3.5.3 Job Based Seismic Processing

Jobs are basically multistep processing tasks applied to seismic data. The job can be created by selecting several processing modules as shown in 3.5a. All the processing modules have their own parameters which needs to be adjusted according to the requirement. The setup parameters for the processing modules are shown in 3.5b & 3.5c

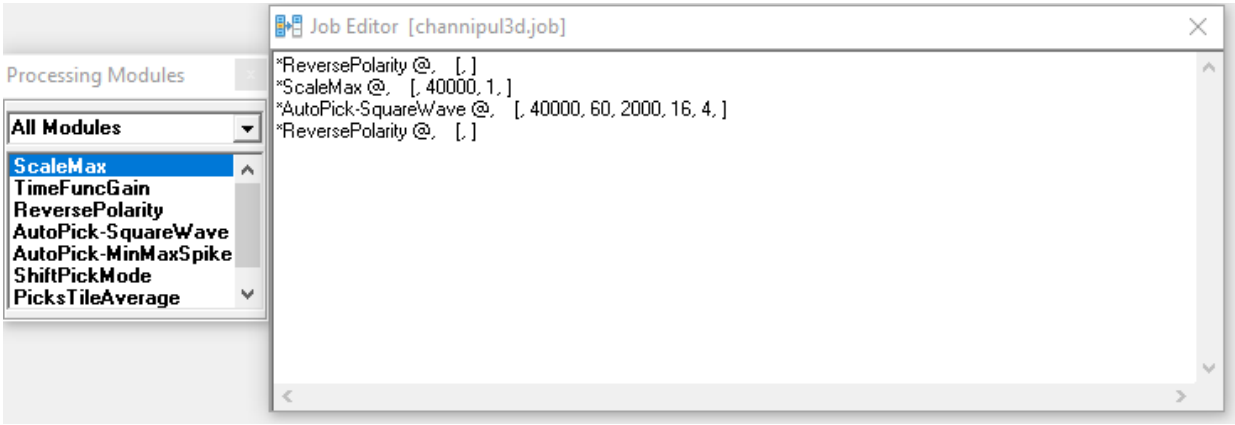

Fig 3.5(a). Processing Modules & job editor

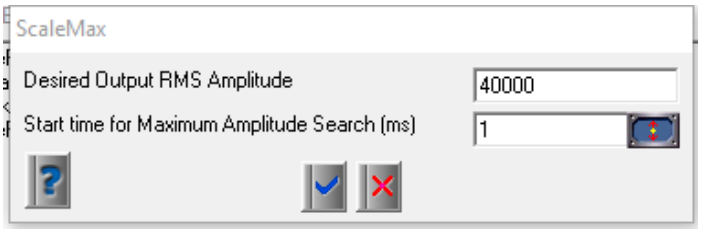

Fig 3.5(b). Parameter of scale max

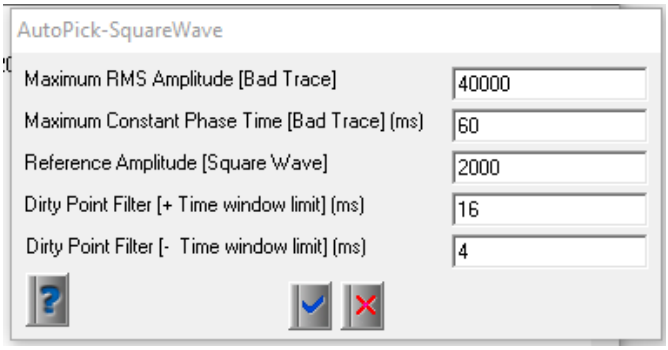

Fig 3.5(c). Parameter of AutoPick-SquareWave

- **Job Files:**

The following two processing steps have been applied to the seismic data by the job:

- ScaleMax
- AutoPick-SquareWave

The software has automated neural network based automated first break picking as well as interactive manual picking tools. If neural network is not able to pick first correctly, the user has a full range of interactive tools through which first breaks can been interactively modified. Fig 3.6 shows interactive tools and processing modules.

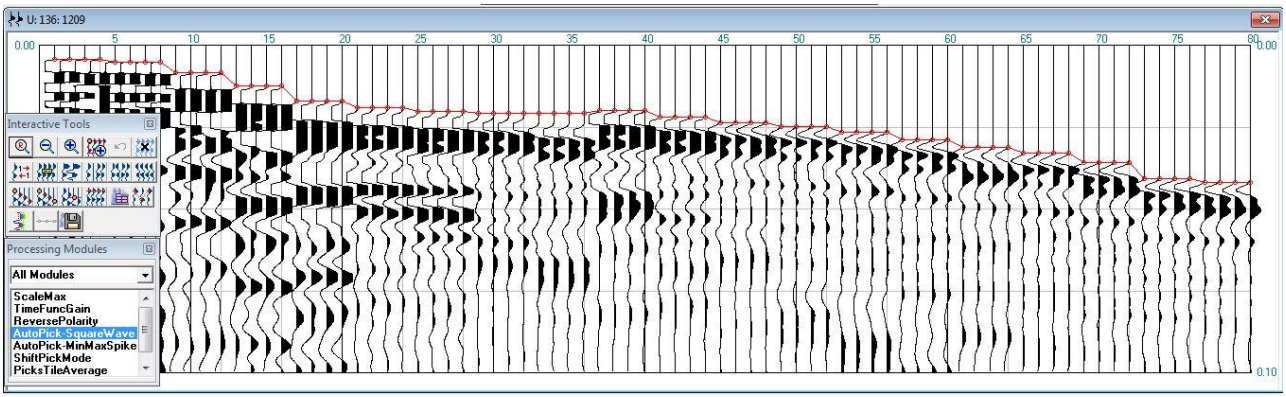

Fig 3.6. Automated Picking along with Processing Modules and Interactive Tools

3.5.3.1 ScaleMax

In order to apply the Auto Picking module, we must balance the amplitudes from near to far offset traces. Usually the near offset traces have very high amplitudes as compared to far offset traces. The Scale Max Gain will balance the amplitudes of all near to far offset traces. An example from Rawat project is given. Figure 3.7a shows the amplitude decay with offset. Fig-3.7b shows the adjustment of traces after applying ScaleMax.

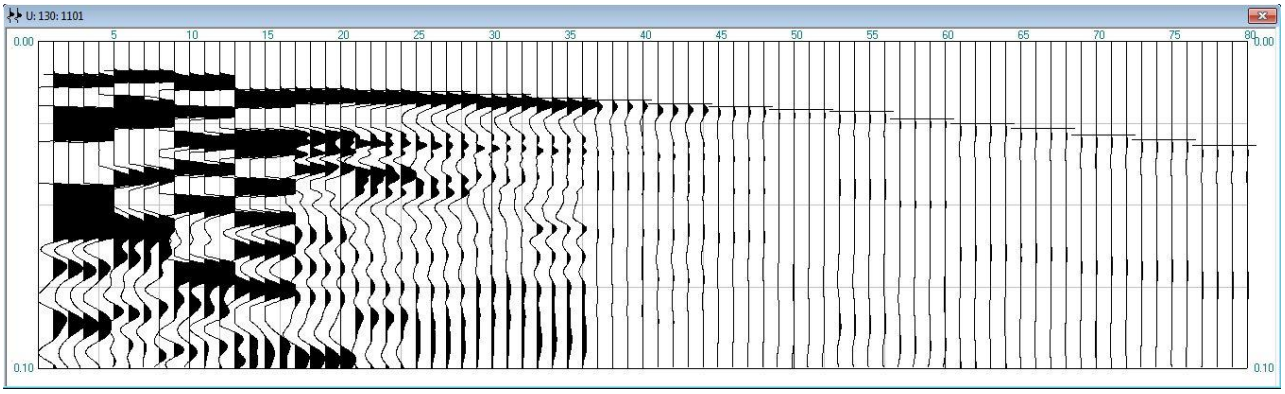

Fig 3.7(a). Amplitude decay with offset before ScaleMax.

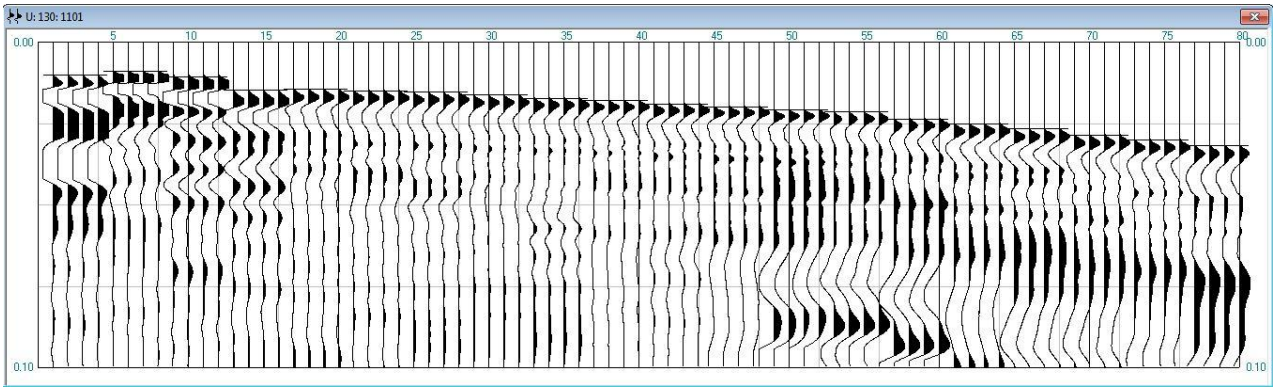

Fig 3.7(b). Trace balancing after appling ScaleMax

3.5.3.2 AutoPick-SquareWave

This is the processing module which automatically picks the First breaks. It is completely automated two step first break picking method. The first step picks the first breaks, while the second step acts as a quality control stage to validate the picked times and refine them if necessary (Khan 2007). The picking algorithm is shown in Figure 3.8.

Steps involved in Auto Picking are:

1 A time invariant gain is applied to the input seismic traces by scaling their maximum amplitudes to the desired RMS amplitude Arms. Each trace is scanned to get its maximum amplitude Amax.

$$Ascale = 1.414Arms\ (Ai/Amax)$$

For reflection records an optional time variant exponential gain, sandwiched between the above-mentioned scaling gains, is also applied.

2 After this initial preprocessing of traces, the data is input to the main step for automatic first break picking. Internally this step consists of several stages.

- Each trace is scanned to get the time of its maximum amplitude sample. A linear regression trend through these times helps in identification of the near offset.
- Near offset trace is used as pilot trace for starting the first break picking.
- Bad traces are identified by analyzing all the input traces.
- Trace to trace tracking is done. If the picked first breaks contain mispicks they are refined through the automated quality control step. This step also has several internal stages.
- Spike search window is created for each trace around its first break.
- Trace is scanned to get maximum and minimum amplitudes thus reducing trace in to spikes.
- To get relative change in spike amplitude from its preceding spikes, the ratio of spike amplitude Ai to the average of all preceding spikes Ak of the same polarity is computed by

$$AR_i = \frac{A_i}{\sum_{k=1}^{i-1} A_k /(i-1)}$$

- Similarly, the spike amplitude ratio is also computed for all negative spikes. To further differentiate the first break from preceding noise the energy of its side lobes is also included by adding the absolute *Ari* of the preceding and following negative spikes to twice the *Ari* of the positive spike as given by

$$AE_i = \left| -AR_{i-1} \right| + 2AR_i + \left| -AR_{i+1} \right|$$

- These enhanced spike amplitudes *Aei* are sorted according to their magnitude and the largest four are selected.

Once the final first breaks have been picked, they are shifted to one of the desired pick modes; crest, trough, zero crossing positive slope or zero-crossing negative slope.

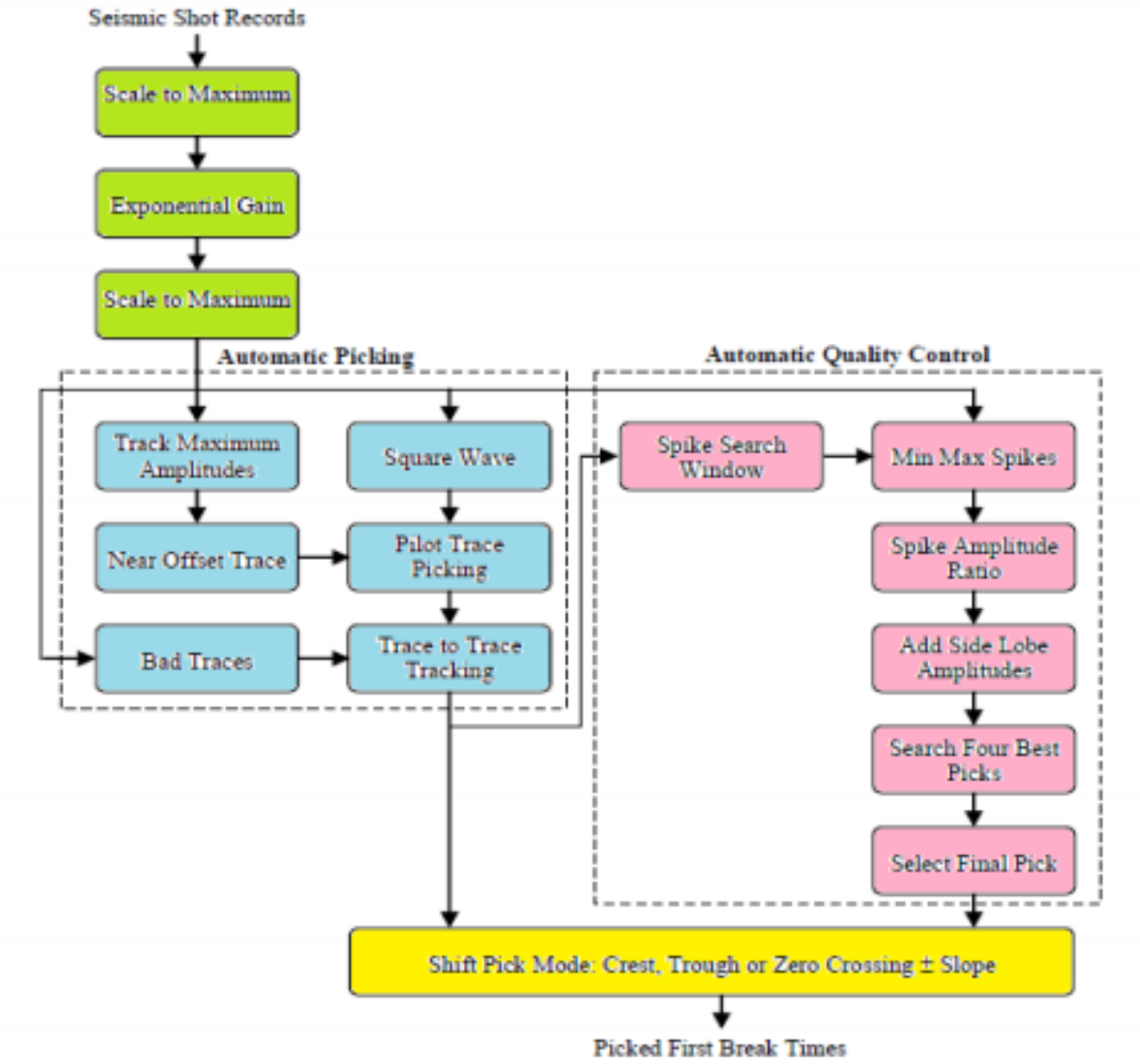

Fig 3.8 . Processing Flowchart of the Automated First Break Picking and Quality Control Method. (Khan, 2007).

3.6 Full Project Processing

Project processing has been done in a systematic way; whole project is set for first break picking alog with processing job.

Full project processing can be done in two ways (Fig 3.9).

3 Job based background processing.

4 Job based automatic and interactive processing.

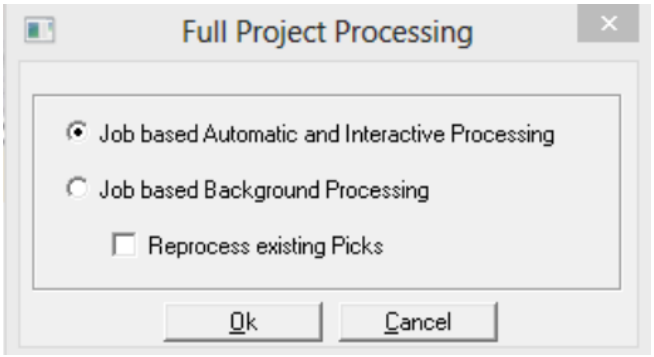

Fig 3.9. Modes of Processing

The first option involved automatic processing of the whole project in the background i.e. it does not display its results to the user and later the user has to review for Quality Control.Thus this option is not used.

In the Automatic and Interactive Processing, the system automatically picks arrival times for a refraction point and shows them to the user. The user in turn can check the picked arrival times. If required, the user can modify the picks by using manual picking options in the Interactive Tools. Selected shot of forward-reverse shooting (Coloured Display) is shown in Figure 3.10 and that for uphole shooting is shown in Figure 3.11.

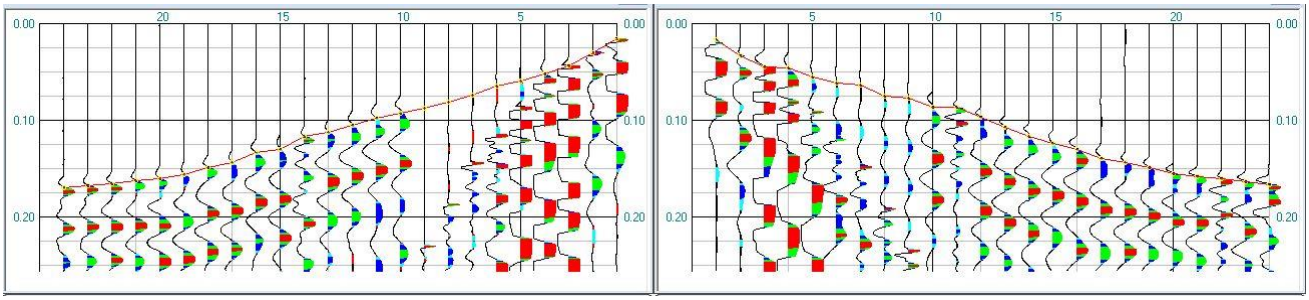

Fig 3.10. Seismic Traces (Coloured Display) with First Breaks Picked (Surface Shoots)

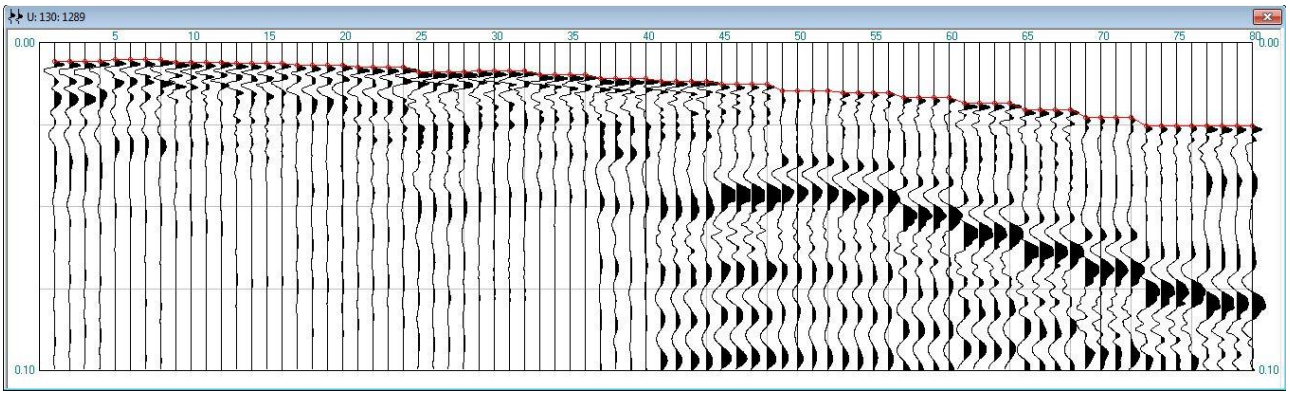

Fig 3.11. Seismic Traces with First Breaks Picked (Uphole)

3.7 Reference Amplitude Visualisation

Interactive modules have variety of applications that are useful for visualization purposes. Color reference amplitude tool helps in deciding the reference amplitude to used for Auto Picking as shown in Figure 3.12.

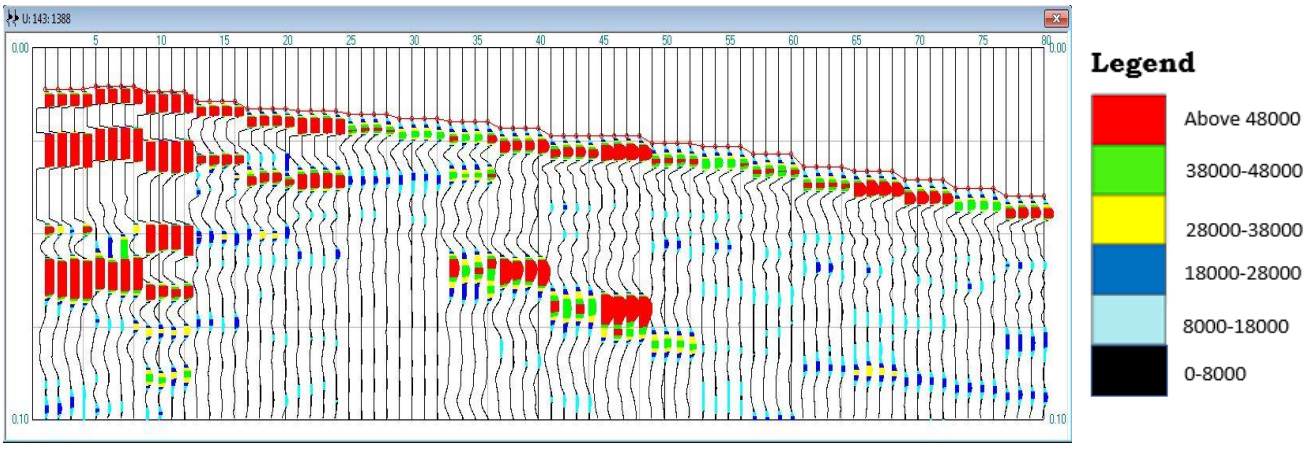

Fig 3.12. Reference Amplitude set by Coloer Attribute

In addition, Visual OIL script can export the seismic data to a grid format which can be used to generate a 3D view of seismic record with first break amplitudes prominently shown (Figure 3.13).

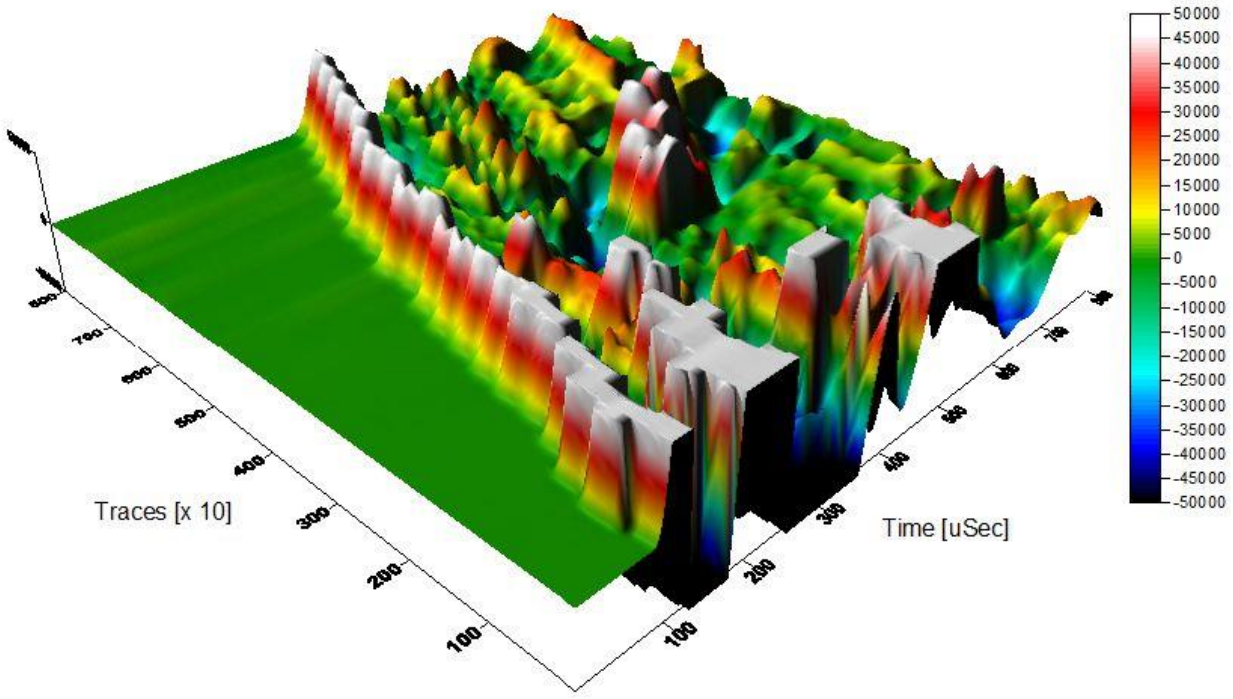

Fig 3.13. 3D Display of Seismic Shot Record with prominent continuity of First Breaks.

3.8 Travel Time Inversion

Refract is the next SeiRA application which generates T-X graphs by passing best fit lines for each picket and slopes of these lines are used to calculate velocities of weathered and sub-weathered layers along with thickness of the weathered layer. These parameters are further used for the calculation of statics in StatCalc. Refract has auto layering algorithm as well as manual layering options that helps the user to model the refractor and compute its parameters. After processing several parameters are computed such as, Average, True, Harmonic, Up-Dip, Down-Dip velocities depths, critical angles and cross-over distance.

- **T-X Graphs:**

T-X graphs plot first arrivals times as a function of offset distances. The software uses neural network to auto-layer and fit best fit lines for velocity computations shown in Figures 3.14 a and b. If required manual layering can also be done interactively.

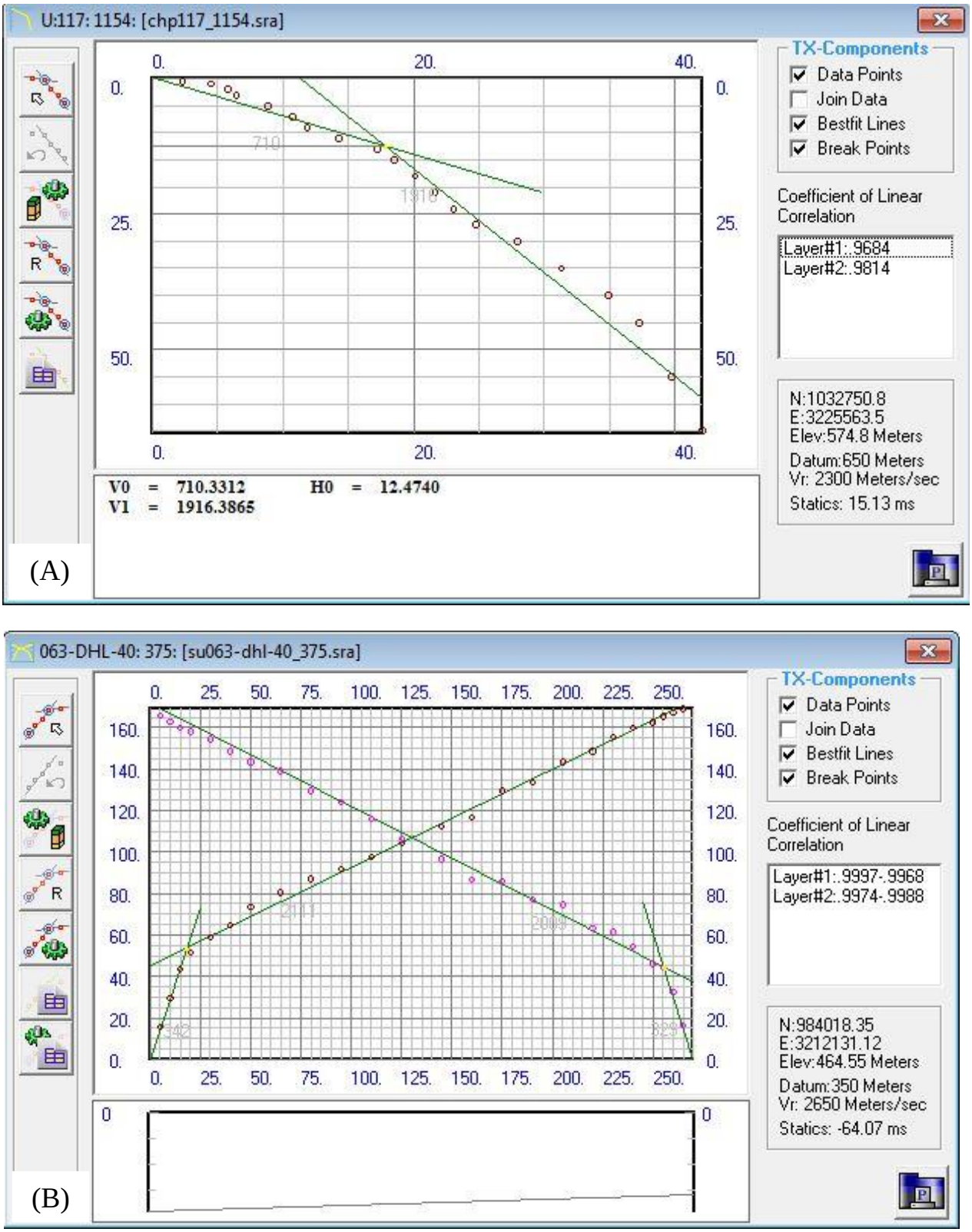

Fig 3.14 (a). T-X Graph for uphole logging (b). T-X Graph for Forward and Reverse (Surface) Shooting

T-X graphs are exported to DesignCAD for final display. Some DesignCAD images for both surface shooting and uphole logging of the study area are shown in Fig 3.15.

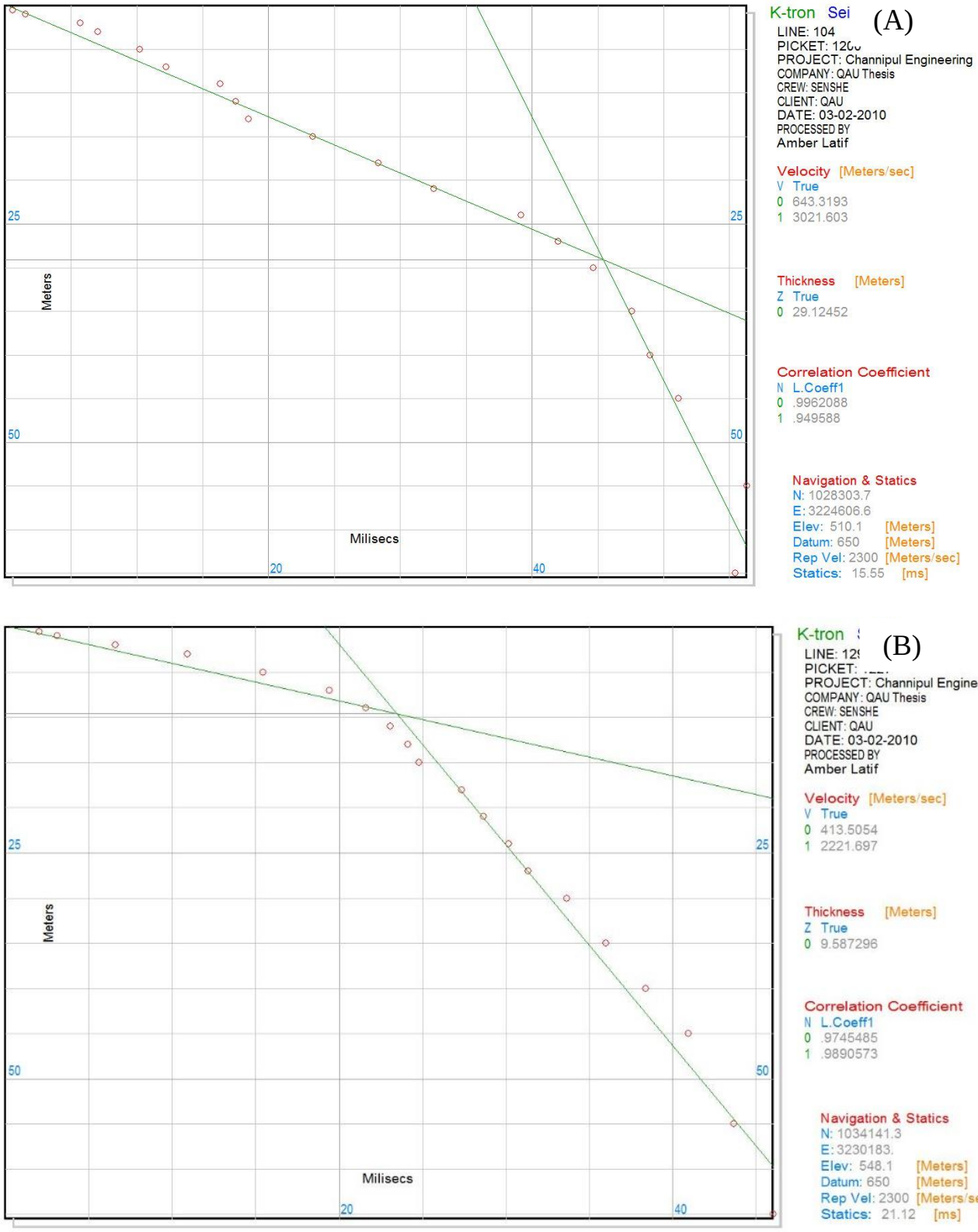

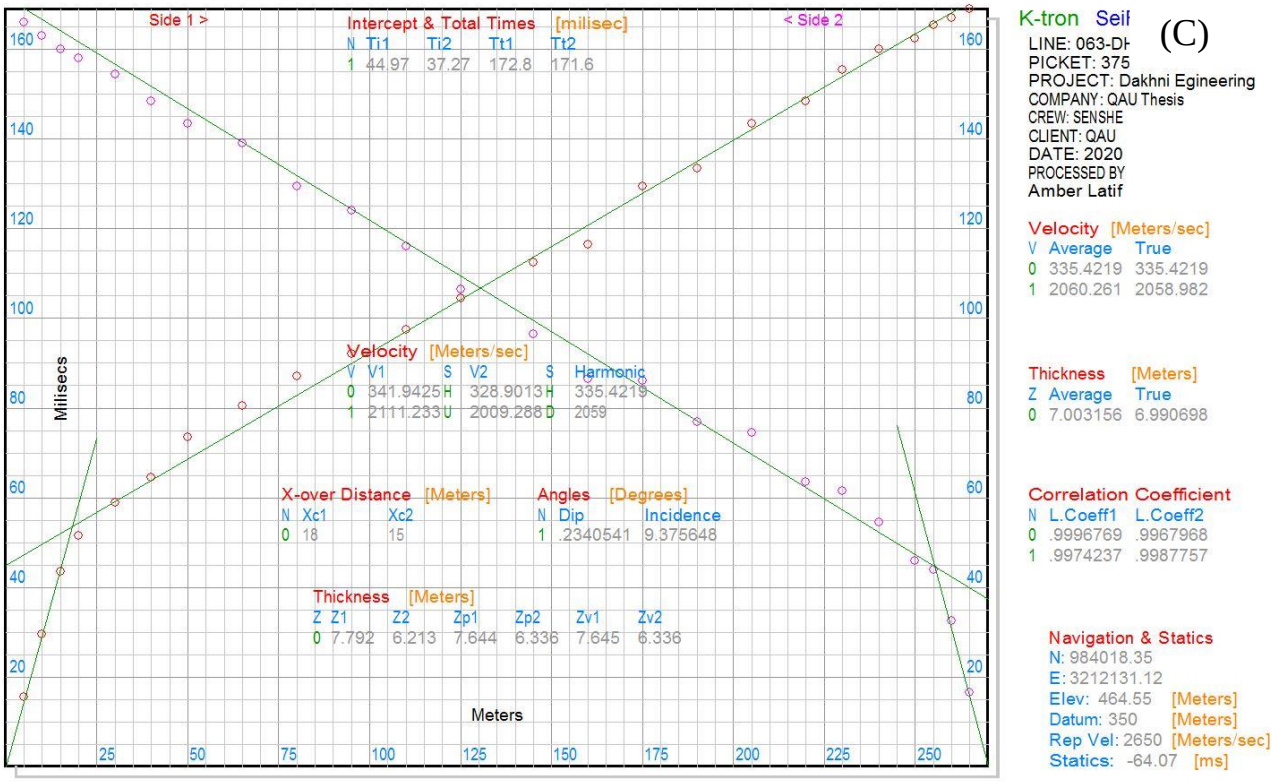

Fig 3.15 (a). TX Graph Plot of of line number 104 and picket number 1200 - Uphole-logging.
(b). TX Graph Plot of line number 129 and picket number 1227 - Uphole-logging.
(c). TX Graph Plot of line number 131 and picket number 1100 - Surface shooting.

It can be observed from the above TX graphs that they are mostly two layers cases; thus the computed parameters are Weathered Layer velocity (V0) and Thickness (H0) and Sub-Weathered Layer Velocity (V1).

3.9 StatCalc

The current study is mainly concerned with Engineering work but the software also has features for computing statics, thus statics have also been computed. StatCalc is a final processing module which is used to generate statics report for the project using 3D gridding. For computation of statics the datum height is chosen according to the ground topography and replacement velocity is adjusted a little above the sub-weathered layer velocity. Inverse Distance Weighted (IDW) Average with 6 neighbors is applied for interpolation. The computation of statics requires selection of a datum plane as well as replacement velocity as shown in Figure 3.16. The percentage tolerance filter checks the value of velocity to be within the specified percentage of tolerance as compared to the IDW average of its 6 neighbors.

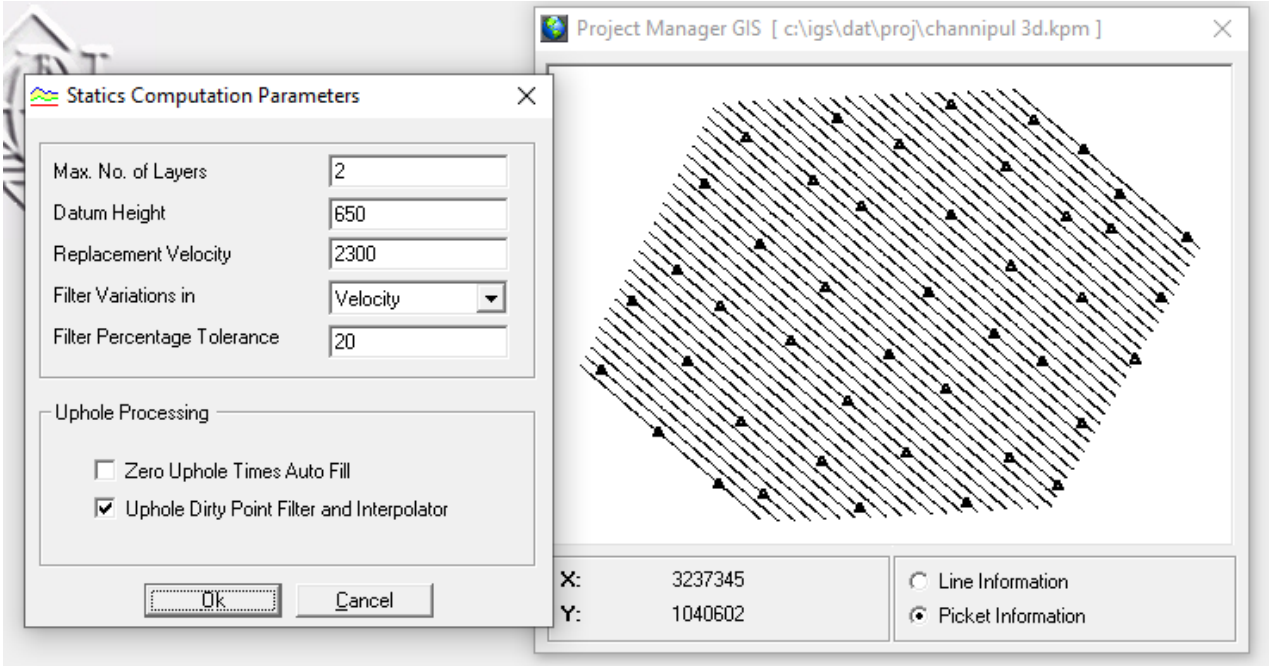

Fig 3.16. StatCalc: Setup Parameters for computation of Statics.

For the current project the processing parameters are as follows:

- Replacement velocity 2300 m/s.
- Datum is taken M.S.L (50m).
- Filter percentage tolerance 50 %.

3.9.1 Attribute Maps

Attribute Maps are the Color Maps of Elevation and Statics that can be generated by StatCalc. StatCalc generated these maps by loading Color Spectrum.

- **Elevation Map**

Figure 3.17 shows elevation colour contour map of the project.

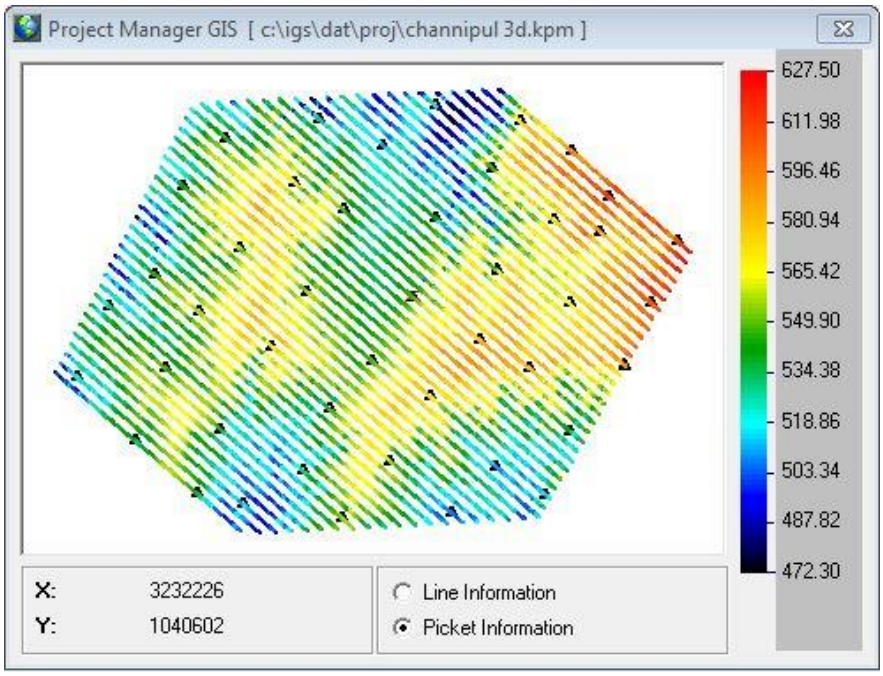

Fig 3.17. Attribute map of elevation of study area.

- **Static Map**

Figure 3.18. shows the statics color map for study area. Prominent variation can be seen in map due to weathered layer undulations.

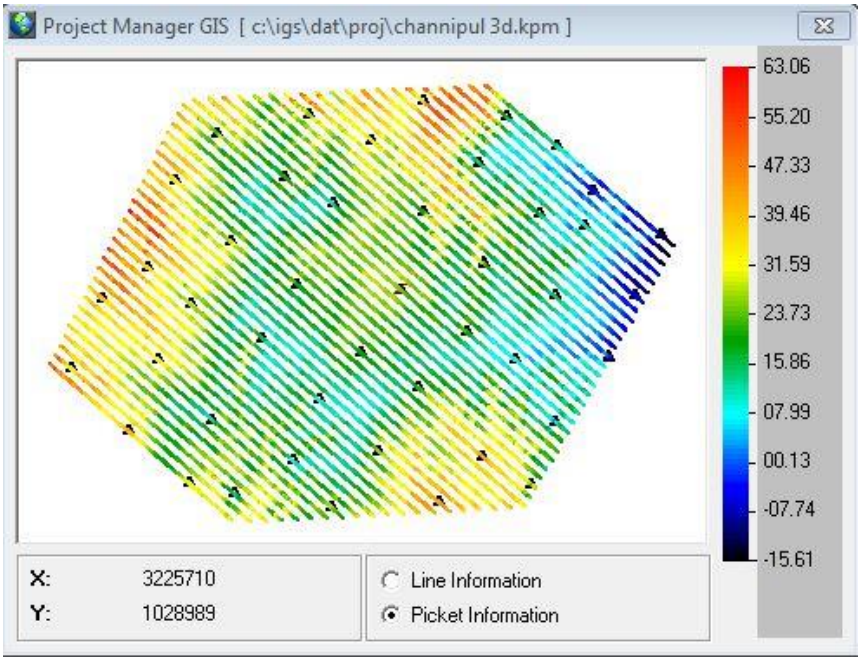

Fig 3.18. Attribute map of statics of study area.

3.10 Surfer

Surfer 8 is a full function 2D/3D visualization, contouring and surface modeling package that runs under Microsoft Windows. Surfer is used extensively for surface analysis, contour mapping, landscape visualization watershed and 3D surfaces mapping and gridding. Grid files obtained from other sources process through Surfer to obtained outstanding contour of 3D surface, watershed, and shaded relief also post maps.

Surfer's sophisticated interpolation engine use Grid files to generate Contour maps and 3D surfaces of Elevation, Statics, weathered layer velocity V0 , sub weathered layer velocity V1 and thickness of Weathered Layer h0.

3.11 Contour Maps

Surfer provides full control over all map parameters. 3D surfaces of topographic Elevation and Weathered Layer thickness are generated while contour maps of the velocity of Weathered and Sub-weathered layers are generated. Figure 3.19 shows the 3D visualization of Elevation, Weathered layer thickness, Weathered layer velocity and sub-Weathered layer velocity.

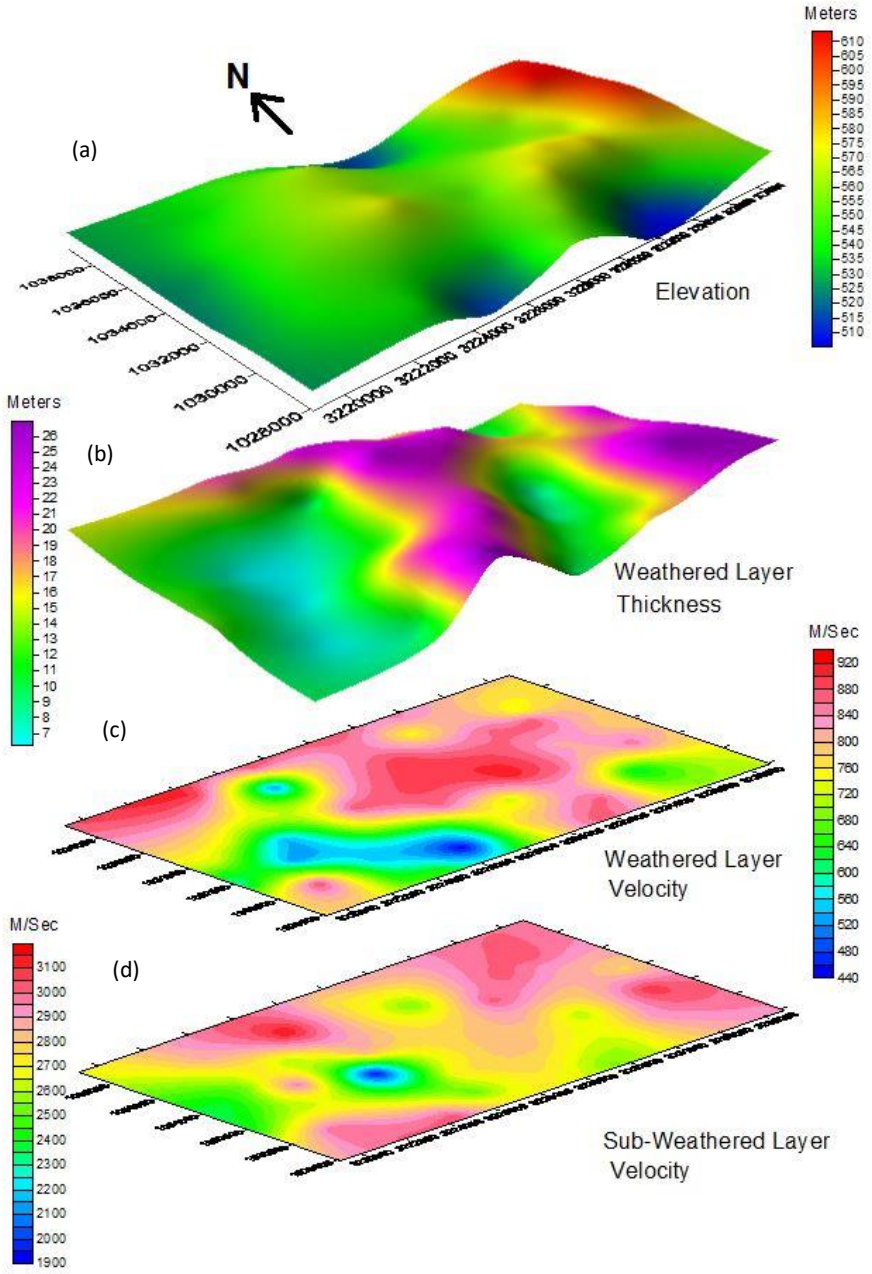

Fig 3.19. 3D Visualisation of (a) 3D Surface of Elevation. (b) Thickness of Weathered Layer. (c) Weathered Layer Velocity Contour Map (d) Sub-Weathered Layer Velocity Contour Map.

From the figure it can be seen that:

a) In Elevation surface the topography in the middle of the region is elevated to 550 meters while in a small portion of northern side there is a depression and similarly in the southern side there are two depressions while north-eastern region is highly elevated where elevation reaches to a maximum of above 600 meters.

b) From Weathered layer thickness in the middle portion from north toward the south have a higher thickness around 25 meters and parallel towards the eastern side there is continuous decrease in thickness around 12 to 13 meters while again going towards south-eastern region the thickness again increases and reaches a maximum of 25 meters and then coming towards the eastern side the thickness drops to around 10m/s and in some portion, it drops to a minimum of about 7 m.

c) Weathered layer velocity Contour map (V_0) indicates that in the central region the velocities are higher in the range of 800m/s to 900m/s whereas it decreases to 600m/s towards south-east region and it drops to 400 to 450m towards south-west region while in the north-western region velocity is again higher.

d) Sub-Weathered layer velocity Contour map indicates that it is higher throughout in the eastern side in the range of 3000m/s or above and it gradually reduces to 2200m/s towards south-western direction but finally in the south-east direction it again increases to 3000m/s while in the north-western side the velocity remains higher in order of 3000m/s.

Based on the variations in the topography, the weathered layer thickness and its velocity, the static contour map is shown in Figure 3.20.

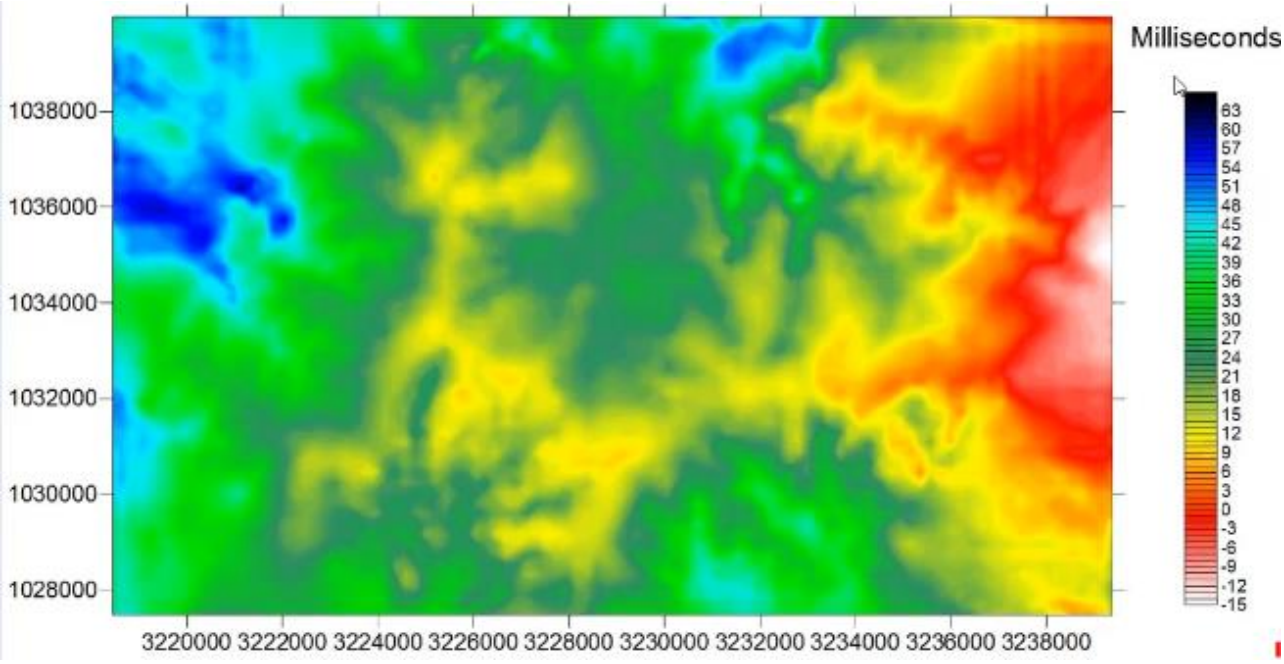

Fig 3.20. Statics Contour Map of Rawat

In Figure 3.20 red color shows negative statics and blue colour shows positive statics. Except red color, all other colors give positive statics, since the datum has been selected at 650 milliseconds. When Statics Contour Map is correlated with Elevation layer topography, as we can see in previous figure (a) mostly topography of area lies in the range of 500 to 660 milliseconds so there are just few peaks in the eastern side which are slightly higher than 650 where statics is negative while rest of the area lies below the datum plane therefore elevation static correction is positive.

Keeping In view the topographic undulations and thickness of weathered layer and its velocity variation, statics values are higher in north-eastern part and at some locations in the northern side, while most of the area in the middle of this region has statics in the range of 10 to 30 milliseconds. Generally, as we move towards the southern side the statics increases, while as we move towards the east the statics value is decreases and ultimately at some points it become negative up to 15 milliseconds.

Chapter 4

Geophysical Engineering Properties for seismic based zoning

4.1 Introduction to the Geophysical techniques

Geophysical techniques are becoming common day by day due to their wide applications for site selection for civil engineering problems like construction of highways, Highrise buildings, construction of dams, stable sites for industries as well as sites for nuclear plants. As strength of the ground must be known to estimate how much overload and vibrations it can withstand, which is necessary for the construction of a building or a highway. A seismic survey provides velocity information about sub-surface layers. Once the P or S wave velocity of a material is determined, its density and all elastic moduli, engineering, and seismicity parameters. can be computed. These parameters all together are referred as engineering and seismicity properties.

Seismic refraction survey are widely used methods in engineering applications to obtain the elastic properties of subsurface layers. The seismic methods are best suited to sediment thickness analysis, bedrock quality determination and detection of the presence of weaknesses in the bedrock before the erection of any civil engineering structures such as bridges, tunnels, dams and portals. As a result, seismic method has evolved into a cost-effective tool for rapidly determining depth to bedrock in engineering and construction projects. Seismic refraction surveys are used to map the depth to bedrock and to provide information on the compressional and shear wave velocities of the various units overlying bedrock. Velocity information also can be used to calculate in place small-strain dynamic properties of these units.

4.1.1 Geomechanics

Geomechanics involves the study of the mechanics of soil and rock & study of how subsurface rocks deform or fail in response to changes of stress, pressure and temperature and it is becoming increasingly important in oil and gas exploration. In the petroleum engineering industry, geomechanics is used to predict important parameters, such as in-situ rock stresses, modulus of elasticity, leak-off coefficient, and Poisson's ratio. Reservoir parameters that include formation

porosity, permeability and bottom hole pressure can be derived from geomechanically evaluation. Generally, geomechanics is divided into two main disciplines includes:

- **Soil Mechanics**

Soil mechanics is a branch of soil physics and applied mechanics that describes the behavior of soils and provides the theoretical basis for analysis in terms of geotechnical engineering, a subdiscipline of civil engineering, engineering geology or geophysical engineering. It deals with the behavior of soil from a small scale to a landslide scale.

- **Rock Mechanics**

Rock mechanics is concerned with the application of the principles of engineering mechanics to the design of structures built in a rock. The structure could include but not limited to a drill hole, a mining shaft, a tunnel, a reservoir dam, a repository component, or a building. If Rock physics is applied for near surface investigation to find strength of lithology / formation then it termed as **Engineering Property Calculation** or **Engineering Mechanics.** Primary and Secondary waves are used to determine the Engineering properties of ground. (Khan, 2010)

4.2 Geophysical Engineering Workflow

The seismic refraction data is processed & finals results includes weathered and sub-weathered layer velocities and thickness along with elevation and topographic information. All these parameters are used as an input for computation of Elastic Moduli, Engineering properties and Seismicity Characterization.

The workflow adopted for the computation of Geophysical and Seismicity parameters is given in Figure 4.1.

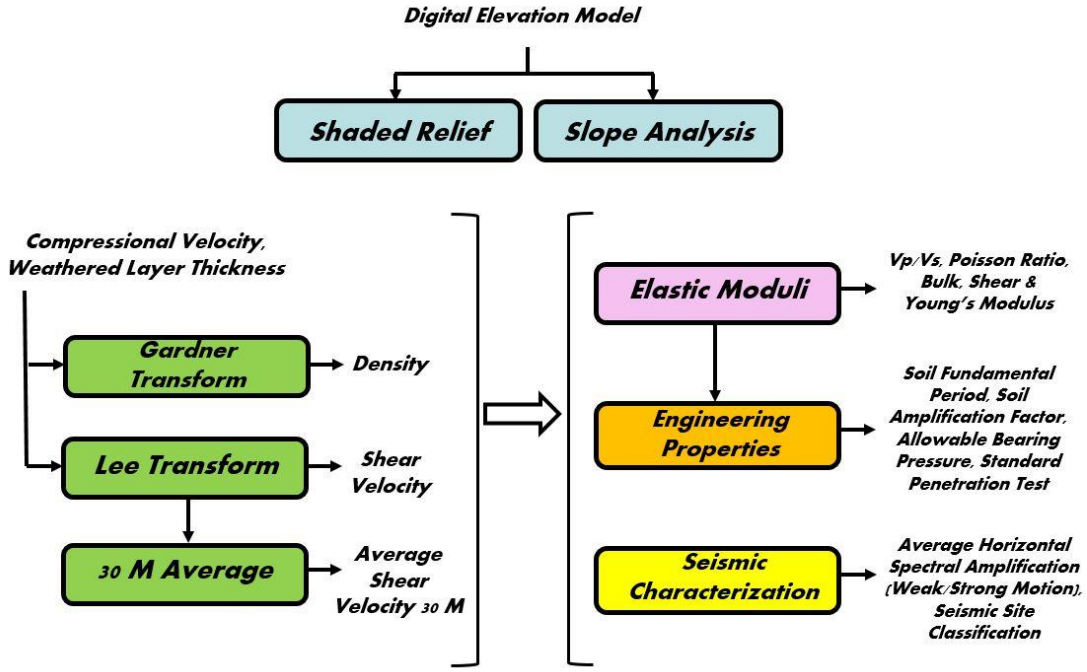

Fig 4.1. Workflow for Geophysical Engineering properties

- **Shaded Relief**

The site area is expanded upto 100 km in all four directions and then Digital Elevation Model (DEM) of the area is obtained from Shuttle Radar Topographic Mission (SRTM) data-based model (Farr et al, 2007). Shaded Relief Map of area is generated from DEM as shown in Figure 4.2.

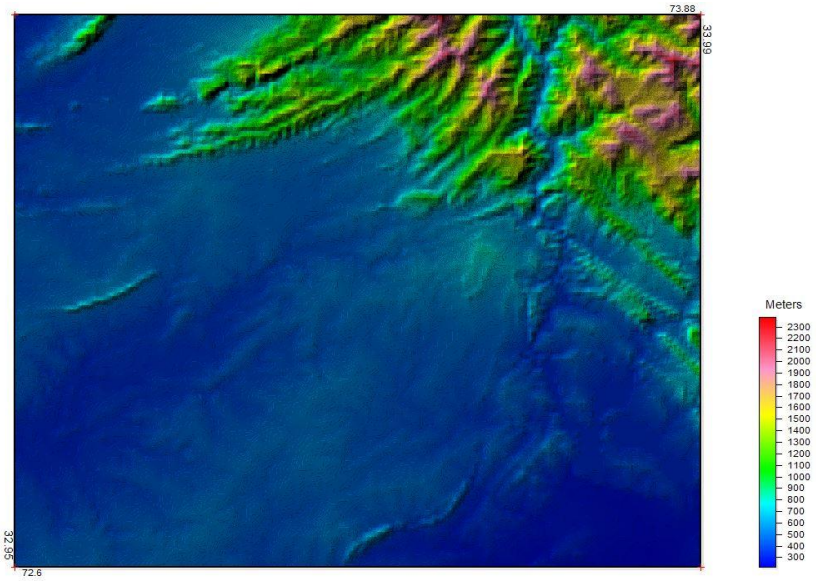

Fig 4.2. Shaded Relief Map of Rawat

Shaded Relief Map is based on the concept that face of the topographic features facing the light source appear brighter, while sides on the other side appear darker giving a shadow effect. The angle between the light source (Sun) and the topographic surface is used to compute the brightness or darkness at a given point. Direct light will give the highest brightness but as the angle increases and become oblique, the brightness reduces and ultimately changes to darkness.

Shaded relief map shown in Figure 4.2 above, indicates that the site of study area lies in the middle where topography of elevation is stable within range of 600 meters above mean sea level whereas in the North-eastern sides, topography rises to an elevation as high as 2300 meters above mean level. Lowest elevation of shaded relief map is nearer to 300m.

- **Slope Analysis**

For all Engineering work we need slope analysis which is basically the derivative of elevation.

2-D slope analysis is carried out on DEM and slope map is generated which provides the dip of the topography. DEM slope or dip map is shown in Fig 4.3.

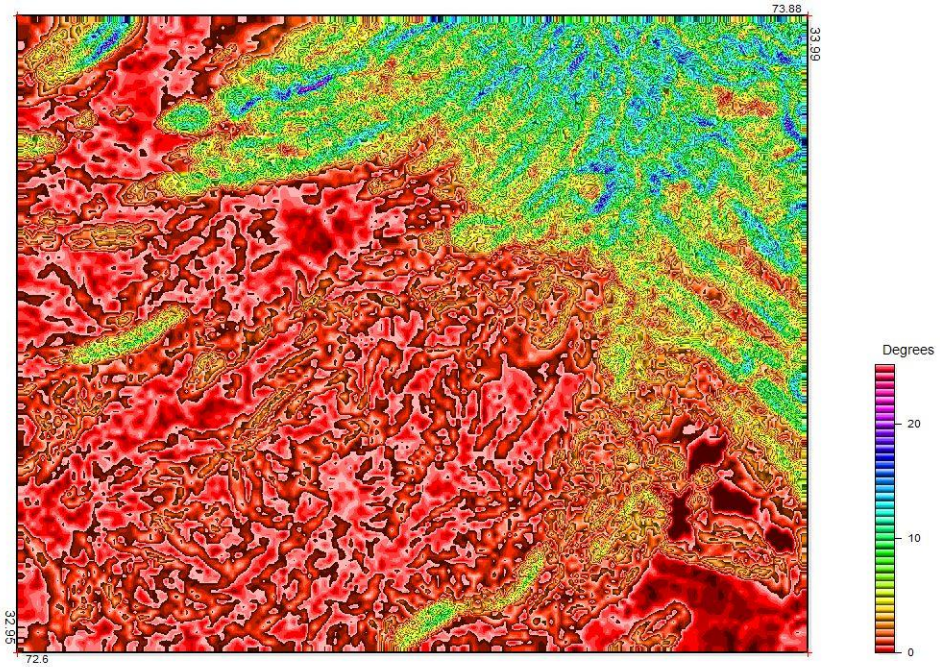

Fig 4.3. Slope Analysis of Rawat

Slope analysis is also an important component for analysing stability, land sliding and site selection analysis of the area. In the Fig 4.3, the site area which lies in the middle part of region have very low topographic dips around 0 to 5 degrees. The red portion is showing stable areas having 0 or a little above degree's slope while yellow shows 5 degrees, green shows 10, blue shows 15 whereas the purple is showing 20 degrees with steeper slope. This change is giving the rate of change of elevation which is the slope.

The workflow in Figure 4.1 shows the following three types of properties being computed.

- Elastic Moduli
- Engineering Properties
- Seismic Characterization

4.3 Elastic Moduli

An elastic modulus, or modulus of elasticity measures an object or substance's resistance to being deformed elastically (i.e., non-permanently) when a force is applied to it. The elastic modulus of an object is defined as the slope of its stress–strain curve in the elastic deformation region. As we have compressional velocity, shear wave velocity and density of weathered and sub-weathered layer, thus we can compute Elastic Moduli for both weathered and sub-weathered layer. A set of rock physics equations are listed below:

- P-Wave Velocity $V_p = 1.16 * V_s + 1.36$
- S-Wave Velocity $V_s = (V_p - 1.36) / 1.16$
- Density $\rho = 0.31 * V_p^{0.25}$
- V_pV_s Ratio $V_pV_{s\ Ratio} = \text{sqrt}(K / \mu) - 4/3$
- Bulk Modulus $K = \rho (V_p^2 - 4/3\ V_s^2)$
- Young's Modulus $E = 9K\mu / (3K + \mu)$
- Shear Modulus $\mu = \rho * V_s^2$
- Lames's Constant $\lambda = K - 2\ \mu / 3$
- Poisson's Ratio $\sigma = 0.5 (V_p^2 - 2V_s^2) / (V_p^2 - V_s^2)$
- P-Wave Modulus $M = K - 4\ \mu /3$

From seismic refraction data we compute thicknesses, velocities of weathered and sub weathered layer. The data would be used to compute various Elastic, Engineering and Seismicity parameters.

Initially Gardner equation (Gardner, 1974) is used to compute density and Lee equation (Lee,2010) is used to compute Shear wave velocities for unconsolidated rocks. Once compressional velocity, shear velocity and density are available all elastic moduli are computed for the weathered and sub weathered layers and then all these computed parameters are used to compute various Geophysical engineering parameters such as Soil Fundamental Period (SFP), Standard Penetration Test (SPT), Soil Amplification Factor (SAF), Allowable Bearing Pressure (ABP). Finally, Seismic Characterization/zoning parameters are computed such as Average Horizontal Spectral Amplification (ASHA), Seismic site Classification.

4.3.1 Density

Density of deeper layers is higher than density of near surface unconsolidated layers because compaction increases with depth. The density of the material directly affects the P-Wave velocities passing through it. The variation in the density of the sub- surface material can be studied by analyzing the velocities. For calculating density following Gardner equation (Gardner, 1974) is used:

$$\boldsymbol{\rho = 0.31 * V_P^{0.25}}$$

Where,

Vp = P-Wave Velocity

Contour map of density of weathered, and sub weathered layer are shown in Figure 4.4.

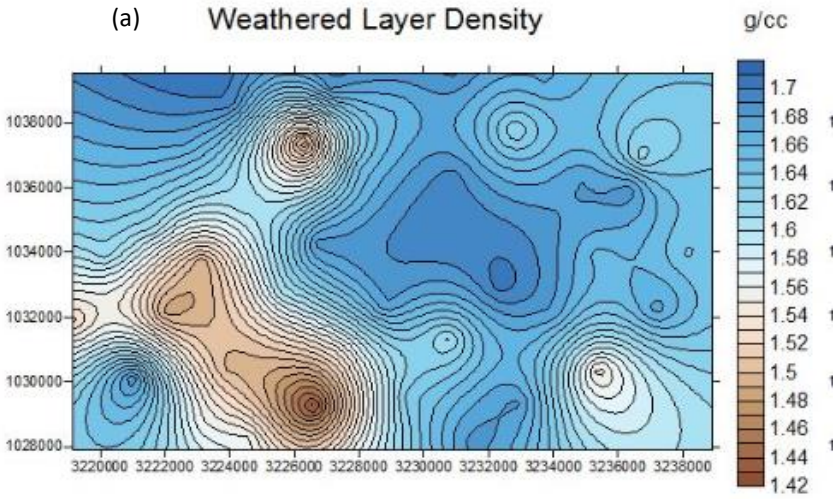

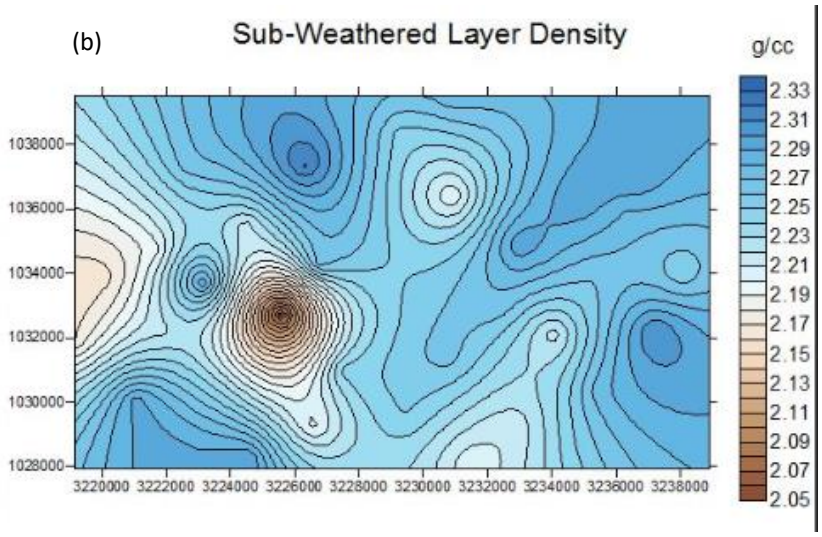

Fig 4.4. Contour Maps of Density (a) Weathered and (b) Sub-Weathered Layer

In Fig 4.4(a), density contour map of Weathered layer shows that the density is higher around 1.6g/cc. Whereas in the south-western side there is a cluster of low-density area around 1.4g/cc while in the north-western side there is also the portion of low density and in the south eastern part density value lies in the middle range of density around 1.5g/cc.

In Fig 4.4(b), density contour map of Sub-Weathered layer shows that mostly density is around 2.3g/cc whereas there is cluster zone where density decreases as low as 2.1g/cc as we move towards west.

4.3.2 Porosity

Porosity is the ratio of pore space volume to the total bulk volume of rock. Porosity is important parameter for estimation of strength of the material and compaction required. Velocities have an inverse relation with the porosity, high velocity value indicates low porosity value. Porosity decreases with compaction and thus velocity increases. Thus, porosity of weathered layer is higher than Sub weathered layer as shown in Figure 4.5 a and b.

$$1/V_{bulk} = \Phi/V_{fluid} + (1- \Phi)/V_{matrix}$$

Where

Φ = Porosity

Vbulk = Wave velocity of rock formation

Vfluid = Wave velocity through the pore fluid

Vmatrix = Wave velocity through solid matrix

Above formula is used to calculate porosity of rock unit.

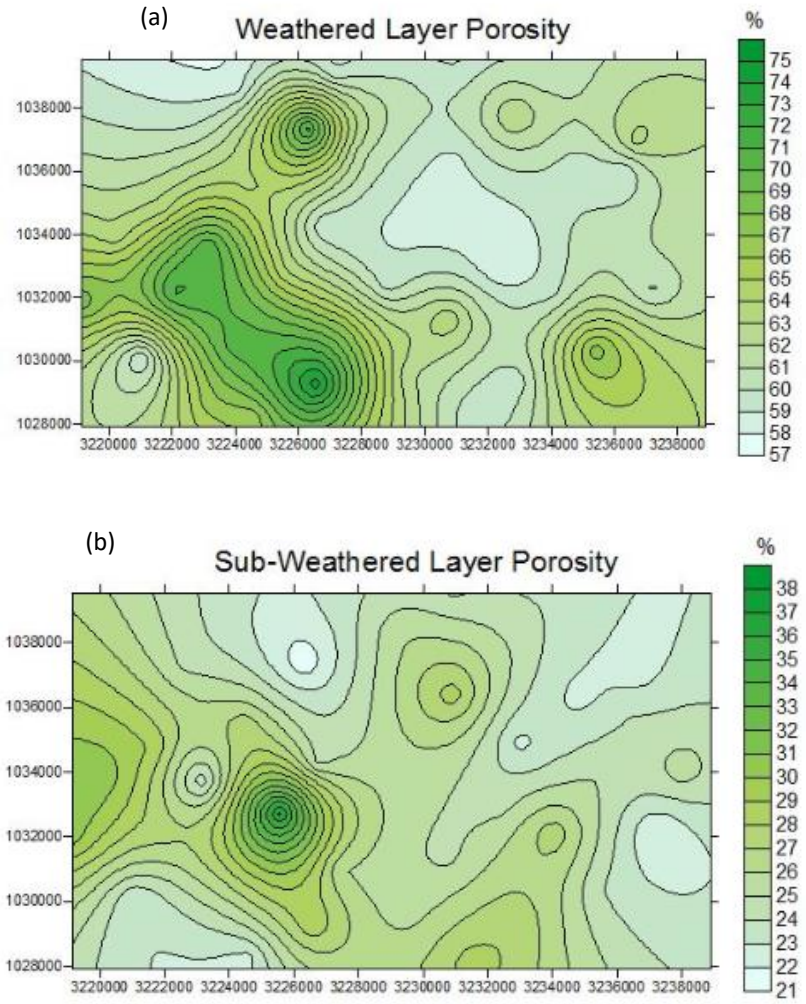

Fig 4.5 Contour Map of Porosity (a) Weathered and (b) Sub-Weathered Layer

Density is inversely proportional to porosity. Porosity interpretation is almost like density in inverse i.e. the places where density is higher porosity is lower and where density is lower porosity is higher. In Fig 4.5(a), Porosity contour map of Weathered layer shows that porosity is higher in the south western part around 75% where in the middle Porosity is around 57%. In Fig 4.5(b), Porosity contour map of Sub-Weathered layer shows that Porosity in most of the region is around 20% whereas we move towards west porosity is around 30 to 35%.

The seismic refraction method provides the velocity of compressional P-waves in subsurface materials. Although the P-wave velocity is a good indicator of the type of soil or rock, it is not a unique indicator. Shear waves velocity are also used to calculate the engineering parameters by using P-wave. The most common Castegna's equation (Castagna et al., 1985) for the calculation of S-wave velocity is:

$$Vs = \frac{(Vp-1.36)}{1.16}$$

Above equation is used for Carbonates and Siliciclastic rocks, but it does not hold true for near surface unconsolidated layers. Thus, when Vp < 1.36 (km/s) the above equation gives negative values of Vs. Thus instead of Castegna equation, Lee (2010) equations are used for computation of Vs from Vp.

Lee (2010) equations for unconsolidated rock are given below:

$$V_s = (V_P/2.286)^{1/0.672} \quad ; Vs > 1Km/sec \quad Eq\text{-}1$$

$$V_s = (V_P/2.042)^{1/0.103} \quad ; Vs < 0.6\ Km/sec \quad Eq\text{-}2$$

Lee used some samples of Vp and Vs to derive these two equations as shown in Figure 4.6.

Figure 4.6 shows the relation between P- and S-wave velocities from various sources. Data by Han and others (1986) are for consolidated sediments and other data are for unconsolidated sediments. There are two distinct trends: one is for S-wave velocity greater than about 1 km/s and the other is for velocity less than about 0.6 km/s.

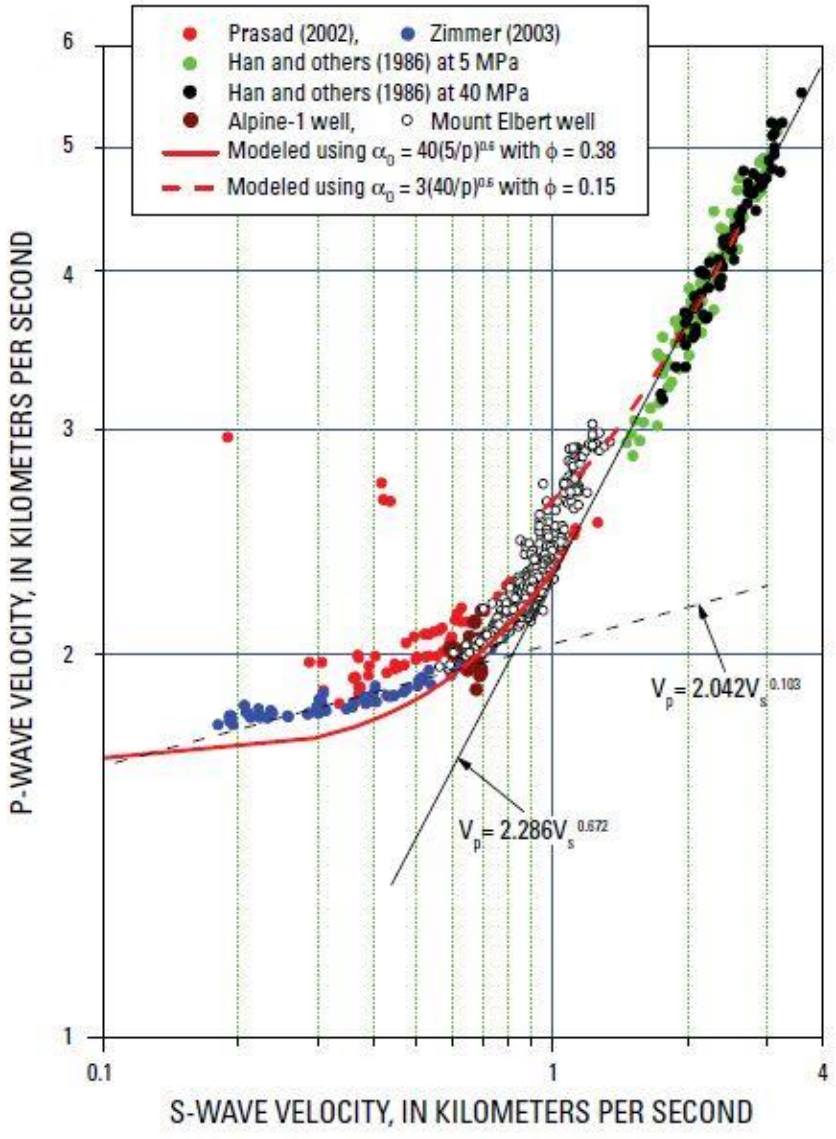

Fig 4.6. Graph of V_p & V_s , samples used by Lee (2010) (Relation between P-wave and S-wave velocities from various sources; laboratory data from Han and others (1986), Prasad (2002), and Zimmer (2003), and well log data from the Mount Elbert and Alpine–1 wells, North Slope of Alaska.).

4.3.3 S wave velocity for 30 meters Average

Vs is calculated by using Visual OIL scripts and contours are generated for both weathered and sub-weathered layers. Engineering projects require a 30 meters shear wave average. We have already computed s-wave by (Lee,2010) equation. Now we have to compute S velocity for 30 meters average from S wave velocities of 1st & 2nd Layers (Vs1,Vs2) and thickness of 1st layer (H1):

$$Vs30 = 30/((H1/Vs1) + ((30 - H1) / Vs2))$$

Contour map of S-wave velocity for weathered sub-weathered 30 Meters average is shown in Figure4.7.

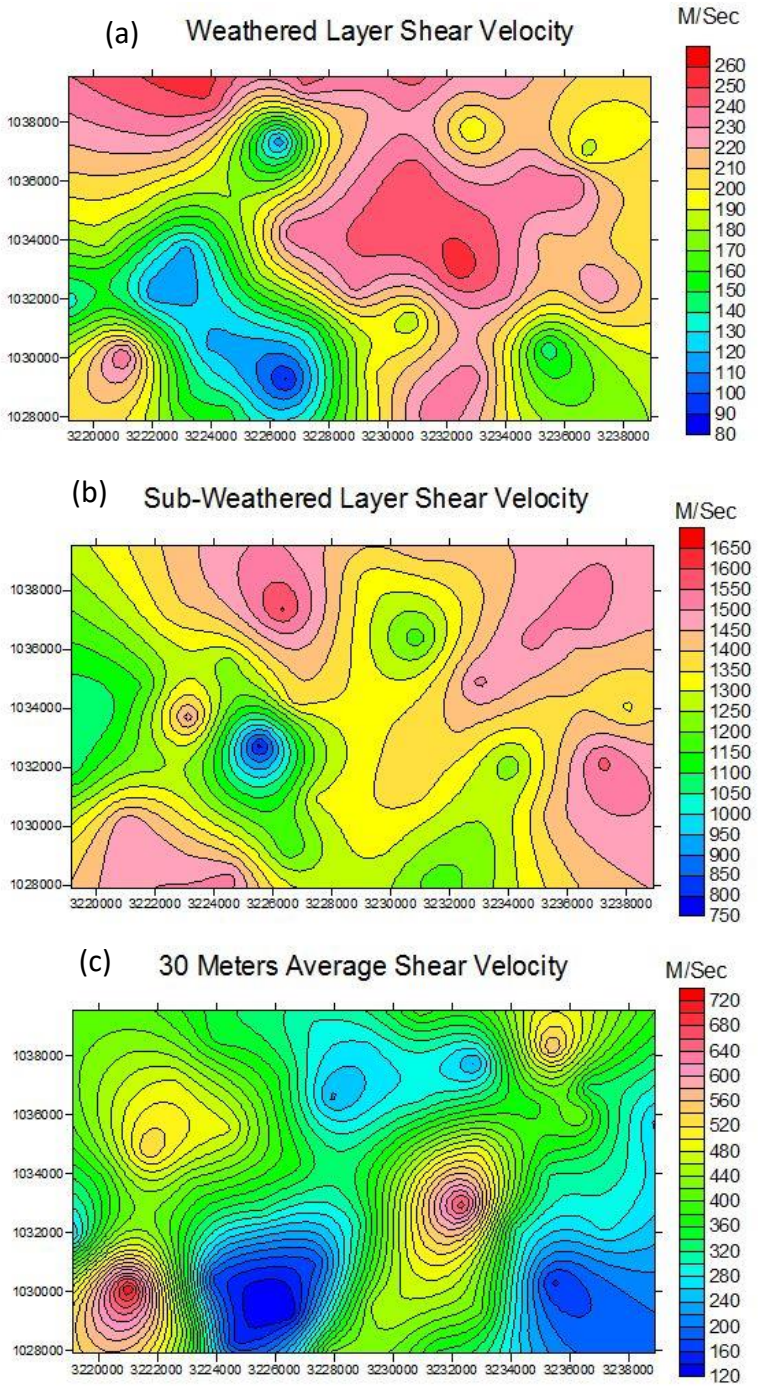

Fig 4.7. Contour Maps of Shear Wave Velocity (a) Weathered Layer, (b) Sub-Weathered Layer (c) 30 Meters Average.

a) In Fig 4.7(a), contour map of weathered layer shows that weathered layer shear velocity is higher in the middle region within 220 to 270m/s and as we move towards south-west their shear velocity for the weathered layer decreases around 100m/s.
b) Similarly, in Fig 4.7 (b) the shear velocity for sub-weathered layer is higher in the north-eastern region around16000m/s and as we move toward the south-west velocity decreases upto 1000m/s. In civil engineering work mostly shear velocity of 30 meters of top lock of Earth is very important. By using shear velocity of weathered and sub-weathered layer 30 meters average shear velocity has been computed that is important for engineering work.
c) Fig 4.7 (c) shows the 30 meters average shear velocity that indicates in the south-eastern part velocity is as low as 200m/s. Similarly, as we move toward west there is another portion that is cluster region which have again low Shear wave velocity upto 200m/s while in most of the other region Shear velocity range within 300m/s to 500m/s. Whereas in some portions like in around middle of the region and south-western portion the velocity become as high as above 600m/s.

4.3.4 Bulk Modulus, Shear Modulus & Young's Modulus

Elastic parameters have been computed by using the standard equations. Elastic moduli is important for computing strength of any material in engineering works and in computation of other parameters. Contour maps of Bulk Modulus, Young's Modulus and Shear Modulus for Weathered and Sub-Weathered layer are shown in Figure 4.8.

a) In Figure 4.8 (a) Bulk Modulus for weathered layer indicate that it is higher in the middle of the region around 1.2GPa and as we move towards east it decreases to 0.9 GPa. Similarly, as we move towards the south-western portion the Bulk Modulus again reduces to a value of 0.3 GPa..
b) Shear Modulus for weathered layer in Figure 4.8 (c) shows the similar trend as for bulk modulus. It indicates that Shear Modulus in the middle of the region around 0.15 GPa and it reduces to 0.02 GPa as we move towards the south-west.
c) Similarly, Young's Modulus for weathered layer in Figure 4.8ure (e) also shows the similar trend. It indicates that Young's Modulus in the middle of the region around 0.33 GPa and it reduces to 0.03 GPa as we move towards the south-west.
d) The contour map of Bulk Modulus, Shear Modulus, Young's Modulus for Sub-Weathered layer in Figure 4.8 (b) (d) (f) shows almost same ties of trend. They show Modulus is higher

in the north-eastern portion where Bulk Modulus has a highest value of 15 GPa, Shear Modulus has a highest value of 6 GPa, Young's Modulus has a highest value of around 16 GPa. But as we move towards the middle region the Bulk Modulus reduces to 11 GPa, Shear Modulus reduces to 4 GPa, Young's Modulus reduces to 11 GPa.

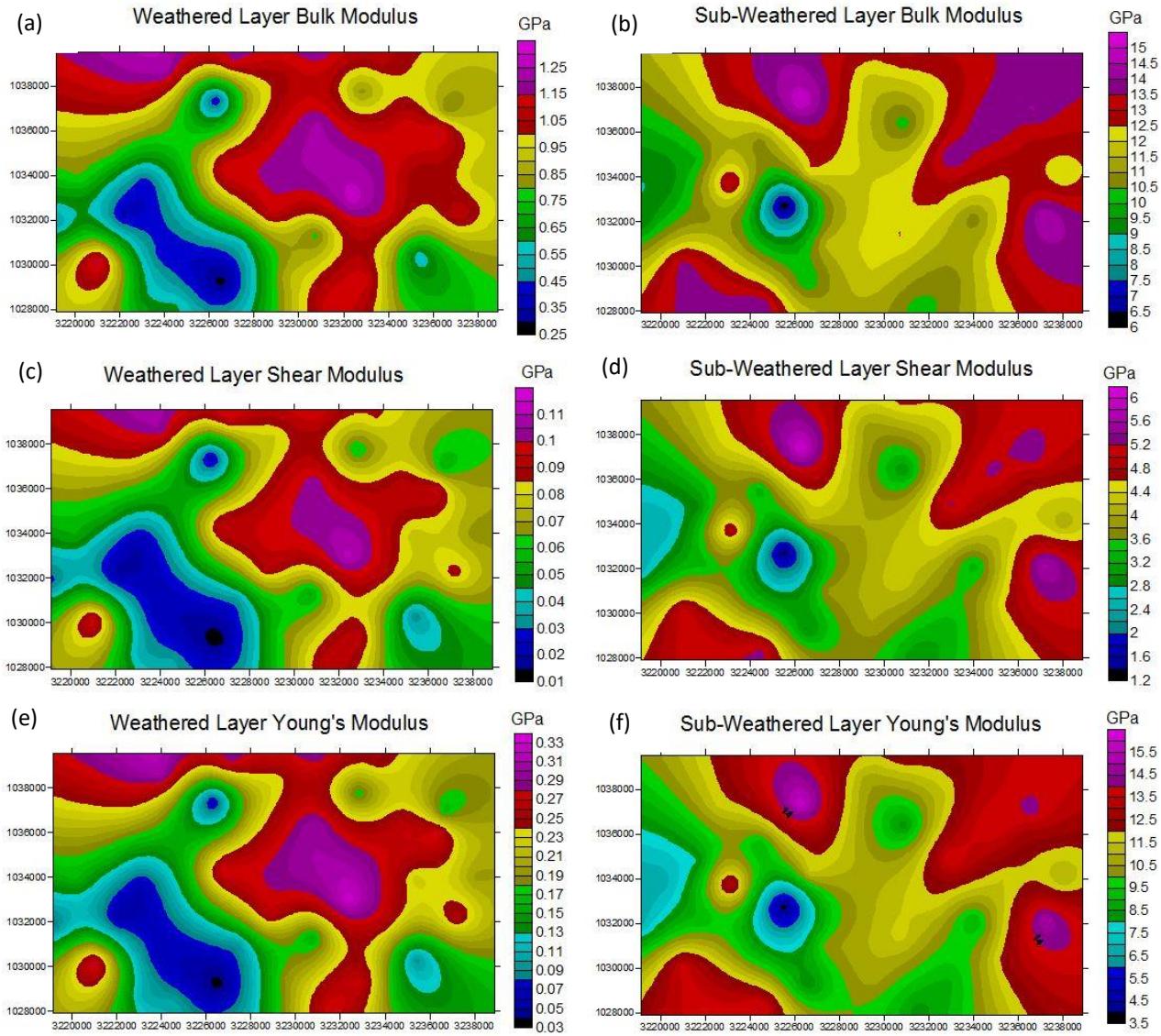

Fig 4.8. Contour Maps for Bulk Modulus, Shear Modulus and Young's Modulus (a) Weathered Layer of Bulk Modulus, (b) Sub-Weathered Layer of Bulk Modulus (c) Weathered Layer of Shear Modulus (d) Sub-Weathered Layer of Shear Modulus (e) Weathered Layer of Young's Modulus (f) Sub-Weathered Layer of Young's Modulus

These parameters have been computed not for interpretation but used in further computation of other Geophysical properties as well as Seismicity properties.

4.3.5 Vp-Vs Ratio & Poisson's Ratio

Another important parameter in Engineering work is Vp-Vs Ratio and Poisson's Ratio. Similarly contour maps of weathered and sub-weathered layer for Vp-Vs Ratio and Poisson's Ratio are shown in Figure 4.9.

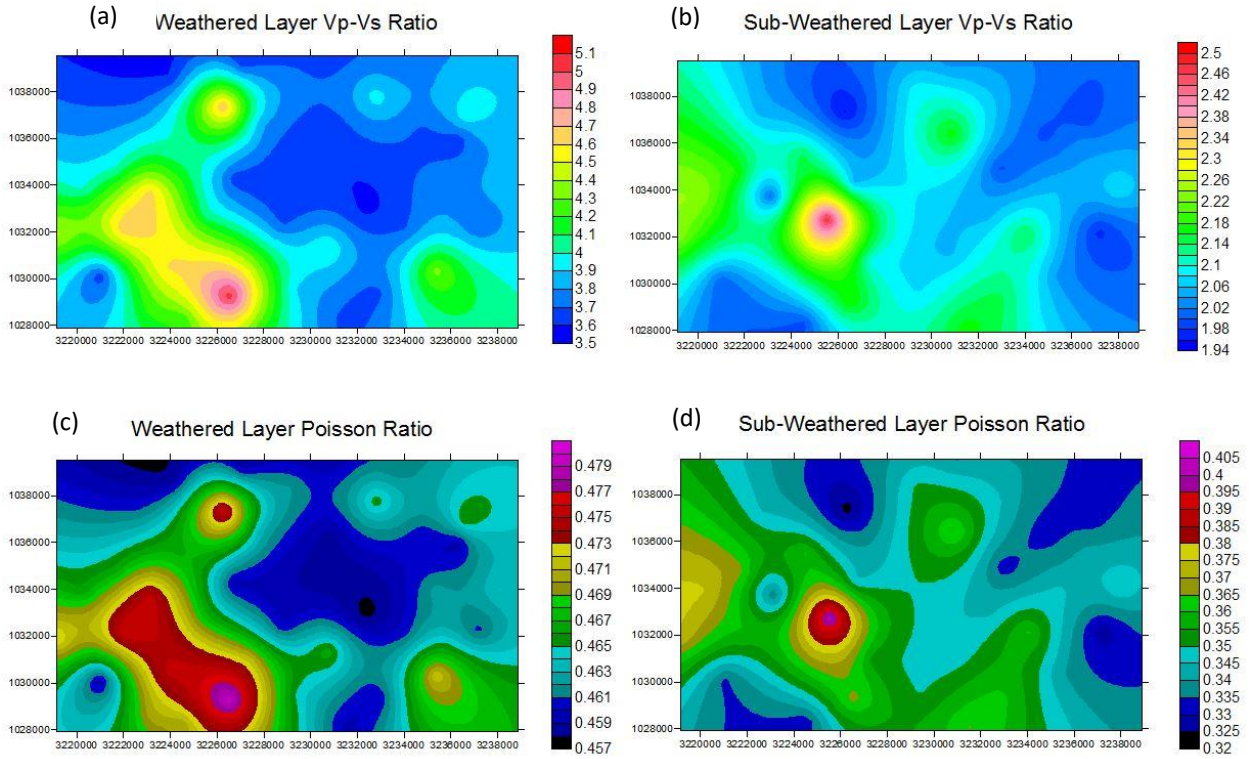

Fig 4.9. Contour Maps for Vp-Vs Ratio and Poisson's Ratio (a) Weathered Layer of Vp-Vs Ratio, (b) Sub-Weathered Layer of Vp-Vs Ratio, (c) Sub-Weathered Layer of Poisson's Ratio, (d) Sub-Weathered Layer of Poisson's Ratio

a) Vp-Vs ratio for Weathered layer in Figure 4.9 (a) indicates that in the South-Western region Vp-Vs ratio is highest around 4.6 and as we move towards North-Eastern portion Vp-Vs ratio reduces to 3.8.

b) Similarly, in Figure 4.9 (c) Poisson Ratio for Weathered layer shows that it has the higher value in South-Western region around 0.47 and as we move towards North-Eastern portion Poisson's ratio reduces to 0.46.

c) Vp-Vs ratio for Sub-Weathered layer in Figure 4.9 (b) indicates that in the Western region it has higher value around 2.25 and as we move towards East Vp-Vs ratio reduces to around 2.

d) Similarly, in Figure 4.9 (d) Poisson Ratio for Sub-Weathered layer shows similar trend and indicated that it has the higher value in Western region around 0.375 and it gradually decreases as we move towards Eastern portion Poisson's ratio reduces to 0.35.

All these parameters are further used in the computation of Engineering Properties as well as Seismic Characterization which are discussed in the next section.

4.4 Geophysical Engineering Properties

In this section we would be computing various Geophysical properties that would be useful for site selection for high building and sensitive engineering site. So key parameters that are computed and useful are discussed below:

4.4.1 Soil Fundamental Period

As earthquake waves propagate through soil media, their amplification or attenuation is mainly dependent on fundamental natural period of the soil deposit. The fundamental period of a soil deposit is dependent on its thickness, low strain stiffness and density. Thus, it is essential to estimate this parameter for site selection of roads and constructions. The Soil Fundamental Period computed using Kanai Method (Kanai, et al.,1983):

Contour map for Soil fundamental period is shown in Figure 4.10.

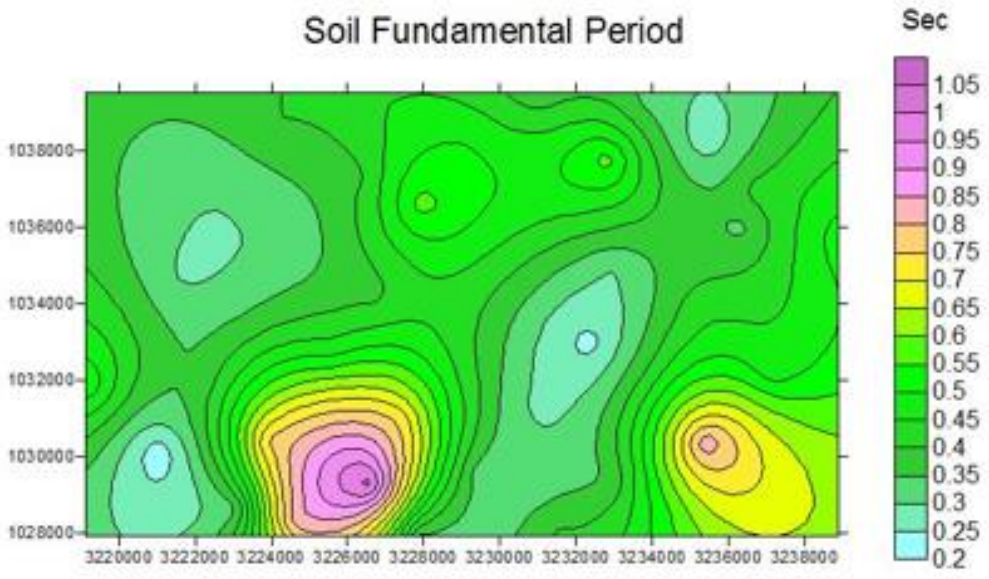

Fig 4.10. Contour Map for Soil Fundamental Period (SFP)

Soil Fundamental Period (SFP) in Figure 4.10 shows that most of the area has Soil Fundamental Period (SFP) around 0.6 sec while some clusters in the South indicates Soil Fundamental Period (SFP) has higher value around 1 sec and some portions have low value upto 0.2 sec. As Soil Fundamental Period (SFP) increases time decreases because they have inverse relationship. As we can see in the Fig. Green colour have lower Soil Fundamental Period (SFP) values its mean it give good response to higher frequencies whereas yellow color give response to lower frequencies.

4.4.2 Soil Amplification Factor

Soil amplification phenomenon is well known for soil amplify earthquake vibrations. Softer soil are worse than firmer soil in terms of amplification. Soil amplification is a phenomenon observed in many earthquakes where the strength of the shaking increases abnormally in areas where the seismic-wave velocity of shallow geologic layers is low. Seismologists have observed that some districts tend to repeatedly experience stronger seismic shaking than others. This is because the ground under these districts is relatively soft. Soft soils amplify ground shaking. The Soil Amplification Factor is computed from S Wave Velocity for 30 Meters Average using Midorikawa Method (Midorikawa, et al.,1987).

Contour map for Soil Amplification Factor is shown in Figure 4.11

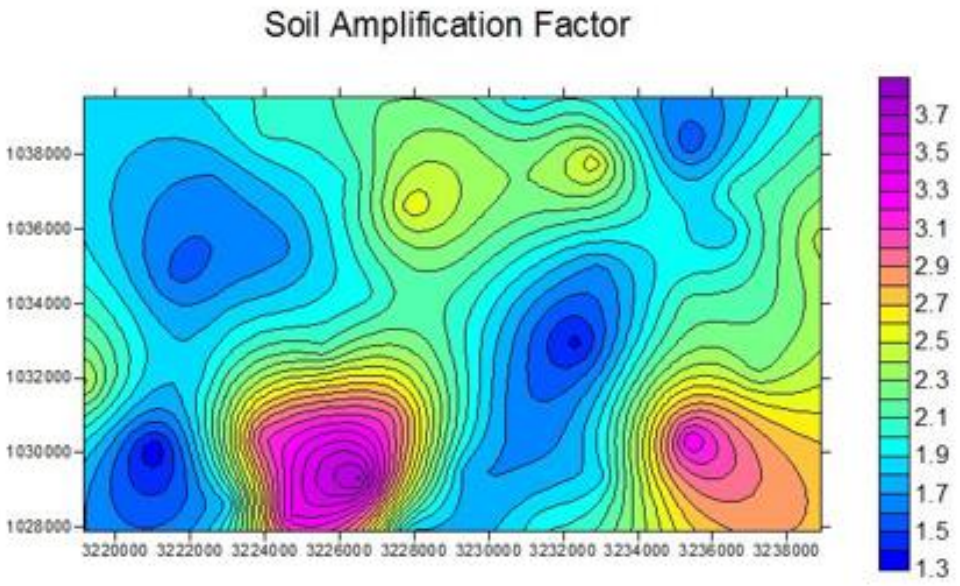

Fig 4.11. Contour Map for Soil Amplification Factor

Soil Amplification Factor (SAF) in Figure 4.11 shows that in most of the area Soil Amplification Factor (SAF) has the lower value around 1.3 and as we move towards North, in the middle portion of North, it gradually increases to 2.5 while in South-Eastern part and another cluster towards the West has highest Soil Amplification Factor (SAF) around 3.3.

It is important to note that for stability of area Soil Amplification Factor (SAF) should have lower value because higher values tend to amplify the ground shaking.

Table 4.1 identifies the soil types on the basis of shear wave velocities.

- **Soil Types Of Classification**

Table 4.1. Soil Types Identification (A.Hadjian, 2002)

Soil type A	*Vs.> 1500 m/sec*	Includes unweathered intrusive igneous rock. Occurs infrequently in the bay area. We consider it with type B (both A and B are represented by the color blue on the map). Soil types A and B do not contribute greatly to shaking amplification.
Soil type B	*1500 m/sec >Vs.> 750 m/sec*	Includes volcanics, most Mesozoic bedrock, and some Franciscan bedrock. (Mesozoic rocks are between 245 and 64 million years old. The Franciscan Complex is a Mesozoic unit that is common in the Bay Area.)
Soil Type C	*750 m/sec >Vs.> 350 m/sec*	Includes some Quaternary (less than 1.8 million years old) sands, sandstones and mudstones, some Upper Tertiary (1.8 to 24 million years old) sandstones, mudstones and limestone, some Lower Tertiary (24 to 64 million years old) mudstones and sandstones, and Franciscan melange and serpentinite.
Soil Type D	*350 m/sec >Vs.> 200 m/sec*	Includes some Quaternary muds, sands, gravels, silts and mud. Significant amplification of shaking by these soils is generally expected.
Soil Type E	*200 m/sec >Vs.*	Includes water-saturated mud and artificial fill. The strongest amplification of shaking due is expected for this soil type.

4.4.3 Allowable Bearing Pressure

Allowable Bearing Pressure is another parameter to check the bearing capacity of soil profile tolerance that it can bear the load of multistory buildings and in terms of road constructions, this parameter define the limit of pressure the soil can bear. The Allowable Bearing Pressure in Soils is computed from S Wave Velocity (Vs) using Uchiyama Method(Uchiyama, et al.,1984).

Contour maps for Allowable bearing pressure for weathered and sub-weathered layer are shown in Figure 4.12.

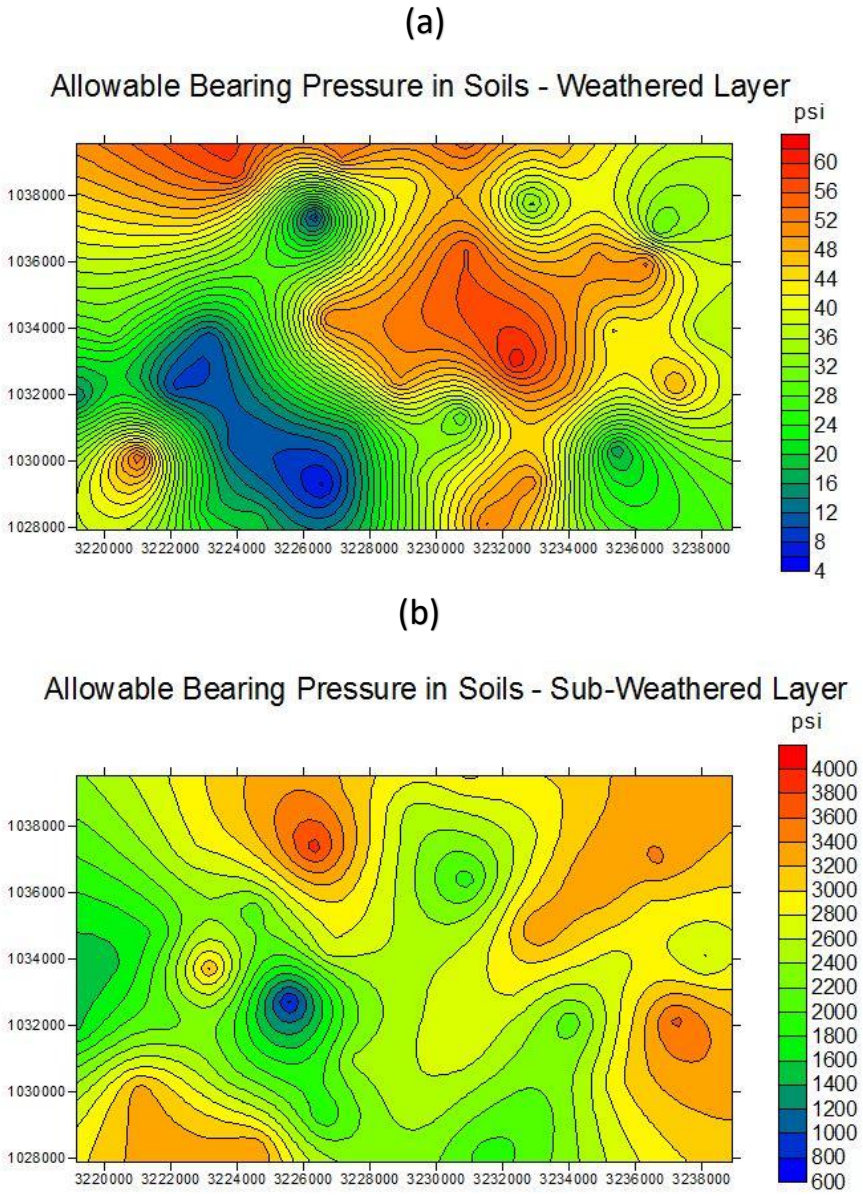

Fig 4.12. Contour Maps for Allowable bearing pressure(ABP) (a) Weathered Layer (b) Sub-Weathered Layer

a) Allowable Bearing Pressure (ABP) for Weathered layer in Figure 4.12 (a) indicates that central region has higher value of Allowable Bearing Pressure (ABP) around 60 psi and as we move towards south-west the Allowable Bearing Pressure (ABP) reduces to as low as 8 psi.
b) Now in Figure 4.12 (b) the Allowable Bearing Pressure (ABP) for Sub-Weathered layer indicates that in central portion Allowable Bearing Pressure (ABP) is around 2200 psi whereas in north-eastern and south-western portion the value of Allowable Bearing Pressure (ABP) further increases to around 3000 to 4000 psi.

For Engineering and construction point of view the Weathered layer has much lower Allowable Bearing Pressure (ABP). Thus, it is not suitable and need to be bulldozed.

4.4.4 Standard Penetration Test (SPT)

The standard penetration test (SPT) is measure of loading capacity of ground. It is an in-situ dynamic penetration test designed to provide information on the geotechnical engineering properties of soil. Imai and Yoshimura in 1970 develop a model. We can compute Standard Penetration Test in Blow Counts from S Wave Velocity (Vs) using Imai and Yoshimura Method (Imai and Yoshimura, et al.,1970).

This test method provides a disturbed soil sample for moisture content determination and still used because of its simplicity and low cost. It can provide useful information in very specific types of soil conditions. For this test, a sample tube, which is thick walled to endure the test environment, is placed at the bottom of a borehole. A heavy slide hammer (140 lbs) is dropped repeatedly 30 inches onto the top of the sample tube, driving it into the soil being tested. The operation entails the operator counting the number of hammers strikes it takes to drive the sample tube 6 inches at a time. Each test drives the sample tube up to 18 inches deep. It is then extracted and if desired a sample of the soil is pulled from the tube. The borehole is drilled deeper and the test is repeated. In cases where 50 blows are insufficient to advance it through a 150 mm (6 in) interval the penetration after 50 blows is recorded. The blow count provides an indication of the density of the ground, and it is used in many empirical geotechnical engineering formulae. Schematic assembly of SPT is shown in Figure 4.13. The main purpose of the test is to provide an indication of the relative density of granular deposits, such as sands and gravels from which it is virtually impossible to obtain undisturbed samples.

The usefulness of SPT results depends on the soil type, with fine-grained sands giving the most useful results, with coarser sands and silty sands giving reasonably useful results, and clays and gravelly soils yielding results which may be very poorly representative of the true soil conditions. Soils in arid areas, such as the Western United States, may exhibit natural cementation. This condition will often increase the standard penetration value.

The SPT is used to provide results for empirical determination of a sand layer's susceptibility to earthquake liquefaction, based on research performed by Harry Seed, T. Leslie Youd, and others. (Youd et al, 2001)

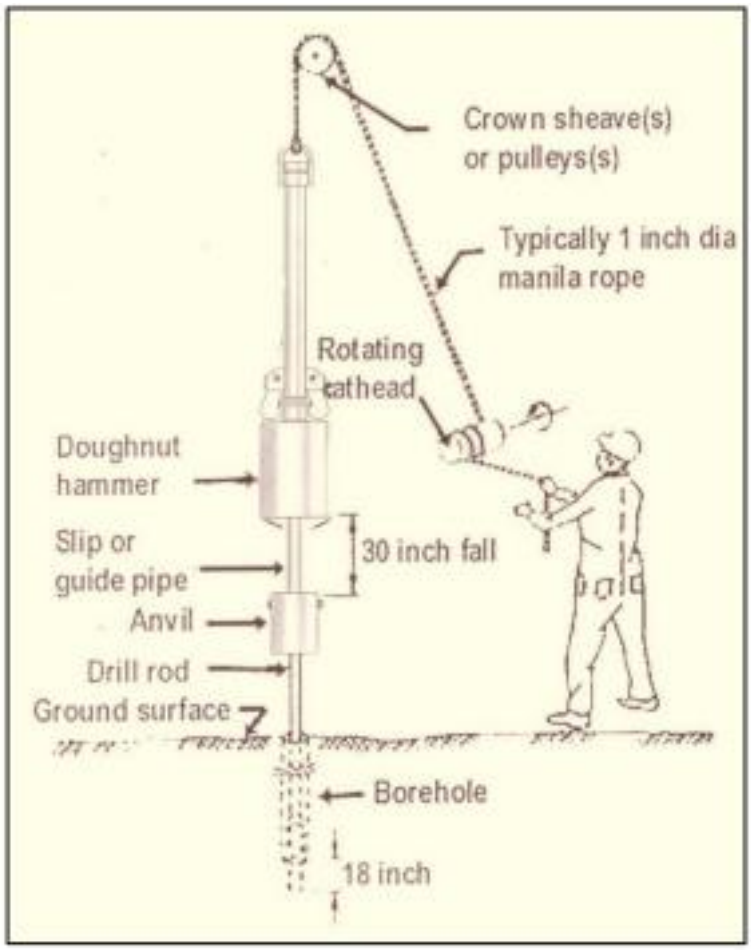

Fig 4.13. Schematic Assembly of SPT.

Contour map for Standard Penetration Test (SPT) for weathered and sub-weathered layer are shown in Figure 4.13.

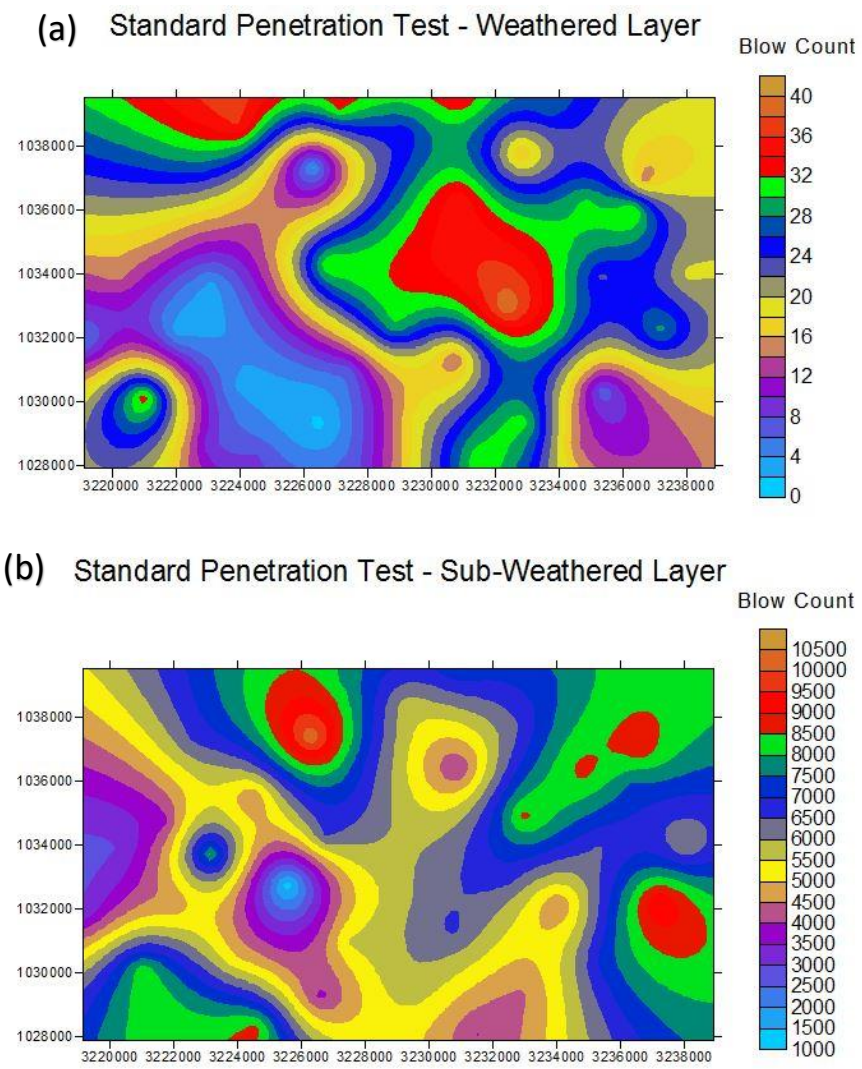

Fig 4.14. Contour Maps for Standard Penetration Test (SPT) (a) Weathered Layer (b) Sub-Weathered Layer.

a) Standard Penetration Test (SPT) for Weathered layer in Figure 4.14 (a) indicates that middle portion and some Northern portions have higher value of Standard Penetration Test (SPT) around 36 Blow count which is much lower than that is acceptable value which is 50 blow count. Rest of area have much low blow count as low as 4 blow count. So from this we conclude that weathered layer is not suitable for Engineering point of view so it need to be bulldozed.
b) By looking in Figure 4.14 (b) Standard Penetration Test (SPT) for Sub-Weathered layer indicates that minimum value is 4000 blow count and goes as high as 9000 blow count or

above. From this we can conclude Sub- Weathered layer is perfect for Engineering point of view.

As the minimum allowable value of SPT is 50 blow count for any site construction so most of the top layer need to be compacted before construction. Its mean from survey it is clear that all the top layer soil needs to be compacted otherwise survey would be reconducted. So it is recommended the site would not be recommended for construction unless the top soil properties should not exceed 50. Originally it should be above 100 low count. Soo for our results Sub- weathered layer is perfect.

4.5 Seismic Site Zoning/Characterization

Seismicity characterization is defined as zoning of a site based on seismicity of the area which is usually based on Average Horizontal spectral amplification of weak and strong motion and then developing various site characterization standards. Different countries have their own standards for site characterization. Similarly, National Earthquake Hazard Reduction Program (NEHRP) has developed a site-based characterization based on weak and strong motion was developed by the Building Seismic Safety Council (BSSC) of USA in 2001. Using these standards Average Horizontal spectral amplification (AHSA) weak and strong motion contour maps have been generated and finally site has been characterized.

It is well known that local site conditions could give rise to significant local amplification of ground motion during earthquakes. The intensity of ground motions during the 1906 San Francisco earthquake were strongly related to the local site conditions. Investigations of ground motion properties indicate that the amplitude, frequency content, and shape of seismic waves are modified by the soils and sediments through which they are transmitted (Borchardt et al., 1991)

4.5.1 Average Horizontal Spectral Amplification (AHSA)

AHSA is associated with earthquake engineering, incorporated with site response investigation in every micro zonation study. ASHA has weak and strong motion between 0,4 and 2,0 sec period from S wave velocity for 30 meters average in m/sec. One of the best approaches found for stable standing the geological structures is to observe the seismic ground motions on the ground surface.

Different approaches in site effect evaluation are used but to enhance the signal to noise ratio and to acquire real data, the most valuable and widely used approach is called Horizontal to Vertical Spectral Ratio (H/V) first introduced by Nakamura in 1989, assuming that the vertical component

is not amplified by surface layers required the single station recording and uses the vertical component. Now Average of Spectral ratios over specified period bands provide estimate of ground response useful for summarizing variation on regional scale and variations pertinent for different types of structures. Ratios for period 0.4 to 2.0 sec provide a useful parameter to summarize variations in ground response on a regional scale. These ratios are computed with respect to local "Rock" sites and results confirms that reality in general that **"**Largest influence of local deposits occurs for horizontal motion at sites underlain by alluvium and mud so maximum average spectral amplification observed at those sites ranges 1.4 to 6.6**".**

The two types of horizontal spectral amplification are

- AHSAw (average horizontal spectral amplification for weak motion)
- AHSAs (average horizontal spectral amplification for strong motion)

- **ASHA-Weak:**

We can compute Average Horizontal Spectral Amplification (AHSA) - Weak Motion between 0,4 and 2,0 Sec periods from S Wave Velocity for 30 Meters Average using Borchardt Method (Borchardt, et al.,1991).

Average Horizontal Spectral Amplification (AHSA) Weak motion represents the aftershocks after main earthquake. Contour Map for AHSA-weak motion is shown in Figure 4.15

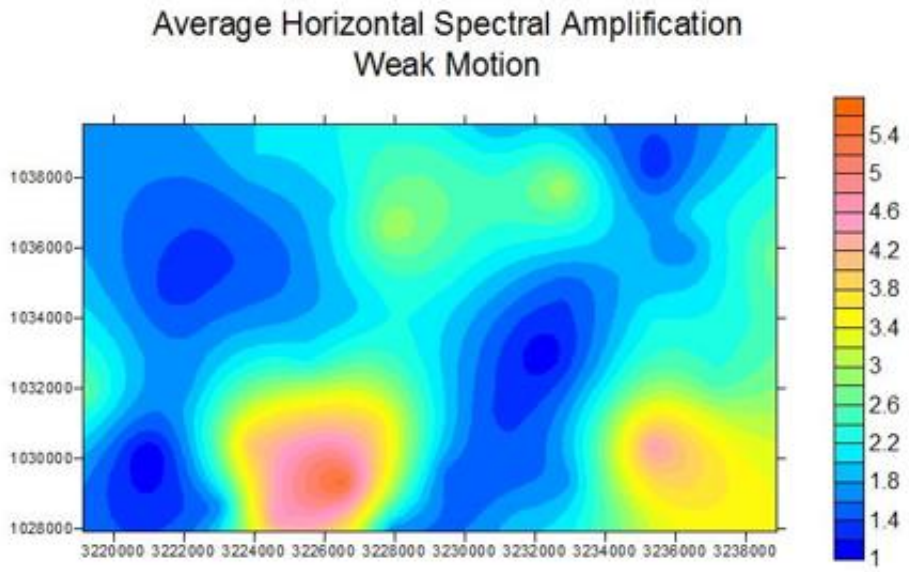

Fig 4.15. Contour Map for Avearge Horizontal Spectral Amplification (AHSA)-Weak Motion

Usually both strong and weak Average Horizontal Spectral Amplification (AHSA) have almost same trends. Average Horizontal Spectral Amplification (AHSA) in Figure 4.15 for Weak motion shows that most of the area has a lower value of Average Horizontal Spectral Amplification (AHSA) is around 1 to 1.8. However, it increases to 3.1 in some portions as we move towards North in the middle. It also attains higher value upto 4.5 in south-eastern portion as well as in another cluster portion in Southern part.

- **AHSA-Strong:**

Average Horizontal Spectral Amplification (AHSA) - Strong Motion between 0,4 and 2,0 Sec periods from S Wave Velocity for 30 Meters Average can also be computed using the Borchardt Method (Borchardt, et al.,1991).

Average Horizontal Spectral Amplification (AHSA) Strong motion represent the main Earthquake. Contour Map for AHSA-Strong motion is shown in Figure 4.16.

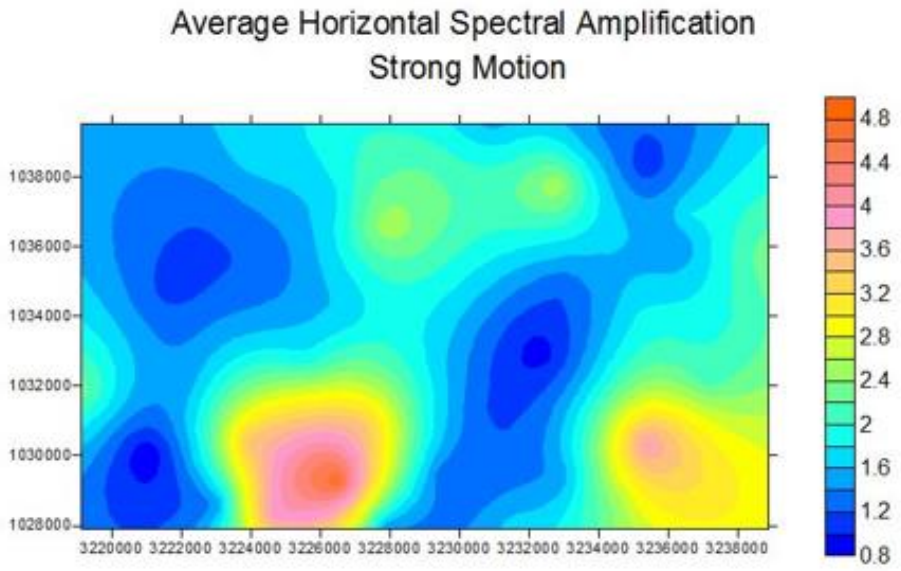

Fig 4.16. Contour Map for Avearge Horizontal Spectral Amplification (AHSA)- Strong Motion

Average Horizontal Spectral Amplification (AHSA) for Strong motion has almost similar trend and from Figure 4.16 it shows that its values are slightly Lowe than Weak motion. In this Fig most of the area has a lower value of Average Horizontal Spectral Amplification (AHSA) is around 0.8 to 1.6. However, it increases to 2.5 in some portions as we move towards North in the middle. It

also attain higher value upto 4 in south-eastern portion as well as in another cluster portion in Southern part.

Overall, from map interpretation of Average Horizontal Spectral Amplification (AHSA) shows that all that blue shaded region indicates that from seismicity point of view these are safer zones and red or pinkish indicates danger zone.

4.5.2 Site Classification based on Vs (30)

National Earthquake Hazard Reduction Program (NEHRP) has set up standards for site classification. Using these standards finally site has been characterized and its contour map is shown in Figure 4.17.

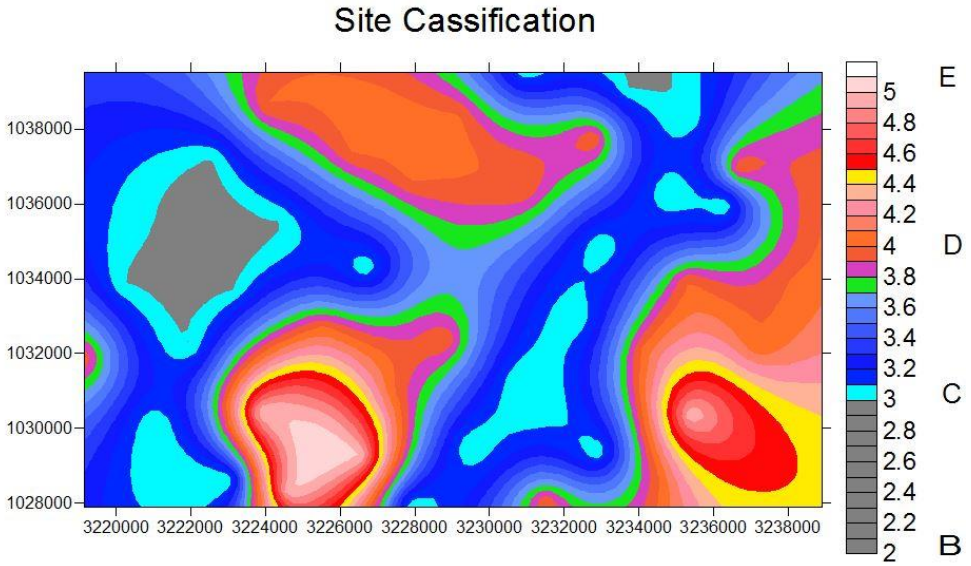

Fig 4.17. Contour Map for Site Classification

According to siting based on National Earthquake Hazard Reduction Program (NEHRP) standards A is the most safest region, B is second safest zone and then C is the third category of safer zone and after that category D & E are not considered safer site zones from seismicity point of view. The contour map for Site Classification in Figure 4.17 shows that the area has no A type of region. Category B indicated by Gray and Category C indicated by cyan colored region are shown in different portions of map are safer site or zones from Seismicity point of view and this interpretation is also compared with Average Horizontal Spectral Amplification (AHSA) for strong and weak motion map which also highlights the same safe zones. All yellow and red zones are not considered safe for construction.

Chapter 5

Development of Moisture Recording Instrument & Computation of Moisture-Velocity Transform

Seismic refraction techniques are used in the petroleum industry, to delineate the weathered layer, for computation of static corrections that are applied to seismic reflection data (Cox, 1999). In addition, these techniques are also helpful in identification of soil types, strata boundaries and depth of bedrock. The Soil Moisture Sensor is used to measure the amount of water inside the soil and provide the moisture level or the level of dryness or dampness of the soil. The output of this sensor helps to judge if there needs water or not in the soil. The sensor is mostly used in the cultivation land to reduce human involvement.

5.1 Introduction

In this chapter our aim is to develop a low-cost moisture recording instrument using Arduino open-source micro controller which is connected to a computer serial port along with a moisture sensor. Using this instrument along with seismic velocity instrument, velocity & moisture are measured. The moisture & velocity pairs at recording stations a cross plotted and a regression equation is derived between velocity & moisture which can be used to compute either velocity from the moisture or moisture from the velocity.

5.2 Arduino Circuit

Arduino is an open-source electronic microprocessor developed by Massimo Banzi and David Cuartielles (2005). The initial Arduino core team consisted of Massimo Banzi, David Cuartielles, Tom Igoe, Gianluca Martino, and David Mellis. In early 2008, the five co-founders of the Arduino project created a company, Arduino LLC to hold the trademarks associated with Arduino (Hernando Barragán e.t 2016). It is a one board solution where all the input output ports, micro-controller and APROM are available on a singal board along with the USB port and it can be connected to a Laptop where we have Arduino programming environment. In Arduino we can attach different gadgets like GPS gadget, Bluetooth gadget, mobile SIM gadget and we can attach different sensors. In our case we are going to use moisture sensor along with two electrodes that would be connected with the Arduino.

5.2.1 Arduino Language

Arduino code is written in C++ with an addition of special methods and functions. So its language is similar to C++ but it is called "*sketch*", a variant of C-language.

5.2.2 Arduino IDE

The Arduino Integrated Development Environment (IDE) is the main text editing program used for Arduino programming. The code is written and loaded to the board using this IDE.

The Arduino board is connected to a computer via USB, where it connects with the Arduino development environment (IDE). The user writes the Arduino code in the IDE, then uploads it to the microcontroller which executes the code, interacting with inputs and outputs such as sensors, motors, and lights.

5.3 Moisture Recording Instrument

Using the Arduino Nano board as well as soil moisture sensor, a moisture measurement system is assembled. The block diagram of the moisture recording instrument is shown in Figure 5.1.

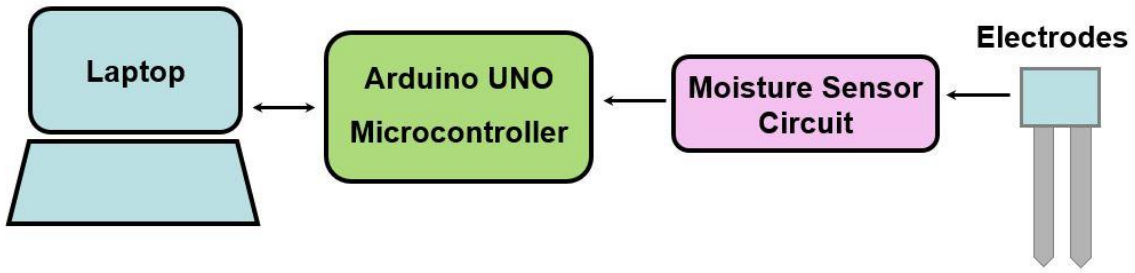

Fig 5.1. Block Diagram of Moisture Recording intrument.

As can be seen in the above figure Moisture sensor passes electric current through electrodes which are inserted into the ground and resistivity is measured. The Moisture sensor calibrates the resistivity value and convert the resistivity into moisture value and then convert into digital value within 0 to 1023 range. 1023 means completely dry which means highest resistivity and 0 means 100% moisture. These values are input to the Arduino UNO Microcontroller through the analog inputs and the program convert these values to percentage value. Finally, these values are sent into the Laptop through USB Serial Port.

The Arduino Nano board along with moisture sensor and its two electrodes is and this complete electronic circuit is shown in Figure 5.2.

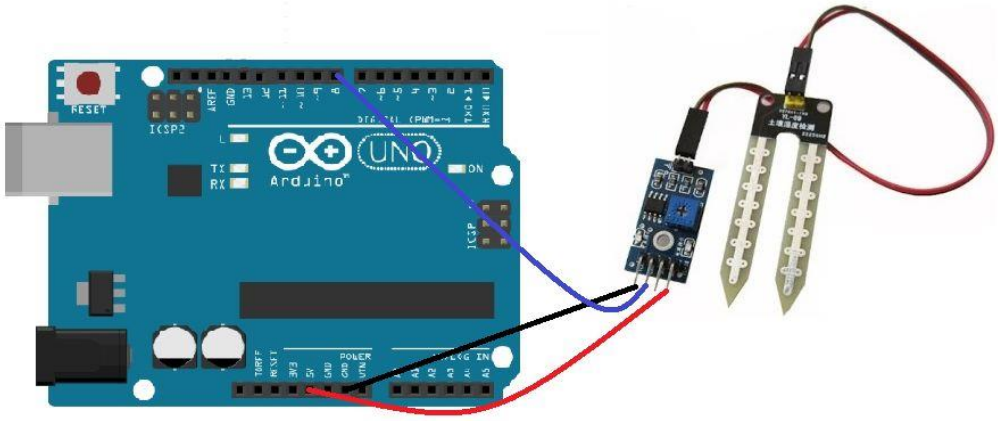

Fig 5.2. Arduino board along with the moisture sensor and electrodes.

This instrument is assembled as shown above and connected with serial port to a laptop. This instrument is continuously transmitting values which are received by the computer into a text file.

Soil moisture sensor's output can be used both as analog and digital output. Digital has 0 value below the threshold limit and 1 above the threshold limit thus this mode is not required as we need a variable value of moisture from 0 to 100%. In analog interfacing mode, the sensor will give the percentage value of the moisture. The sensor gives value from 0 to 1023 and microcontroller will map the value to the percentage from 0 to 100. The range can be changed depending on the climate of that place. Developer can change the range in the code according to the requirements.

5.3.1 Working of Soil Moisture Sensor

A moisture sensor has two long probes as shown in Figure 5.2, which are pushed in the soil to measure the amount of water in the soil. The current flows through the soil and the resistance of the soil is measured which is converted to the moisture value. Where there is more water, soil conducts more current, so the resistance will be lower and moisture level will be higher. On the other hand, dry soil conducts very less amount of electricity because of very low amount of water, so the resistance is higher, and moisture will be lower. There is a mapping for the level of moisture.

Sensors are mainly mapped within 0 to 1023 values after analog to digital conversion. The moisture sensor values can be interpreted as:

- If the sensor value is 1000 or more than that then the sensor is not in the soil or sensor is disconnected.
- If the sensor value is more than 600 but less than 1000 then the soil is dry.
- If the sensor value is 370 to 600 then the soil is humid.
- If the sensor value is less than 370 then the sensor in the water.

An now using Arduino development environment a program is written in its Sketch. The short program converts all the values and returns the moisture percentage value. The Program code is given in Annexure A.

5.4 Two Geophones Seismic Recorder

For the measurement of top-soil layer velocity we have used a seismic recorder with only two geophones which are directly connected to the computer along with the software and geophones are planted at 1 meter apart. This seismic recorder is build on built-in PC Sound Card and we just have to connect a pair of geophones along with a cable which has an audio jack connected to the PC (Khan et al., 2012)

The seismic recorder requires a PC laptop with a stereo audio input, installed with the seismic recording software and Digi Seis component. The schematic of this instrument is given in Figure 5.3.

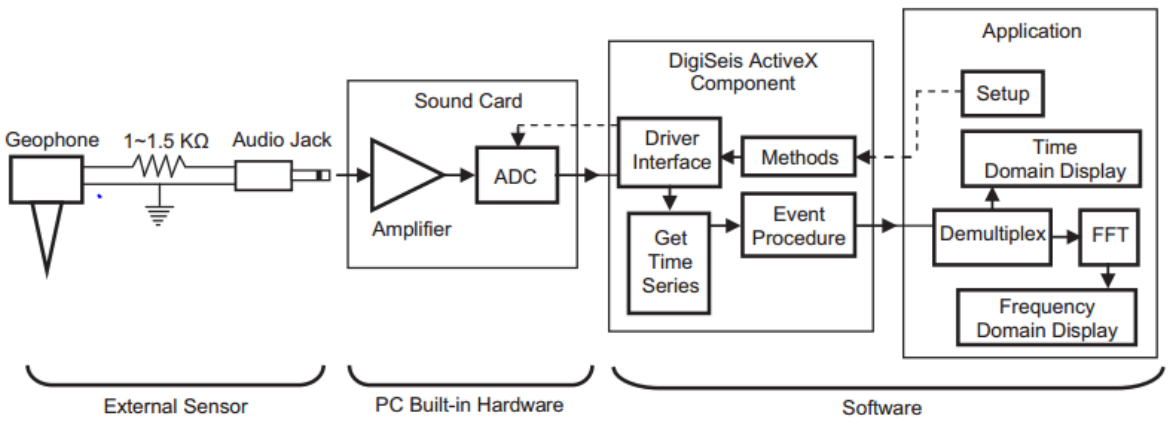

Fig 5.3. Block Diagram of Seismic Recorder (Khan et al., 2012)

The PC-based seismic refraction recorder along with its two geophones is shown in Figure 5.4.

Fig 5.4. Field acquisition with the PC-based two geophone seismic refraction recorder.

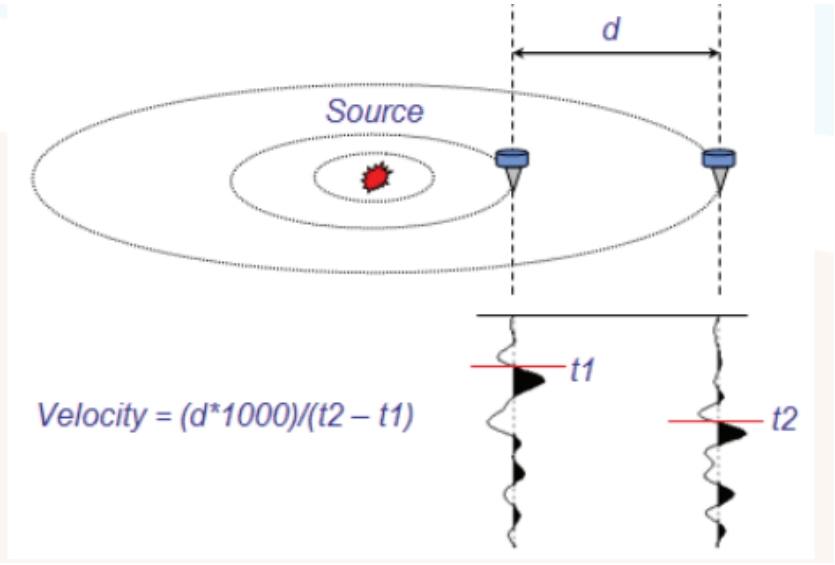

Fig 5.5. Working of two geophones for measurenment of top layer velocity. (Khan, Akhter, G & Ahmed, 2012)

Just with a single jump or with a hammer we make a bang near the first geophone. Waves travel to first geophone and recorder records the time t_1 then gradually wave mover towards second

geophone and recorder records the time t_2. The distance between the two geophones is set to one meter and using the two recorded times the velocity is computed as.

$$V = (d * 1000) / (t_2 - t_1)$$

This above discussed procedure is demonstrated in Figure 5.5.

The instrument has a specialized recording software. Thus, when the geophones are planted and software is set in recording mode it will continuously records the waves and take the time difference at the two geophones. The measurements can be repeated at a location to average out the results. Instead of doing one-time measurement we take 12 measurements for accuracy. The software recordings repeated 12 times are shown in Figure 5.6.

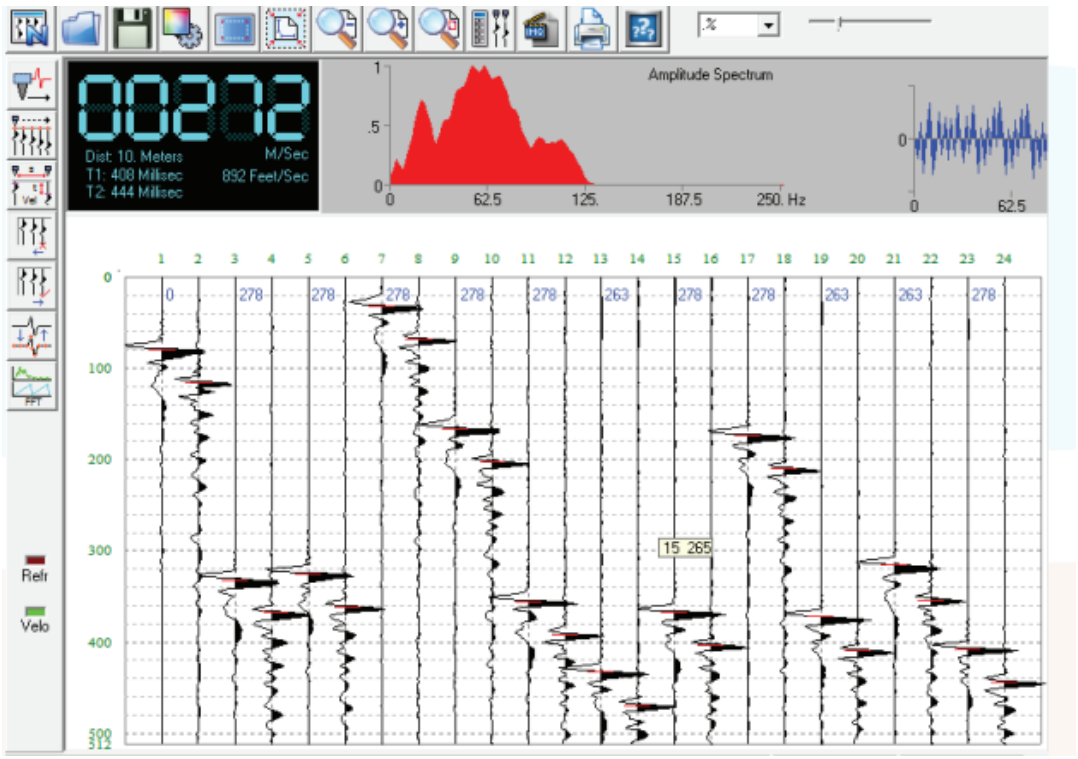

Fig 5.6. Software display of Seismic Recording instrument for measurenment of Top layer velocity, using the arrival times from each pair of traces

5.5 Velocity-Moisture Measurements in the Field

Using the moisture instrument and two geophones seismic recorder, both connected with the Laptop. Velocity-moisture survey has been carried out in the surrounding grounds in the vicinity of Railway General Hospital or Ripah medical institute in Rawalpindi.

Base Map for Velocity-moisture measurement stations is shown in Figure 5.7.

Fig 5.7. Base Map of Survey area for Moisture & Velocity measurement

Map shows that data has been acquired at total a of the 17 stations and Moisture & velocity is measured at these stations. Table 5.1 shows the values of measured velocities & moisture percentage at the these stations.

Table 5.1. Velocity-Moisture Saturation data

Station ID	Compressional Velocity M/Sec	Moisture Saturation %
MV-1	299.9	17.5
MV-2	168.0	25.1
MV-3	205.7	22.7
MV-4	124.2	31.5
MV-5	131.7	28.1
MV-6	167.1	30.4
MV-7	111.0	27.7
MV-8	243.5	22.3
MV-9	334.6	15.3
MV-10	390.7	12.6
MV-11	347.8	21.1
MV-12	342.8	22.3
MV-13	216.7	24.6
MV-14	122.6	29.1
MV-15	171.3	37.8
MV-16	189.4	29.9
MV-17	309.0	16.7

Our aim in this study is to use the velocity-moisture values and establish a relation between these two parameters using linear regression. Thus velocity-moisture transform is established using an imperical relationship. The data points are input into Wavelets software (Khan et al. 2006; Khan and Akhter 2015) for regression analysis. The regression analysis interface in Wavelets software is shown in Figure 5.8.

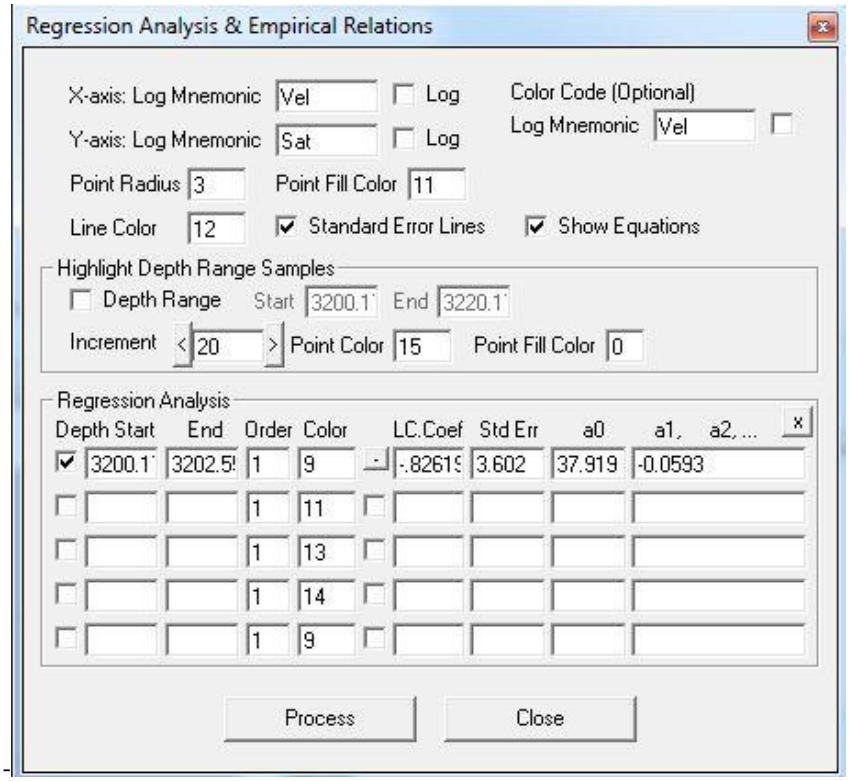

Fig 5.8. Software Interface of Regression Analysis.

The Velocity-Moisture Saturation cross-plot along with the best fit regression line are shown in Figure 5.9.

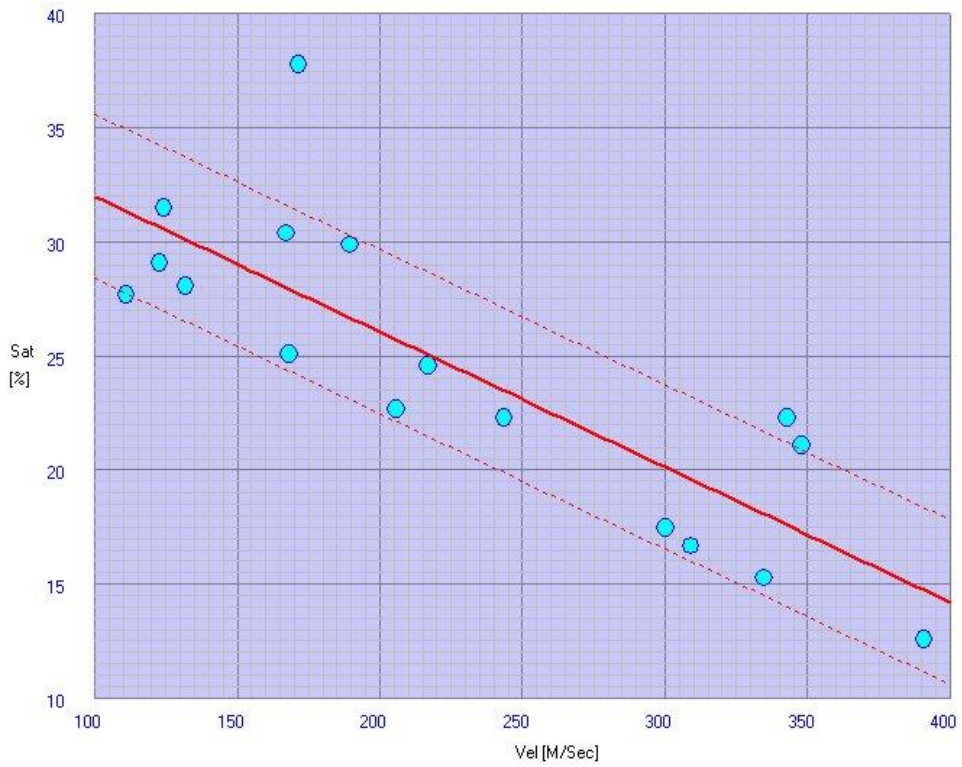

Fig 5.9 Cross plot between Velocity and Moisture Saturation along with best-fit regression line (red-solid) and standard error lines (red-dash).

Looking at the cross-plot it is evident that probably velocity is decreasing as moisture percentage is increases. The Velocity to Moisture linear equation is given as:

$$\boldsymbol{Sat = 37.919 - 0.0593\ Vp}$$

Where ***Vp*** is compressional velocity and ***Sat*** is Moisture Saturation in percentage.

This equation has a Coefficient of Linear Correlation 0.82 with a standard error of only 3.6%.

By using this equation, we can now measure the velocity and then derive the moisture without using the moisture instrument.

Conclusions & Recommendations

Conclusions

- Uphole Logging and Near surface Seismic refraction survey was carried out which indicates that the weathered layer thickness varies from 7 meters to 26 meters and weathered layer velocities are lies between 400 meters to 900 meters while Sub-weathered layer velocities are lies above 2000 meters to 3200 meters.
- The DEM indicates that area has a stable topographic variation ranging between 500 to 600 meters above mean sea level and slope analysis indicate that the stable area has a dip below 5 degrees. Thus, from accessibility point of view this area is suitable for construction of any Engineering site.
- Various Engineering parameters computed from Seismic Refraction survey such as Soil Amplification Factor, Soil Fundamental Period, Allowable Bearing Pressure of Soil that indicates some portions in the Eastern part of the region are highly unstable for Engineering and construction point of view.
- Similarly, Standard Penetration Test also indicates that Eastern part of the region has lowest value of 4 blow count however the value increases to the maximum of 40 blow count as we move toward the north but overall maximum value is lower than the minimum acceptable value of 50 blow count therefore for construction of heavy site weathered layer need to be retreated before the construction.
- Seismicity study indicates that Average Horizontal Spectral Amplification for two regions in the southern and south-eastern part has a Spectral Amplification factor of 5.4 which indicates that region is unstable for construction point of view.
- Based on National Earthquake Hazard Reduction Program (NEHRP), the seismicity of site classification has been carried out which indicates that South-Eastern region of the area as well as some patches in the South as well as in North lies in Zone 5 which is is highly unstable zone and not suitable for construction while rest of the area characterized from 3 to 3.8 is stable and therefore those zones are suitable for construction of heavy Engineering plant.

- An Arduino Based Moisture Recording Instrument has also been developed which is capable of recording moisture of topsoil and it can be used as an useful instrument for Engineering studies.
- Using the soil moisture instrument along with measurements of seismic velocities a localised survey in Rawalpindi has been carried out to measure the velocity and moisture content of topsoil and regression based velocity-moisture empirical relation has been derived. This Equation can also be used to compute moisture from the velocity.

Recommendations

- Standard Penetration Test of weathered layer indicates the some portions in the South-Eastern region has lowest values of SPT less than 10 Blow counts & weathered layer thickness also indicated that these portions have a weathered layer thickness around below 10m. Thus, it is recommended that the weathered layer should be bulldozed in order to make site stable before construction for an Industrial site.
- However, when we move towards North Standard Penetration Test values reaches maximum of 40 blow count and weathered layer thickness is also higher. Therefore, in those regions it is recommended that area should be compacted in order to improve its Engineering properties before construction for an Industrial site.

Annexure A

Script of Moisture Saturation Program.

```
//Aurdino Program to get Moisture Data through serial port
//The program measures the resistivity and inverts it into moisture.
//Finally the moisture is converted into % saturation
//Setup the Serial Port Baud Rate and Analog Pin0 to get Input from Sensor
void setup()
{
  Serial.begin(9600);
  pinMode(A0, INPUT);
}
//Aurdino Main Loop
//Read Resistivity from Sensor and convert it into Moisture Saturation
//Send the Mositure Saturation values to computer
void loop()
{
  int resist = analogRead(A0);
  int moist= 1024 - resist;
  int moistpercent = 100 * moist / 1024;
  Serial.println(moistpercent);
  delay(5000);
}
```

References

Akademi Ltd. Sti., 2002. “Erbaa Organize Sanayi Bolgesi Jeoloji-Jeoteknik Etut Raporu”, Aki, K. and G. Richards, *Quantative Seismology*, v.1., 557 pp., W. H .Freeman.

A.H Hadjian, 2002, Soil Dynamics and Earthquake Engineering

Book, Seismic data analysis techniques in hydrocarbon exploration / Enwenode Onajite.

Borcherdt, C. M. Wentworth, A. Janssen, T. Fumal, and J. Gibbs, 1991, Methodology for Predictive GIS Mapping of Special Study Zones for Strong Ground Shaking in the San Francisco Bay Region, CA, Proc. 4th Int. Conf. Seismic Zonation, 545-552

Building Seismic Safety Council (BSSC) (2001): NEHRP recommended provision for seismic regulations for new buildings and other structure, 2000 edition, part 1 provision, prepared by the Building Seismic Safety Council for the Federal Emergency Management Agency, Report FEMA 368, and Washington, DC.

Cox, M., 1999, Static corrections for seismic reflection surveys: Soc. Expl. Geophys.

Castagna, J.P., Batzle, M.L., and Eastwood, R.L., 1985, Relationships between compressional-wave and shear-wave velocities in clastic silicate rocks. Geophysics, V.50, pp.571-581.

Dobrin, M. B., & Savit, C. H., 1988. Introduction to Geophysical Prospecting. Mcgrew Hill Company

Farr, T. G., et al., 2007. The Shuttle Radar Topography Mission, Review of Geophysics., Vol. 45, RG2004. doi:10.1029/2005RG000183.

Gardner, G.H.F., Gardner, L.W., and Gregory, A.R., 1974, Formation velocity and density – the diagnostic basics for stratigraphic traps: Geophysics, 39, 770-780.

Hernando Barragán.,2016. The Untold History of Arduino arduinohistory.github.io. Retrieved 2016-03-06.

Imai, T. and Yoshimura, Y., 1970, Elastic wave velocity and soil properties in soft soil, Tsuchito-Kiso 18 (1), 17–22 (in Japanese).

Jadoon I A K, Khawaja AA, Jamshed S Q. 1995. Thrust geometries and evolution of the eastern North Potwar Deformed Zone, Pakistan [J]. Geol Bull Univ Peshawar, 28: 79–96.

Jaswal, T. M., Lillie, R.J. and Lawrence, R.D., 1997. Structure and Evolution of the Northern Potwar Deformed Zone, Pakistan. AAPG Bulletin., 81,2,308-328.

Kanai, K., 1983, Engineering Seismology, University of Tokyo Press, pp-251.

Kazmi, A.H., And Jan, M.Q., 1997, Geology and Tectonics of Pakistan, Graphic Publishers Karachi, Pakistan.

Kadri, I. B., 1995. Petroleum Geology of Pakistan. Karachi: Ferozsons (Pvt) Ltd.

Kearey, P., Brooks, M., & Hill, I., 2002. An Introduction to Geophysical Exploration. Blackwell Science Ltd.

Khan, K. A., Akhtar, G., Ahmed, Z., Khan, M.A., and Naveed, A., 2006, Wavelets - A Computer Based Training Tool for Seismic Signal Processing, Pakistan Journal of Hydrocarbon Research, Vol. 16, pp.37-43.

Khan, K.A., 2007. Artificial Intelligence Based Automated First Break Picking And Quality Control, 77th Annual International Meeting, SEG, Expanded Abstracts, Pp.1103–1107. Doi:10.1190/1.2792598.

Khan, K.A., 2009, Seismic Methods, Digital Courseware Series, 2nd Edition.

Khan, K.A., 2010, Seismic - The Next Step Series: Seismic Attributes, OIST, Islamabad

Khan, K.A., Akhter, G. and Ahmad, Z., 2010. OIL - Output Input Language for Data Connectivity between Geoscientific Software Applications, Computers & Geosciences, Vol.36(5), pp. 687-697. doi:10.1016/j.cageo.2009.09.005

Khan, K. A., Akhter, G., Ahmad, Z., Khan, M.A., and Naveed, A., 2006. Wavelets - A Computer Based Training Tool For Seismic Signal Processing, Pakistan Journal Of Hydrocarbon Research, Vol. 16(1), and Page.37-43.

Khan, K.A., 2004. An intelligent and efficient approach to picking first breaks, 56th Annual Conference and Exhibition, European Association of Geoscientists and Engineers, Extended Abstracts, P155.

Khan, K.A., Akhter, G., and Ahmad, Z., 2012, DigiSeis – A software component for digitizing seismic signals using the PC Sound Card, Computers & Geosciences, Vol.43, 217-220. doi:10.1016/j.cageo.2012.02.024

Khan, K.A., 2000. Integrated Geo Systems - A Computational Environment for Integrated Management, Analysis and Presentation of Petroleum Industry Data, In: T. C. Coburn and J. M Yarus (Eds.), Geographic Information Systems in Petroleum Exploration and Development, American Association of Petroleum Geologists, AAPG Book on Computers In Geology, Pp.215-226.

Khan, K.A., Akhter, G., and Ahmad, Z., 2009. The Real meaning of Geoscience Data and Process Integration, Proceedings of IAMG International Conference, Computational Methods for Earth, Energy and Environmental Sciences, Stanford Univ., CA.

Khawar Ashfaq Ahmed**,** "Seismic Facies Modelling of Potwar Basin Using Seismic and Well Log Data", Scientific & Academic Publishing, p-ISSN: 2163-1697 e-ISSN: 2163-1719 , 2012; 2(6): 192-211.

Khan K.A. and Akhter, G., 2015, Computer-Based Experiments for Learning Seismic Signal Processing Concepts, Computer Applications in Engineering Education, Vol. 23, 959-966. Doi: 10.1002/cae.21669

Lee, M.W., 2010, Predicting S-Wave Velocities for Unconsolidated Sediments at Low Effective Pressure, Scientific Investigations Report 2010–5138, USGS

Mari, Jean-Luc, "Signal Processing (For Geologist & Geophysicist)" , p 1-2, 1999.

Midorikawa, S., 1987, Prediction of isoseismal map in the Kanto plain due to hypothetical earthquake. Journal of Structural Engineering 33, 43-48

Michael D. McCormack et al., 1993. First-break refraction event picking and seismic data trace editing using neural networks. Geophysics, Vol.58, No.1, P. 67-78

Palmer, D. (1980). "The Generalized Reciprocal Method of Seismic Refraction Interpretation." Soc. of Exploration Geophysicists. Tulsa, OK.

Pennock E.S., Lillie R.J., Zaman A.S.H., Yousaf M., Structural interpretation of seismic reflection data from eastern Salt Range Potwar Plateau, Pakistan. American Association of Petroleum Geologist Bulletin, 1989, 73(7), 841-857.

Robinson. E. S., And Coruh. C., 1988. Basic Exploration Geophysics, John Wiley and Sons, Inc. Newyork.

R. Borcherdt, C. M. Wentworth, A. Janssen, T. Fumal, and J. Gibbs, 1991, Methodology for Predictive GIS Mapping of Special Study Zones for Strong Ground Shaking in the San Francisco Bay Region, CA, Proc. 4th Int. Conf. Seismic Zonation, 545-552.

Sheriff, R. E. And Geldart, L. P., 1995. Exploration Seismology, 2nd Ed., Cambridge Univ. Press.

Shami B.A., Baig M.S., Geomodelling for the Enhancement of Hydrocarbon Potential of Joya Maier Oil Field, Potwar, Pakistan. Annual Technical Conference, Islamabad, Pakistan, 2002, 124-145.

Shah, S.M.I., 2009. Stratigraphy of Pakistan. Geological Survey of Pakistan, Memoirs, v.22.

Sheriff, R. E., 1991, Encyclopedic Dictionary of Exploration Geophysics: Society of Exploration Geophysics.

Shah, S.M.I., Ahmed, R., Cheema, M.R., Fatmi, A.N., Iqbal, M.W.A., Raza, H.A., and Raza, S.M., 1977. Stratigraphy of Pakistan. Geological Survey of Pakistan, Memoirs, V. 12, P.137.

Telford, W. M., Sheriff, R. E., & Geldart, L. P., 1990. Applied geophysics. Cambridge University Press.

Uchiyama, S., Tonouchi, K., Imai, T., 1984, Measurement of S Wave Velocity of Ground and Application of S Wave Velocity Data for Civil Engineering, OYO Technical Note, No:52.

William J. Sercombe., et al., 1998. Wrench Faulting in the Northern Pakistan Foreland [Journal]. - [s.l.]: The American Association of Petroleum Geologists, Vol. 82

Yilmaz, 2001, Seismic Data Analysis and Processing, Inversion and Analysis of Seismic Data, Society of Exploration Geophysics, Tulsa.

Youd, T. L.; Member, Asce, I. M. Idriss, Chair; Fellow, Asce, Ronald D. Andrus, Co-Chair; Arango, Ignacio; Castro, Gonzalo; Christian, John T.; Dobry, Richardo; Finn, W. D. Liam; et al. (2001). "Liquefaction Resistance of Soils: Summary Report from the 1996 NCEER and 1998 NCEER/NSF Workshops on Evaluation of Liquefaction Resistance of Soils". Journal of Geotechnical and Geo-environmental Engineering 127*:* page 297–313.

K-tron Research Incorporated

605, 6th Floor, Kohistan Tower
The Mall, Rawalpindi

Email: support@k-tron.net
www.k-tron.net

No: KRI-SYS-522

19th November, 2020

Education Software Licence(s)

Educational licenses for the following K-tron Software Applications have been issued to Amber Latif, BS Student, Quaid-i-Azam University, Islamabad.

Application	Version	Issue Date	Expiry	Licence Key
SeiRA	4.3-5.0	06-09-2019	31-12-2021	B91558C-32A7C6B-2071-1558-25B9-B04-72F
Precision Matrix	5.10	06-09-2019	31-12-2021	B919542-32A97B9-BD2-B9-37F7-F91-6BC
Visual OIL	2.10	06-09-2019	31-12-2021	B828E3F-68E3A3B-216B-3E3-3A09-FE6-743
Wavelets	7.00 R2020-07	11-11-2019	Perpetual Non Expiring	14D70-33B4F
GeoStudio	8.50 R2020-02	14-01-2020	31-12-2022	C6E3E52-3D8A4C7-A5-830-3F62-1379-6E2

Umair Khan
Systems Support

SENSHE
西安森舍电子科技有限责任公司
Xian Senshe Electronic Technology Corporation (Pvt) Ltd

Ref: S2019-P152

December 8, 2019

Near Surface Seismic Data for Engineering Studies.

Ms. Amber Latif, BS Geophysics student, Quaid-i-Azam University, Islamabad, has been provided Seismic Refraction and Uphole Logging data of Rawat Area to carry out engineering studies of the site as part of her thesis research work.

The student is required to submit the outcome of the research work to Xian Senshe Electronic Technology Corporation (Pvt) Ltd.

Malik Shoaib Afzal Khan
Party Chief
Senshe Crew-112

House 377, Street 25, Sector E-11/4, Islamabad, Pakistan
Phone No.: +92-51-2153065 **Fax NO**.: +92-51-2153064 **Website**: www.senshe.com